Influence of spectra model on the ship response

Luccas Zulliane Marquetti da Silva

Thesis to obtain the Master of Science Degree in

Naval Architecture and Ocean Engineering

Supervisors: Dr. Roberto Vettor

Prof. Dr. Alexandre Nicolaos Simos

Examination Committee

President: Prof. Dr. Carlos Guedes Soares

Supervisor: Dr. Roberto Vettor

Member of the Committee: Dr. Serge Sutulo

October 2019

Acknowledgements

This work is mostly dedicated to those that effectively contributed on the construction of my very being. Firstly, I thank my parents, as they have always been supportive, more than I could ever deserve. I thank my brother, and best friend, who always willingly and kindly looked after me, in such way that every moment I felt supported and beloved. I thank my fiancée who gently have been supportive and comprehensive during this time of hard working and distance.

I thank my home university, the Polytechnic School of the University of São Paulo, for providing me the solid basis I needed to be able to overcome my own limits. I thank my supervisor Professor Alexandre Simos who willingly and gently helped me out innumerable times with both the academic and life decision subjects, which teachings and suggestions made me go beyond I could ever imagined.

I thank The Technical University of Lisbon for hosting me in such amazing period in which I attended a great master course, which experience will never be overlooked. I thank Professor Carlos Guedes Soares for being totally supportive and for managing the course as head of the department in such an outstanding way. I thank both secretaries Miss Fátima and Sandra for kindly guiding me during this period as foreign student, which suggestions became crucial for a better experience abroad.

I feel it is also crucial also to thank my landlord, Doron, who helped me out innumerable times and supported me more than I could ever expect, who now I consider as a good friend of mine.

Finally, I tenderly thank my supervisor Professor Roberto Vettor, who so gently supported me during this entire period and showed to be an excellent supervisor with such a great commitment on our work. I felt I could account on him anytime and that became crucial for me to go further, to grow academically and, as said on the beginning, he inherently contributed significantly on the growth of the personality of my very being.

Abstract

The prediction of the ship responses in ocean-waves excitement is of marked importance on the design, as well as in lifetime operations. The structures have to withstand the wave induced loads as to guarantee motions and accelerations to be contained within acceptable limits, so that the comfort and safety of people and cargo onboard are not overlooked. Wave energy spectra parametric models can be used to describe the distribution of wave energy into both the frequency and directional domains. The ship responses can be estimated from them, regarding the correspondent RAOs. This work aims at investigating the influence of the spectra models on the ship responses, studying the significance of the wave climate on the differences between the models, so that suited spectral models can be recommended according to the seaways the vessels are designed to operate. Cases in which the traditional uni-directional single-peaked approach provides enough accurate responses are to be highlighted, as also those in which a better description of the wave field energy in terms of wave components and directionality is needed. Single and double-peaked models were found to present agreeing results in dominated wave fields. Uni- and multi-directional models did not show to provide expectable agreement, although higher similarity in more severe wave climate was verified in heave, suggesting that simpler models can be used. A more marked variability on the differences in roll was observed, meaning that a better description of the wave field energy is suggested.

Keywords: Spectra Models, Ship Responses, Wave Climate

Resumo

A predição das respostas do navio em excitação de ondas oceânicas é de acentuada importância no projeto, bem como no tempo de vida operacional. As estruturas devem resistir os carregamentos induzidos por ondas tanto quanto garantir que movimentos e acelerações estejam dentro de limites aceitáveis, de forma que o conforto e segurança de pessoas e carga a bordo não são esquecidos. Modelos paramétricos de espectro de energia de onda podem ser usados para descrever a distribuição da energia de onda nos domínios de frequência e direcional. As respostas do navio podem ser estimadas por ele, a respeito das funções de transferência correspondentes. Esse trabalho visa investigar a influência dos modelos de espectro nas respostas do navio, estudando a relevância do clima de onda nas diferenças entre eles, de forma que modelos de espectro adequados podem ser recomendados de acordo com as vias marítimas nas quais as embarcações são projetadas para operar. Casos nos quais a abordagem tradicional unidirecional de pico único fornece respostas suficientemente acuradas serão destacados, bem como aqueles nos quais é necessária uma melhor descrição da energia do campo de onda em termos de componentes de onda e direcionalidade. Modelos de pico único e duplo mostraram apresentar resultados semelhantes em campos de onda dominados. Modelos uni e multidirecionais não mostraram concordância expectável, embora maior semelhança em clima de onda mais severo foi verificada em *heave*, sugerindo que modelos mais simples podem ser usados. Uma variabilidade mais acentuada nas diferenças em *roll* foi observada, significando que uma melhor descrição da energia do campo de onda é sugerida.

Palavras-chave: Modelos Espectrais, Respostas do Navio, Clima de Onda

Contents

List of tables

List of figures

List of symbols

T_m	Average Wave Period
S_ζ	Heave Response Spectrum(a)
$\Phi_{\zeta_w\zeta}$	Heave Transfer Function
θ_H	Relative wave direction
MWD	Mean Wave Direction
S_φ	Roll Response Spectrum(a)
$\Phi_{\zeta_w\varphi}$	Roll Transfer Function
ζ_s	Significant Heave Amplitude
φ_s	Significant Roll Amplitude
H_s	Significant Wave Height
S_{ζ_w}	Wave Energy Spectrum(a)

Chapter 1

Introduction

A major design concern about man-made marine structures is the capability of withstanding wave induced loads that shall act upon them during the operating life. Besides, motions, such as accelerations, are, in most cases, design priority, as they are intended to not be violent, which express the concerning about the safety of people and cargo on-board.

Loads and motions can be obtained, for instance, either from experiments in model basins or computationally. Numerical methods, such as strip theory, are applied in this latter case, mostly to solve the seakeeping problem on regards of the potential theory, in such way to obtain the correspondent transfer functions. The Response Amplitude Operators (RAOs), meaning the module of the transfer functions, reflect the expected behavior of the ship under wave excitation and depend on the ship characteristics such as the main dimensions, mass, moments of inertia and so forth. The ship responses are dictated, therefore, by that inherent expected behavior and the external forces, these latter related with the energy of the incident waves.

The description of the wave energy is crucial part of the ship response computations. The wave energy spectrum is largely for the description of the wave energy distribution into both the frequency and directional domains. Full representation of the wave energy spectrum is in most of the cases impractical, thus parametric models are usually adopted to fit the energy distribution to classical distributions proposed in the literature. Integral parameters required to describe the wave field main characteristics are, for instance: H_S, T_m and MWD. The energy spectrum can be expressed by different parametric models, such as uni- or multi-directional, single or double-peaked ones, reflecting the presence of multiple wave systems. Depending on the sea-state characteristics, the variability on the ship response estimations when changing the parametric model can be more or less significant, in such way that it shows the importance of selecting a reliable model in order to avoid eventual under-estimations on the calculation of loads and motions. Obviously the most complete model, in which the separate contribution of the wave components, swell and wind-sea, and the energy directionality are considered, would be the most suggested one, though criticalities related, for instance, to the estimation of appropriate spreading functions, may compromise their outputs. Simpler models, however, can still provide similar results

compared to that latter, which application can be interesting from the point of view of computational time saving and modeling simplicity.

Unidirectional models are those in which the wave energy distribution is performed only about the frequency domain while in the multidirectional ones, frequency and directional energy spreading are considered. The relation between the MWD and the ship course produces θ_H, the relative wave direction, meaning the angle with which the waves approach the ship, varying from following to head waves. The relative wave direction performs an important role about the calculation of the ship response, as it directly influences on how the wave energy spectrum relates with the RAOs. As on the uni-directional models the wave field energy is entirely concentrated at θ_H, in some cases when this latter is found to be a high excitation direction, which is dictated by the RAO, the ship responses computed from it are more likely to be over-estimated compared to the directional models. On the other hand, when θ_H is a low excitation direction, the responses are likely to be under-estimated.

Single-peaked models are those in which the wave field is a resulting wave system from the interaction between the wave components, swell and wind-sea, composing a combined wave field. The wave components separate characteristics such as their own H_S, T_m and MWD are not in fact taken into consideration, therefore, but the characteristics resulting from an *average* system. Double-peaked models, on the other hand, take into consideration the separate characteristics of each component. Wave fields where the two wave components show to be energetically relevant about the total energy and which the MWDs differ significantly are those which the single-peaked models may provide not so reliable information, as the particular θ_H associated to each component will be lost on the process, as result of the representation of that crossing wave system into an average field with average MWD. Depending on the θ_H of each component and their energetic relevance about the total energy, the combined θ_H to be described by the single-peaked model can be, for instance, a high excitation direction, which eventually yields in over-estimated responses compared to the case when the separated contributions with their own relative wave directions are used. Low average excitation direction can also result from the interaction between both components, so that the correspondent responses are likely to be under-estimated.

The influence of the parametric model on the ship responses depends on the wave climate, as discussed. The knowledge of the wave field characteristics of the sea-ways the marine structures are designed to work at can be quite handy for the selection of a model that describes well its energy content. Depending on the wave climate, simpler models such as the uni-directional ones can provide similar responses compared to those from the more complete models, in such way that they can be chosen over these latter for the estimation of the desired responses. The sea-state classification for instance, can be handy for the definition of the wave climate for which the models tend to produce similar results. For instance, when dominated wave fields are more likely to occur, meaning either swell or wind-sea is energetically irrelevant, it implies that double-peaked models will naturally turn into single-peaked ones, as the peak which refers to the irrelevant component will show to be negligible. Single and double-peaked models

tend, in this case, to provide similar results, in such way that directional single-peaked models can be preferably chosen over directional double-peaked ones, implying on a more time saving and simplistic modeling. Sea-ways when both components are relevant have to be studied in detail, as the wave climate is locally dependent so that it is expected that in some locations, agreements between simpler e more complete models can be eventually found. Furthermore, it will be shown that more severe conditions often shows good agreement between the models, suggesting that simpler approaches can be adopted for design purposes then for operational ones.

The influence of selecting either a parametric spectra formulation or the full spectrum on both the ship responses and route planning was investigated [1]. One shows that different decisions on route planning can eventually be derived if using the parametric formulation over the full spectra.

Studies on the relevance of multi-modal wave spectra shown that detailed and reliable estimates on the ship responses such as vertical bending moment, shear stresses and accelerations could be derived thanks to wave spectra partitioning into wave components, swell and wind-sea [2]. Aspects such as operational life extension could be approached for a FPSO operating at the North Sea, which heading was found to be dominated by wind-sea waves. Such information would be lost whether the combined wave field was considered, showing therefore the relevance of the wave directionality on the response computations.

Still regarding the relevance of the wave spectra on response estimations, recent studies on the effect of directional dispersion functions over the ship responses have shown that roll can be highly affected although smaller influence is verified about vertical motions such as heave, pich and bow vertical acceleration. The influence of the dispersion function on the ship responses shows, moreover, to vary according to the relative wave direction [3].

The uncertainties related to the sea state spectra shape and transfer function acquisition from linear models could produce uncertainties in the ship response short-term predictions [4], [5]. On regards of the ship transfer functions, linear theories were found to produce underestimated ship responses in typical weather on the North Atlantic while for short-term predictions, the variability of spectral ordinates plays an important role, which is not the case when considering long-term predictions, when the type of spectra shape, meaning P-M spectrum, JONSWAP or double-peaked spectrum have dominant relevance on the variability of the ship responses.

Aside the mentioned studies, the significance of spectra models on the response estimates is such a subject that has not yet been explored deeply by the scientific community, though. The present work aims at verifying the influence of the spectra model over the responses and deriving the relevance of the wave climate on the difference between the models. The particular cases when the usual approach of describing the wave energy spectrum by a simple single-peaked uni-directional parametric model can be reliable for the ship response estimation are intended to be highlighted such as those when a more

complete description of the wave field energy distribution is suggested. The selection of a suitable model shows to be crucial for the reliable response estimations, being important for both the design and operational purposes.

1.1 Objectives and work motivation

An appropriate description of the wave field energy in terms of energy spectrum shows to be crucial to provide reliable estimations of quantities such as induced loads and motions. Even though the frequency (uni-directional) single-peaked model is currently used in the industry for obtaining the ship responses, not well estimated results can eventually be given. The wave field energy is, in this case, inherently fully concentrated at the main wave propagation direction, which whether being high or low excitation directions, over and under-estimated responses can be obtained, respectively, which could be avoided whether using multi-directional models, where the energy directionality is taken into account. The relevance of the wave components over the total wave system might not be overlooked as well, since swell and wind-sea can present quite different periods, propagation directions and energy content, which characteristics are lost whether approaching the problem by considering the wave field to be an average system, as described by the single-peaked models. This work aims at identifying when the ship responses can be computed from simpler models by verifying their variability according to the usage of different parametric models, highlighting the wave climate in which that could be made

Four different models based on the JONSWAP formulation are implemented. They vary on the number of peaks and on the wave energy distribution kind, this latter being either uni or multi-directional distributions. The understanding on the mechanisms associated to the agreement between the models is intended, meaning the characteristics of the wave field for which the models tend produce similar responses. The differences between the outputs from single and double-peaked models are to be assessed in sight of the significance of the wave components over the total wave field. The agreement between uni and multi-directional models is to be analyzed taking into account the relevance of the energy directionality on the wave energy representation for the different wave climates. The ship responses from each model are to be computed over the North Atlantic, so that the differences between them can be assessed in sight of the local wave climate, meaning that the locations where they provided agreeing results can be highlighted. The sea-states for which the simpler models can be chosen over the more complete ones are finally intended to be shown. It is intended, therefore, to show that the wave field energy can be fairly well described by simpler models at specific wave climate conditions, which can be handy from computational time saving and modeling simplicity.

The wave field characteristics such as the H_S, T_m and MWD for the resulting average (total) wave system and for the two components are to be retrieved from the ERA-Interim reanalysis database.

The ship transfer functions are to be obtained numerically from an in-house seakeeping code developed in CENTEC, in which strip theory is implemented to solve the seakeeping problem regarding the potential theory. Good estimations on the RAOs, heave and pitch, specifically, were obtained from the code [6], where a comparative investigation between three codes (the in-house developed one, PDStrip and MaxSurf) and experimental data from two fast displacement hulls in head waves derived from model testing was performed. The quality of the estimations showed though to decrease with the ship forward speed.

The computations are based in a code written in *Python*, in which multiprocessing tools are implemented to increase computational performance, which became significantly handy to perform the heavy calculations associate with the multi-directional models.

1.2 Dissertation structure

In the second chapter, the ship from which are to be computed the transfer functions is described, where are presented the main particulars. An overview describing the relevance of seakeeping analysis on the ship design is presented and the seakeeping problem regarding the potential theory is formulated.

The third chapter presents a brief discussion about the wave generation mechanisms. The JONSWAP frequency spectrum formulation, which all parametric models here used are derived from, is presented. The formulation of the double-peaked parametric models is outlined as well as the procedure about the directional energy spreading method used. The validation procedure of the models used is described and the function implemented to compute θ_H as the relative angle between the ship course and the MWD is presented.

In the fourth chapter, the mechanisms that lead to the differences between the models regarding heave and roll responses are described as well as their relation with the wave climate.

In the fifth chapter, the study of the differences between the models regarding a spatial distribution over the North Atlantic is performed. Comments about the patterns found in the mappings are outlined.

In the sixth chapter, the sea state classification procedure use is described and formulated. The differences regarding conditioned wave fields are analyzed.

Finally, the conclusions are outlined, where considerations about the variability on the ship responses regarding the usage of different parametric models are described. Comments on the relevance of the wave climate over the differences between the models are performed and the cases when the simpler approach is enough accurate on providing reliable responses are highlighted as well as those when the usage of a more compete model is suggested.

Chapter 2

Ship seakeeping

2.1 Seakeeping and ship operability

Marine offshore or coastal structures design is performed taking into account the survival capability to numerous hazard events that they eventually are subjected to, such as collision, fire and heavy-weather. As they are commonly defined as *safety at sea,* or *seaworthiness*, aspects as such are generically related to the safety of people onboard, cargo and hull. Fuel consumption, economical navigation and comfort of crew and passengers, for instance, are, on the other hand, considered *lower violent quantities* related to the ship operability, usually called as *seakindliness* [7].

Even though the correspondent problems of seaworthiness and seakindliness are of different magnitudes, both are strongly related with the ship environmental operability, or *seakeepability*, this latter associated with the responses due to wind waves excitation, such as motions, velocities, accelerations and loads. The seakeepability is inherently related with the wave field characteristics, so that a good description of the sea-ways in terms of spectral energy distribution plays an important role during the design stage, as the structures have to withstand to the environmental loads which they are subjected to. Not only dependent on the wave climate, the ship responses are also affected by the mass distribution, ship speed, heading, hull geometry, which turn to be described by the ship likely behavior at sea, expressed by the ship RAOs. The hull geometry was, by the time when the design processes were not fed with seakeeping recommendations, defined according to economic and geometric aspects, mainly. The hull form was, furthermore, majorly selected on the basis of calm-water performance rather than sustained ship speed on *real wave climate*. Thus, basic performance criteria were practiced and subjects such as speed losses on rough weather navigation were not taken into consideration. Such losses are usually caused by added resistance, decreased propulsive efficiency, slamming, propeller racings, etc. Aside these *involuntary losses*, increased motions amplitudes and accelerations in heavy-sea navigation induced to *voluntary losses*, which are meant to avoid structural damages and unbearable operating conditions onboard. An increased detail on the analysis of seakeeping permitted the design to cover

aspects other than those so far established, such as improved seakeepability related to the dynamic behavior in waves in order to obtain better general performance and environmental operability.

The behavior of the ship in irregular sea-ways as well as the influence of rough weather on the ship operability has been under investigation. Studies about the impact of the waves, heading and loading condition on the attainable ship speed, voyage time and emissions are published, [8]. There are evidences that route planning in terms of rough weather avoidance, for instance, can be beneficial on the attendance of the ship mission and also on the emission reduction.

Considerations about the impact of weather conditions on the ship maneuverability have been outlined as well. The maneuvering capabilities in heavy-weather events depend on the ship type and different adverse weather criteria have been proposed in order to guide the ship design in such way that the vessels could consequently be adequately equipped to face such adverse wave climate, on regards of their own missions and environmental operability. The study developed in [9] highlighted such adverse conditions that the ship design should account for, in particular for tree distinct situations: maneuvering in open sea, maneuvering in coastal waters and low-speed maneuvering in restricted areas. On the first case, the rogue-prone sea-states should be taken into account for model tests and numerical simulations, as sea-states with narrow-banded wave spectrum and high steepness in deep water are likely to produce the so-called rogue, or freak, waves. On the second case, one recommends a modified JONSWAP wave energy spectrum parametric model for finite water depth, to be used for the wave field energy representation. In the last case, wind speed values are suggested for maneuverability criteria in low-forward speed and strong wind for ships with large windage area such as cruisers, RO-ROs and container ships.

The description of the sea-ways in terms of the energy distribution into frequency and direction domains, can affect considerably the results, when computing the ship responses, as they depend on how the wave energy spectrum relates with the RAO. The relative wave direction with which the waves approach the ship plays an important role in such relation. In [2] it was verified that, thanks to the direction partitioning of the 10-yr wave spectra field data into both the swell and wind-sea components, the heading of a particular ship located in the North Sea was dominated by wind-sea waves. Responses such as vertical bending moment, shear stresses and accelerations were derived from such detailed analysis so that structural aspects could be meticulously analyzed, permitting, for instance, operating life extension. Such detailed and crucial heading information would be lost whether the partitioning was not performed, in such way that the wave field would be considered as an average condition resultant from the interaction between the components, which would produce different heading and predicted responses.

The accuracy of numerical models on the prediction of the ship responses in extreme sea state has been recently investigated, since nonlinear responses become quite evidenced in such weather condition [10]. 3D panel method based numerical model predictions are compared with model test results and further,

the effect of the ship forward speed on the ship responses in extreme sea state is investigated. The numerical model showed to provide reasonable results for bending moment at mid-ship although in general linear and nonlinear models slightly underestimate ship motions. The ship forward speed shows to increase the ship responses although different behavior regarding the sagging moment sensibility in low speed is observed in both the model tests and numerical simulations. Further improvements on the wave model are still suggested to be performed.

The detailed description of the dynamic behavior of vessels sailing through irregular sea-ways has shown to be significant, as the ship responses such as motions, velocities, accelerations and loads can be numerically obtained with a fairly good accuracy. These quantities can be used as design variables in order to achieve desired criteria for propulsive performance, shipping efficiency and environmental operability, for instance. Route planning, shipping efficiency, maneuverability and ship responses are some of the aspects affected by the wave climate, which when taken into consideration may lead to benefits such as improved seaworthiness, seakindliness and seakeepability.

2.2 Seakeeping problem and strip theory

To compute the ship responses, both the wave energy spectrum and the ship RAOs are needed. The response spectrum, $S_r(\omega,\theta)$, respectively to an arbitrary response *r,* in terms of both the wave frequency and direction domains can be found as formulated in Equation 1 [11]:

$$S_r(\omega,\theta) = \left|\Phi_{\zeta_w r}(\omega,\theta)\right|^2 \times S_{\zeta_w}(\omega,\theta) \quad (1)$$

The terms are such that $\left|\Phi_{\zeta_w r}(\omega,\theta)\right|$ is the module of the ship transfer function, meaning the RAO, and $S_{\zeta_w}(\omega,\theta)$, the wave energy spectrum, which, for instance, can be expressed in terms of integral parameters (H_S, T_m and MWD) such as by the parametric formulation of the JONSWAP spectrum.

The RAO is the complex amplitude of the motion respectively to an arbitrary mode, in response to an incident wave of unitary amplitude, with defined frequency and main direction [12].

RAOs are usually obtained either experimentally from tests in model basins or can be determined computationally, by solving the seakeeping problem with numerical methods such as Strip Theory. This latter methodology is the most commonly used in ship response analysis, and the one applied in this work.

The definition of the fluid loads acting upon a floating structure performing harmonic oscillatory motions and the motion amplitudes, transfer functions and other measurements of interest, define the seakeeping problem. The fluid is considered to be ideal, meaning incompressible, inviscid, irrotational and without surface tension. Incident harmonic waves are present and the water depth is finite. The linearized Bernoulli equation is applied to compute the fluid pressures on the body surface. Such linearization is possible due to the assumption of small amplitudes and motion velocities. The Bernoulli equation depends on the solution of the velocity potential of the fluid.

The velocity potential can be expressed in terms of three components, as by Equation 2:

$$\phi(x, y, z, t) = \phi_r + \phi_w + \phi_d \tag{2}$$

Respectively:

- ϕ_r, the so-called radiation potential, which represents the disturbances in the fluid due to the oscillatory motion of the body.
- ϕ_w, the velocity potential associated to the incident harmonic waves, called undisturbed wave potential.
- ϕ_d, the diffraction potential, which represents the velocity potential of the fluid associated to the diffracted waves by the body, in case of fixed condition.

The solution of the total velocity potential, expressed in the left hand of Equation 2, must satisfy a set of boundary conditions. Furthermore, the imposition of the mass conservation of the fluid is performed, which, regarding the potential theory, turns to be expressed by the Laplace Equation as follows:

$$\nabla^2\phi = \frac{\partial^2\phi}{\partial x^2} + \frac{\partial^2\phi}{\partial y^2} + \frac{\partial^2\phi}{\partial z^2} = 0 \tag{3}$$

The seakeeping problem can be solved computationally, making usage of the strip theory numerical method, for instance. In this case, the 3D hydrodynamic problem is simplified into a set of 2D hydrodynamic problems**.** The strip theory is suitably applicable for slender bodies, which in practice means $B/L \ll 1$. The hull is divided into a finite number of strips which are rigidly connected to each other. The shape of the strips resembles the shape of the part of the hull that they represent. Each strip is considered to be a section of infinitely long floating cylinder from the hydrodynamic point of view. This latter assumption yields that both waves, those generated by the hull oscillatory motions and the diffracted ones, travel perpendicularly to the hull longitudinal plane.

The numerical solution of the seakeeping problem is to be obtained from an in-house code, which a simplified partially non-linear time domain approach showed to provide reliable vertical responses of the S-175 containership in head waves compared with experimental data [13]. The code is based on

Salvensen Tuck & Faltinsen method [14]. Additionally, for the acquisition of the roll transfer function, an additional viscous-damping is required, which is estimated by usage of the Miller method [15].

The description of the hull in terms of a set of transverse sections is required by the program. The definition of the desired frequency domain for the acquisition of the ship transfer functions is needed so as the relative wave directions and the set of forward speeds. The ship body's constants are also to be introduced such as structural moments of inertia, vertical and longitudinal positions of the center of gravity and the transverse metacentric height.

2.3 Ship description

The ship selected is the S-175 container ship due to the considerable number of works already published in which this hull is object of study as for seakeeping analysis such as those carried out during the 15th International Towing Tank Conference (ITTC) in which a comparative numerical study is performed on motion prediction [16], or for loads assessment [13] when nonlinear responses are compared with published experimental data,.

The container ship main particulars are presented in Table 1 and the bodylines, in Figure 1.

Table 1. S-175 container ship main particulars

Length between perpendiculars	L_{pp} [m]	175
Beam	B [m]	25.4
Depth	D [m]	15.4
Draft	T [m]	9.5
Displacement	Δ [ton]	24742
Longitudinal position of CG	LCG [m]	-2.43

Both the heave and roll transfer functions are to be obtained from the seakeeping code. The in-house code input file is prepared, in which the submerged hull is described. The ship forward speed is hereafter considered to be such that $F_n = 0.2$, meaning, approximately 16 knots. Ship courses in a range with step of 10 degrees from $0°$ to $180°$ are implemented to obtain the RAOs. The heave and roll RAOs are displayed in Figure 2.

Other quantities with high level of importance for ship operations such as relative vertical motion, vertical acceleration and vertical bending moment were intended to be analyzed, although it was decided to

restrict the analysis to heave and roll motions only due to the high computational effort that would be required.

Results on pitch motions were also assessed, although a certain similarity with those on heave was verified, in such way the first one was decided to not be included in the further analysis presented in this work.

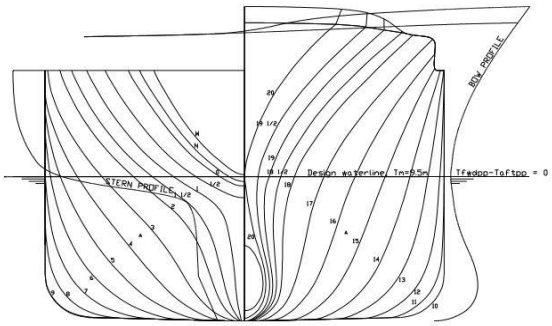

Figure 1. S-175 container ship bodylines. Picture from [13]

A)

B)

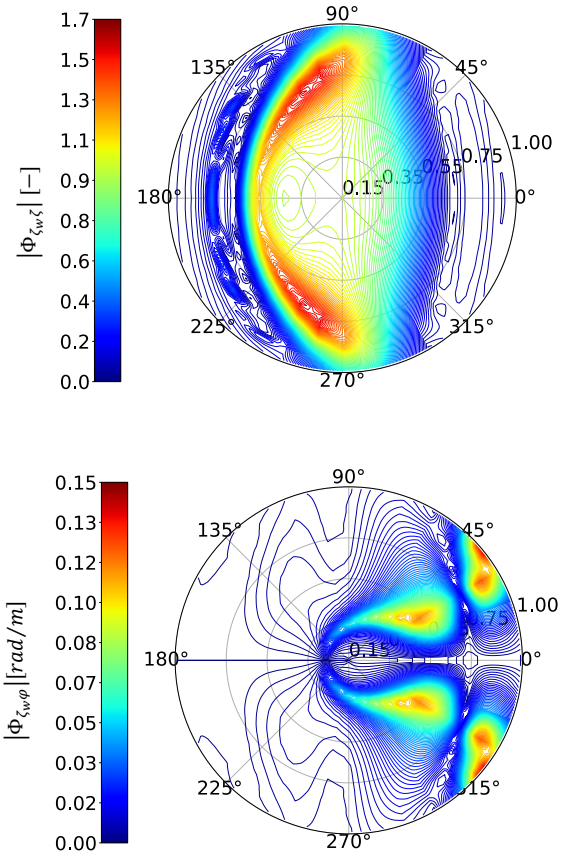

Figure 2. S175 container ship RAOs. A) Heave RAO, B) Roll RAO – Frequency range [0.15 – 1.0 rad/s]

Chapter 3

Wave spectra models and formulations

3.1 Wave generation mechanisms and wave climatology

Before describing the spectra parametric models, a discussion on the physical mechanisms regarding wind waves generation is outlined, as a general understanding of the processes involved on the scenario of wave excitations upon man-made marine structures and the inherent consequences from the point of view of motions and loads generation come to be important. Such discussion is made based on the unified theory of Miles [17] and Phillips [18], which describe two wind waves generation mechanisms, the so-called Miles-Phillips Mechanism. The first mechanism is associated with the generation of tiny ripples on the water surface, which are called *capillary waves*, while the second one drives for the generation of the *gravity waves*.

Capillary waves are tiny perturbations on the water surface in contact with wind. Since such small waves are not largely affected by gravity action, the main mechanism responsible for recovering the sea surface to the mean level is the liquid surface tension, which can be called as capillary action. The presence of capillary waves is the starting point for the generation of gravity waves as they increase the roughness of the sea surface, which strengthen its interaction with the wind. Capillary waves usually have period lower than 0.1 s while gravity waves present periods that can vary in a range from 1 to 30 seconds [19]. The action of gravity is the restoring mechanism that drives the water surface to the mean level about that latter wave modality, as they present higher wave amplitudes.

Wind waves, which are commonly generated through the mechanisms described, can be classified into two basic components: swell and wind-sea waves.

- Wind-sea waves: as described in [11], wind-sea is a train of waves driven by the prevailing local wind field. They are mostly formed by short-crested waves, which crest length is two or three-fold the apparent wave length. Crests are found to be sharp and individual wave crests can propagate towards different directions. A train of wind-sea waves can be quite irregular in terms of wave period and amplitude.

- Swell waves: is a train of waves that have propagated out of the area where they were generated and for that reason they no longer depend on the local wind to exist and can propagate through large distances [20]. In its aspect, swell waves are more uniform in terms of period and wave height. Crests are more rounded compared to those seen in wind-sea waves. Additionally, there are evidences that the JONSWAP frequency spectrum can well describe a swell wave system energy distribution if compared with measured raw swell spectrum [21].

In wave climatology, the global geographical distributions of the wave components aforementioned as well as their frequency of occurrence and relevance on the global wave field are under continuously investigation. Past studies, as such those presented in [22], investigated the seasonal variability of the global ocean and wind wave climate by using satellite altimetry and models hindcast. Some results as the global distribution of the wave height field and wind characteristics were obtained, showing, for instance, that the H_S tends to increase in higher latitudes and wave climate progressively moderates while approaching the Equator. Such studies, however, were mostly based on two main wave field characteristics, the H_S and the T_m. The inclusion of the directionality through the *MWD*, as shown in [23], brought to the wave climatology results even more accurate as for instance in cases when swell and wind-sea show to present significant different propagation direction. The energy distribution representation of the resulting average wave system, in this case, by a multi-directional single-peaked model can differ substantially from the one obtained by the double-peaked modeling, where the energy spreading of each component is suitably performed about their correspondent MWD. The separation of the wave spectra field into two components, swell and wind-sea, and the estimation of the correspondent three main characteristics via spectral integration provide a better understanding of the wave climate variability mechanisms, as swell and wind-sea waves are affected by wind changes in different scales.

When comparing the relevance of these two wave components on the global wave field, it is found that this latter is considered to be swell-dominated, in terms of frequency of occurrence, [23]. The frequency of occurrence calculation of both wave components was performed taking into account the formulation proposed in [24], which relates the peak wave phase speed with the 10-m wind velocity. Even in extratropical areas where severe wave climate is likely to be found (usually wind-sea dominated wave fields are commonly observed in storm events), the wave fields tend in general to be swell-dominated. Also, the variability of the seasonal means of the wave field characteristics was studied and the conclusion is that the interannual variability of swell and wind-sea is strongly associated with the variations on the atmospheric forcing. In both the North Atlantic and the North Pacific oceans, wind velocities are higher during the hemispheric winter and so are the wave heights, while on the Southern Ocean, the wind velocity does not suffer such a big variability and, consequently, the wave heights.

The study of the wave climatology has many practical applications in marine engineering as the understanding of the global wave field characteristics in terms of spatial distribution and time variability are of important knowledge for the design of offshore and coastal structures. Even though weather

forecasting is not perfectly accurate due to the stochastic nature of the variables from which the global climate is dependent, recognizing climate patterns can be critical for the prediction of induced wave loads and motions, for instance. As wave adverse conditions can be harmful for marine structures and for the vessels operability, commonly rough weather avoidance is practiced, which, in long term, influences on the general wave climate experienced by oceangoing vessels, such as reductions on the H_S experienced by the vessels during the operating life [25].

The next sections describe the formulation of the wave spectra models implemented. The models vary on the number of peaks as well as on the wave energy distribution type. The wave field can either be described in terms of the resulting average wave system or in terms of the separate components, which, hereafter, are respectively to be called as single and double-peaked formulations. The energy distribution types are either performed only about the frequency domain (called as frequency or uni-directional model) or about both the frequency and directional domains (called as directional or multi-directional models). The simpler model constitutes of a single-peaked frequency (uni-directional) spectrum (1D1P) while the following constitutes of a double-peaked frequency spectrum (1D2P). The directional spectra, as well as in the first case, constitute of single and double-peaked models, 2D1P and 2D2P, respectively

3.2 The JONSWAP spectrum

Over the last decades, the scientific community has worked on wave statistics to adequately predict ship motions and wave loads acting upon man-made structures in order to feed design processes with increasingly detailed information to, for instance, prevent accidents eventually caused by under-estimation of the environmental scenario and its direct impact over the marine structures. The responses can be estimated if known the correspondent RAOs and the energy spectrum. This latter can be obtained, for instance, from the free-surface elevation time record of a single fixed location, applying a Fourrier analysis [11].

In 1964, Pierson and Moskowitz [24] presented for a fully developed sea-state the uni-directional wave energy spectrum (P-M Spectrum). Developing seas, however, were found to have a more peaked shape, which came to be better described by the JONSWAP Spectrum, where the dependency on the wind speed and fetch was introduced, as proposed by the formulation shown in [26]. This latter is considered to be a generalization of the P-M Spectrum through the introduction of the mentioned parameters, and particularly when the so-called peak enhancement factor equals 1, it simplifies into the P-M formulation.

In 1976, the parametrization of the former JONSWAP spectrum was proposed in terms of H_S and T_m [27]. This latter formulation is used in this work to describe the wave energy distribution into the frequency domain (and further distribution into the directional domain is to be performed over this model in order to obtain the directional ones), with which the ship responses are to be computed. In Equation 4 the JONSWAP parametric frequency spectrum is presented.

$$S_{\zeta_w}(f) = 0.11 H_v^2 T_v (T_v f)^{-5} \exp[-0.44(T_v f)^{-4}]\, F_1^{-1} \gamma^{\exp\left[-\frac{1}{2\sigma^2}(1.296 f T_v - 1)^2\right]} \quad (4)$$

The terms are:

- $H_v = \frac{H_S}{\sqrt{F_1}}$, where H_s is the significant wave height in m;
- $T_v = \frac{T_m}{F_2}$, where T_m is the average period, according to [27] and [28], based on the first moment, meaning that $T_m = \left(\frac{1}{2\pi}\right)\left(\frac{m_0}{m_1}\right)$, where m_0 and m_1 are the spectral moments of order 0 and 1, respectively;
- F_1 and F_2 are correction factors for area and peak period of a P-M frequency spectrum, respectively;
- γ is the JONSWAP peak enhancement factor, and for the "average JONSWAP spectrum" is considered to be such that $\gamma = 3.3$, moreover, whether the factor equals 1, the spectrum turns to be the same as the P-M one;
- σ is a parameter associated to the peak width, which is defined as follows:

$$\begin{cases} \sigma = 0.07 \; for \; f \leq \dfrac{1}{1.296 T_v} \\ \sigma = 0.09 \; for \; f > \dfrac{1}{1.296 T_v} \end{cases} \quad (5)$$

About the definition of the correction factors F_1 and F_2, it is shown in [27] their dependence on the peak enhancement factor. A sample of values are provided in Table 2, where the variability of these factors according to γ is verified.

Table 2. Values of parameters F_1 and F_2 of the JONSWAP Spectrum as function of γ.

$\boldsymbol{\gamma}$	$F_1 = \frac{m_{0,JONSWAP}}{m_{0,P-M}}$	$F_2 = \frac{(m_0/m_1)_{JONSWAP}}{(m_0/m_1)_{P-M}}$
1	1	1
2	1.24	0.95
3	1.46	0.93
3.3	1.52	0.92
4	1.66	0.91
5	1.86	0.9
6	2.04	0.89

In this work, the values of F_1 and F_2 are assumed to be those in which the *average* JONSWAP spectrum is considered ($\gamma = 3.3$), hence $F_1 = 1.52$ and $F_2 = 0.92$. According to Equation 4, the frequency domain is in s^{-1} although hereafter the domain is considered to be expressed in rad/s. Hence, it is necessary to transform the original domain into the desired one as follows:

$$\int S_{\zeta_w}(\omega)d\omega = \int S_{\zeta_w}(f)df \tag{6}$$

Knowing that:

$$d\omega = 2\pi df \tag{7}$$

Then:

$$\int 2\pi S_{\zeta_w}(\omega)df = \int S_{\zeta_w}(f)df \tag{8}$$

Finally, the JONSWAP parametric spectrum in which the frequency domain is expressed in rad/s is given by:

$$S_{\zeta_w}(\omega) = \frac{S_{\zeta_w}(f)}{2\pi} \tag{9}$$

Equation 9 is a parametric formulation of the single-peaked frequency spectrum of a given sea-state.

3.3 Double-peaked parametric model

Assuming the energy spectrum to be single-peaked can eventually be inadequate to suitably represent the wave field energy, as it describes the energy distribution of a resulting average wave system, in such way that the separate contribution of each wave component (swell and wind-sea) is not considered. Depending on the wave climate, both swell and wind-sea can be equally relevant about the total wave field energy in such way that this information as well as the correspondent peak frequencies of each wave component are lost whether considering single-peaked formulation. Even worse, the peak of the spectrum assessed with the single-peak model, can be located relatively far from the ranges of frequencies where there is the highest concentration of energy. This can significantly distort the results that are sensitive to the vicinity of the wave energy to the natural frequency of the motions. As described in [28], some measured spectrum from the Utsira Coastal Station in the North Atlantic during stormy conditions exhibited double-peaked spectra. This occurs when the sea-state results from the interaction of swell and wind-sea waves or when the wind direction changes, producing a developing sea-state. Modeling these events with single-peaked formulation consists in considering the wave field to be an average condition from the interaction between the components. Quite different spectra shape can be

observed in this case when comparing single and double-peaked models so that the way they relate with the RAOs can also diverge, which eventually produces disagreeing responses.

In that way, the double-peaked spectral modeling can be expressed by the sum of two JONSWAP spectra models. Considering swell ($S_{\zeta_w,S}$) and wind-sea waves ($S_{\zeta_w,W}$) as the possible wave components of the wave field system, the total spectrum can be expressed by:

$$S_{\zeta_w}(\omega) = S_{\zeta_w,S}(\omega) + S_{\zeta_w,W}(\omega) \tag{10}$$

Both the swell and wind-sea components are to be formulated according to Equation 9, introducing the correspondent H_S, T_m and MWD.

3.4 Directional energy distribution

The frequency (uni-directional) spectra can be spread into the direction domain, yielding the directional spectrum. Considering a JONSWAP frequency spectrum $S_{\zeta_w}(\omega)$ as expressed in Equation 9, the directional distribution is performed by weighting it with a probability distribution function [29] as follows:

$$S_{\zeta_w}(\omega,\theta) = D(\theta|s,\theta_W).S_{\zeta_w}(\omega) \tag{11}$$

The term $D(\theta|s,\theta_w)$ is defined as *direction dispersion function*. It represents the wave energy distribution at a given frequency into the direction domain around the main propagation direction, θ_{max}. This function holds that:

$$\int D(\theta|s,\theta_W)d\theta = 1 \tag{12}$$

It is, furthermore, formulated as follows:

$$D(\theta|s,\theta_W) = \frac{2^{2s-1}\Gamma(s+1)\Gamma(s)}{\pi\Gamma(2s)}\cos^{2s}(\theta-\theta_W) \tag{13}$$

Where:

- s is the factor of the dispersion function, in this work, considered to be 1;
- θ_W is the dominant wave propagation direction;
- $\Gamma(s)$ is the Gamma Function.

It is important to mention that:

$$|\theta - \theta_{max}| \leq \pi/2 \tag{14}$$

The factor of the dispersion function, *s*, may assume different values for swell and wind-sea, as these two components present quite different directionality, inherently associated to their generation mechanisms. Wind-sea is more commonly to be found propagating in different directions while swell waves usually propagate towards a fairly defined one. The energy directionality of both components at a single point can present, therefore, different distributions. The ship responses are to be, however, computed over a grid of points on the North Atlantic, in such way that the definition of the suitable dispersion factor for each point comes to be impractical, then one assumes the same value for both wave components. Further investigations on the influence of the dispersion factor on the responses may be, nevertheless, requited.

3.5 Ocean-wave data

The representation of the energy spectrum is made through the models so far presented. The H_S, T_m and MWDs of the combined wave field and components, swell and wind-sea, are, therefore, the main ocean-wave data required as prior information. These data are retrieved from the ERA-Interim database, which is an ocean atmospheric reanalysis provided by the European Centre of Medium-Range Weather Forecasts (ECMWF) [30]. Environmental data estimates are performed by combination of data assimilated majorly from satellite observations and prior information from a forecast model. Ocean surface analysis in terms of wave height are performed using observations from space-born radar altimeters and background estimates from such model, which describes the evolution of two-dimensional wave spectrum at the sea surface, considering the contribution of swell and wind-sea waves. The analyzed wave heights are used to continuously adjust the model-predicted wave spectra. A 6-hourly global ocean-wave data from 2017 is retrieved and used in this work.

The forecast model is composed by a set of equations that describe some of the physical aspects associated to climatology in general. The interaction between the global atmosphere and the ocean surface is one of the aspects that this work is most involved with. Locally observed parameters are extrapolated forward in time from the forecast model equations, providing estimates of the desired quantities. The quality of the physical meaning of the estimates inherently depends on the accuracy of the model and on the goodness of the prior observed data.

The spectra representation of the atmospheric dynamic variables constitutes the main role of the atmospheric model on the estimates. The impact of ocean waves on the airflow via transfer of energy and momentum is the main focus of the ocean waves forecast model, on the other hand. Atmospheric

variables that influence the wave growth are introduced to this latter. The consequential impact of the resulting sea-state on the ocean surface roughness is the output of the process.

The wave model is based on the WAM approach. This latter was introduce to the Integrated Forecast System (IFS) and was the first one on solving the energy balance equation, in which nonlinear wave interactions were included. Compared with two other wave hindcasts, HIPOCAS (WAM based model) and NOOA/CFSR (WAVEWATCH based model), ERA-Interim shows to provide similar estimations of the wave height in less severe wave climate while higher disagreement between the models can be verified in extreme conditions (mid-high latitudes on the North Atlantic) [31]. Furthermore, comparing ERA-Interim wave height estimations to satellite observed data, in non-extreme climate, lower deviations are derived if compared to the remaining models while in extreme conditions, the best precision is observed.

A code developed in *Python* was specially implemented for downloading the wave data from the ERA-Interim server.

3.6 Model verification

The goodness of the models presented so far on the representation of the wave field energy have to be verified, as for the physical meaning of the estimated ship responses a good description of the sea-state energy shows to be crucial. The moment of zero order can be used for the estimation of the H_S, which this latter was used as prior wave field information for the model construction itself. That parameter can be estimated and compared to the one that fed the model, so that the model consistency can be verified.

The moment of i^{th} order, m_i, of the spectral curve are computed, as shown in [11], according to the following expression:

$$m_i = \int_0^\infty w^i S(\omega) d\omega \tag{15}$$

Equation 15 yields the spectrum moment of i^{th} order respectively to the frequency spectrum, only. Whether the directional spectrum is considered, Equation 16 is used instead:

$$m_i = \int_0^{2\pi} \int_0^\infty w^i S(\omega, \theta) d\omega d\theta \tag{16}$$

The spectral moments computed either by Equation 15 or 16, in case considering order 0, 2 or 4, represent respectively the:

- Variance of the wave elevation displacement;
- Variance of the wave elevation velocity;
- Variance of the wave elevation acceleration.

According to [11], the H_s (meaning twofold the mean value of the highest one-third part of the amplitudes recorded, $H_{1/3}$) can be estimated from the expression below:

$$H_s = 4.0\sqrt{m_0} \tag{17}$$

The square root of the zero order moment is frequently called as the Root Mean Square (RMS). The equation can be rewritten as: $H_s = 4.0 \times RMS$, therefore. The general verification procedure follows with the estimation of H_s according to Equation 17, which m_0 results from the integration of the spectral curve respectively to the correspondent model. The estimated and retrieved H_S are plotted in charts, in order to give a visual evidence of such comparison. Graphical representation of the general verification procedure can be seen in Figure 3.

The verification focus on the wave data recorded from the month of January of 2017. The point in analysis is located in Azores, which GPS coordinates are 40º N, 26º W. Figure 4 displays both estimated (Equation 17) and retrieved H_S about the 1D1P, 1D2P, 2D1P and 2D2P models, at A, B, C and D, respectively. It is clear that the models can represent well the energy content of the sea-state. The responses can be computed and the models compared to each other as to highlight the main differences between the outputs, then.

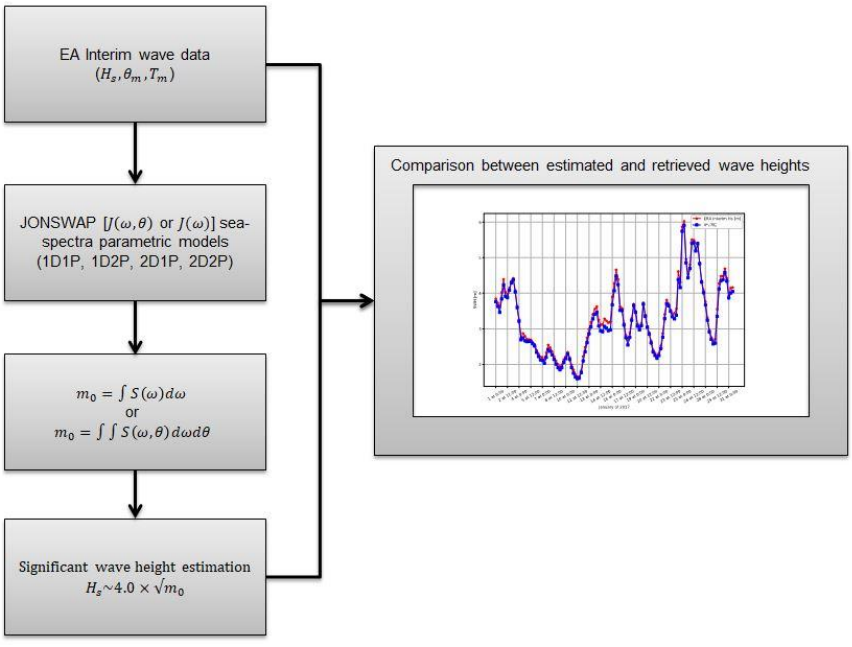

Figure 3. Parametric models verification procedure

3.7 Relative wave direction function

It is crucial to implement a function that can relate both the ship course and the main wave propagation direction in order to obtain the relative angle between these two, with which the waves approach the ship on regards of an appropriate convention. This relative direction is usually called as *relative wave direction*. Usually one assumes $0°$ for following waves and $180°$ for head waves.

According to [32], the main wave propagation direction convention follows the meteorological one. In that way, $0°$ means “waves coming from North” while $90°$ means “waves coming from East”. On the other hand, the ship course convention adopted implies that $0°$ means “ship sailing towards North” while $90°$ means “ship sailing towards East”. In essence, the procedure firstly translates the main wave propagation direction convention into the ship course one and secondly the relative angle between these two is computed. The conversion of this latter into the appropriate convention is performed, yielding finally the relative wave direction.

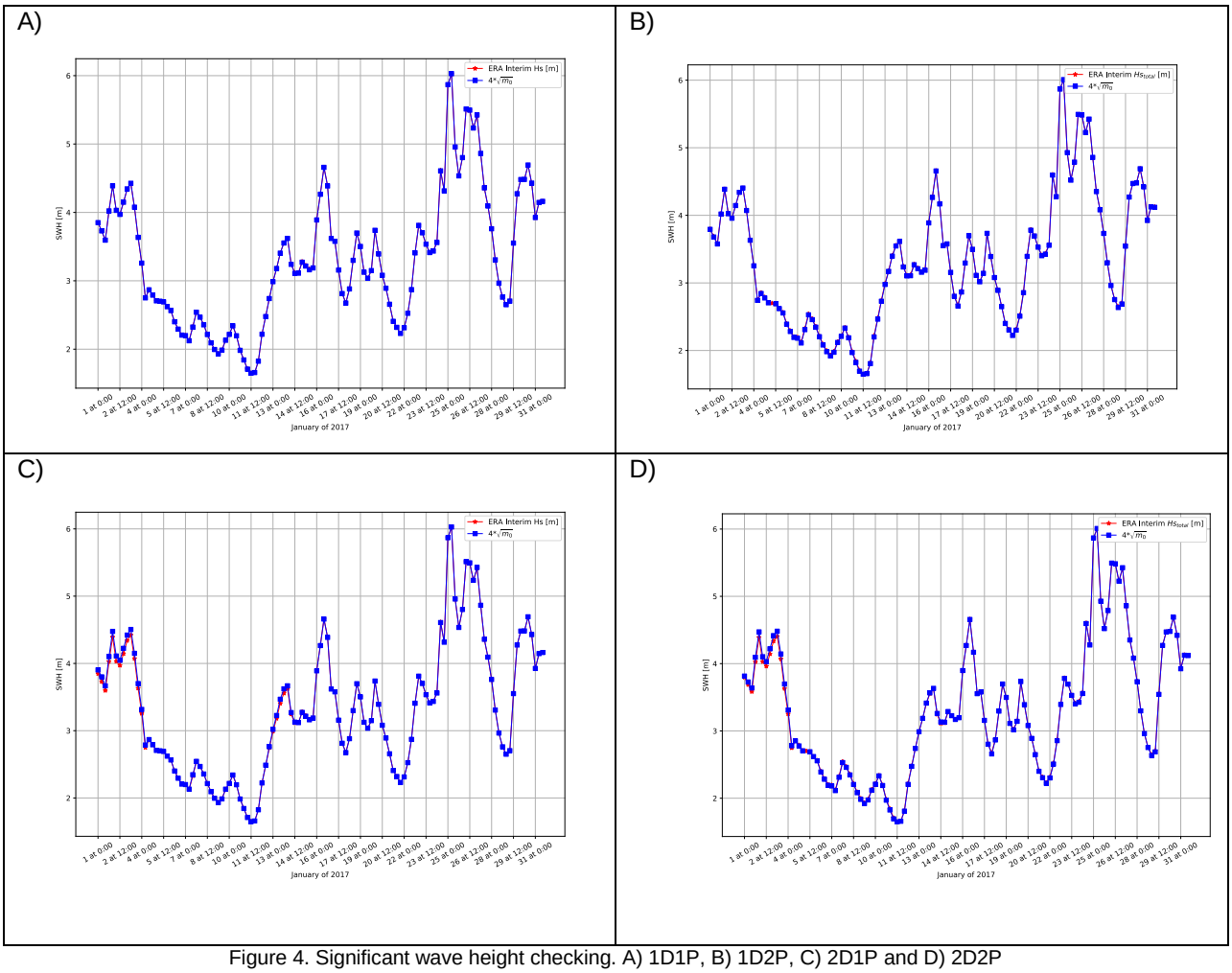

Figure 4. Significant wave height checking. A) 1D1P, B) 1D2P, C) 2D1P and D) 2D2P

Chapter 4

Responses to different spectra models

4.1 Heave response

In this section, some differences between the outputs of the parametric models on heave motion are highlighted. The objective is to verify what they are related to, regarding the influence of the wave climate on the relation between the wave energy spectrum and the RAOs.

In Figure 5, are displayed the significant amplitudes of heave, $\zeta_s = 2 * \sqrt{m_0}$, during the month of January of 2017. The wave data, which the spectral models are related to, are from a point near to the Azores archipelago (GPS coordinates: 40º N, 26º W). The ship is sailing at $F_n = 0.2$, service speed at, approximately, 16 knots and course of 45 degrees, North-East direction.

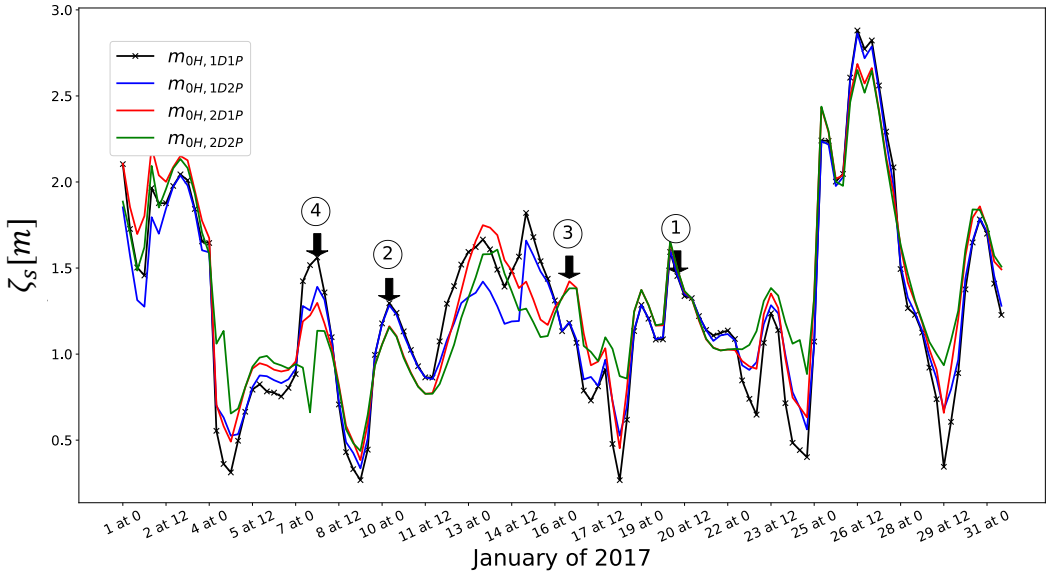

Figure 5. Cases highlighted for heave response

As can be noticed in Figure 5, in several cases the parametric models provide different heave responses. As to figure out some of the possible causes that lead to such differences, four characteristic dates in which the models presented peculiar features are identified (they are highlighted in the chart with arrows

and numbers), so that a correlation between the different representations of the wave energy distribution and the eventual disagreement between the models can be outlined. The wave field main characteristics (significant wave height, H_s, average wave period based on the first moment, $T_{\frac{m_0}{m_1}}$, and mean wave direction, θ_w (this latter according to the meteorological convention [32]) for the highlighted dates are provided in Table 3 about the combined wave system and for the wave components, swell and wind-sea.

Table 3. Main wave data for the dates highlighted about heave response

	H_s [m]			$T_{\frac{m_0}{m_1}}$ [s]			θ_w [deg]		
Date	Combined Wave System (H_S)	Swell Waves (H_S^S)	Wind Sea Waves (H_S^{WW})	Combined Wave System (T_m)	Swell Waves (T_m^S)	Wind Sea Waves (T_m^{WW})	Combined Wave System (θ_W)	Swell Waves (θ_W^S)	Wind Sea Waves (θ_W^{WW})
20/1/2017 06:00 (1)	3.42	3.41	0.17	10.8	10.9	2.65	287	287	288
10/1/2017 06:00 (2)	2.39	2.38	0.21	9.59	9.89	2.16	320	72	320
16/1/2017 12:00 (3)	3.76	1.71	3.35	7.27	9.80	6.81	161	234	158
7/1/2017 18:00 (4)	2.68	2.46	1.04	7.45	8.76	4.05	123	142	100

The *Combined Wave System* represents the resulting wave field from interaction of both swell and wind-sea components. The representation of wave data about swell or wind-sea waves is made by including the superscripts S and WW, respectively. Thus, H_S^S and H_S^{WW} are the significant wave height for swell and wind-sea, respectively. The same is applied for the remaining parameters (T_m and MWD).

Hereafter, a wave component is considered *negligible* if the ratio between the energy carried by that component is lower than 10% of the total spectral energy, such that, with regards to wind-sea:

$$\left(\frac{H_S^{WW}}{H_S}\right)^2 < 0.1 \tag{18}$$

4.1.1 Date (1) – Responses to swell waves: Case 1

Wind-sea waves are considered to be negligible, as $\left(\frac{H_S^{WW}}{H_S}\right)^2 = 0.002$. As seen in Table 4, the combined wave field H_S, T_m and MWD are similar to those of the swell component. The significant wave height of the first system is $H_S = 3.42$ [m] while the latter one is $H_S^S = 3.41$ [m]. The average wave periods are $T_m = 10.84$ [s] and $T_m^S = 10.92$ [s] while the MWD are $\theta_W = 287$ [deg] and $\theta_W^S = 287$ [deg].

Table 4. Main wave data about Date (1) for heave response

	H_s [m]			$T_{\frac{m_0}{m_1}}$ [s]			θ_w [deg]		
Date	Combined Wave System (H_S)	Swell Waves (H_S^S)	Wind Sea Waves (H_S^{WW})	Combined Wave System (T_m)	Swell Waves (T_m^S)	Wind Sea Waves (T_m^{WW})	Combined Wave System (θ_W)	Swell Waves (θ_W^S)	Wind Sea Waves (θ_W^{WW})
20/1/2017 06:00 (1)	3.42	3.42	0.17	10.84	10.92	2.65	287	287	288

A visual comparison between the uni-directional spectra parametric models is shown in Figure 6. The heave RAO is displayed in the same chart. The textbox provides the wave data of the combined wave field and of both swell and wind-sea.

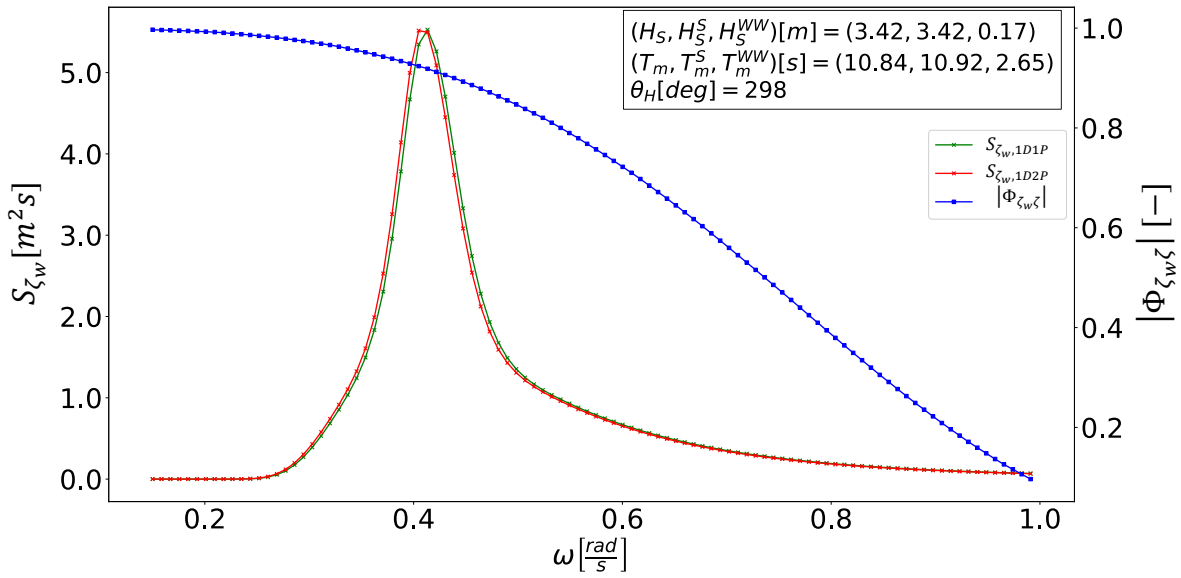

Figure 6. Date (1) – Wave spectra and Heave RAO, 1D models comparison

The comparison between the response spectra is displayed in Figure 7. The textbox indicates the values of the significant heave amplitudes.

The multi-directional energy spectra are presented in Figure 8.A and Figure 8.B about the 2D1P and 2D2P models, respectively. The directional heave RAO is displayed in Figure 8.C and the response spectrum about both models are shown in Figure 8.E and Figure 8.F.

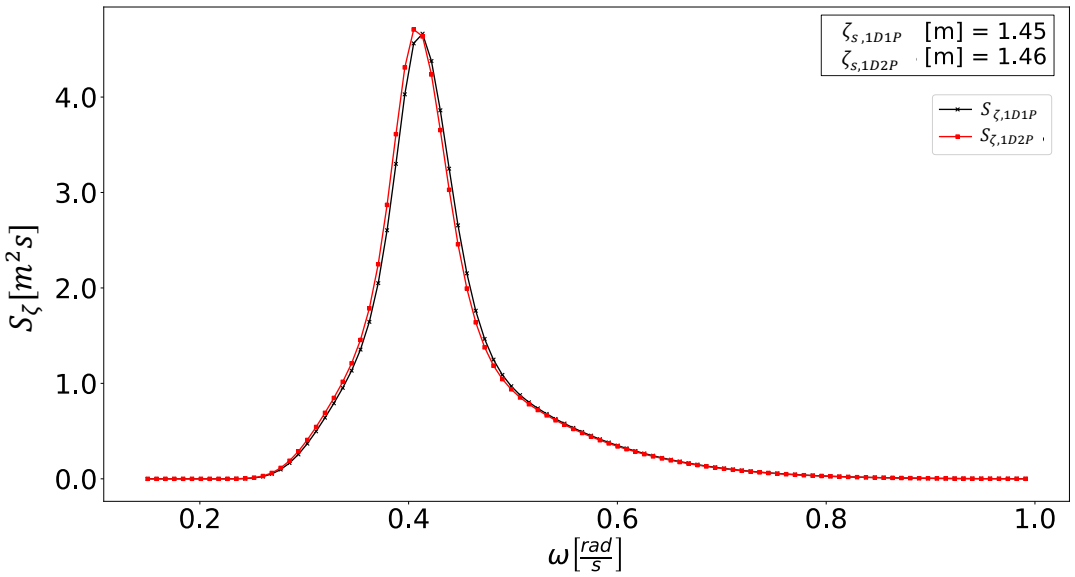

Figure 7. Date (1) – Heave response spectra, 1D models comparison

The wave energy distributions are similar about the frequency spectra models (1D) as well as about the direction ones (2D), as seen in Figure 6 and both Figure 8.A and Figure 8.B, respectively. That comes from the fact that the part of the energy content carried by wind-sea waves is irrelevant compared to the contribution of swell over the total energy. As the average system is basically composed by swell, both the 1P and 2P models end up, in practical terms, to represent the wave energy distribution of that unique wave component. For cases in which one wave component is considered to be negligible, the single and double-peaked models tend to be practically coincident, then similar results can be expected. The significant amplitudes of the frequency models are $\zeta_{s,1D1P} = 1.45$ [m] and $\zeta_{s,1D2P} = 1.46$ [m], and the amplitudes about the directional ones are $\zeta_{s,2D1P} = 1.49$ [m] and $\zeta_{s,2D2P} = 1.50$ [m]. As expected, single and double-peaked models slightly differ from each other, but such differences can be neglected in practical applications.

Frequency and directional models differ by the fact that these latter considers, additionally to the frequency distribution, the energy distribution into the direction domain. Frequency (uni-directional) models concentrate the wave field energy at the wave main propagation direction while directional (multi-directional) ones, on the other hand, spread the wave energy about that direction. Depending on θ_H, frequency models can either produce over or under-estimated responses, as either that concentrated energy is substantially amplified (if θ_H is a high excitation direction) or is "damped" by the RAO (if θ_H is a low excitation direction). For instance, it is known that *beam waves* are, in general, prejudicial for roll motion (high excitation direction), while roll excitations by *following waves* are substantially lessened (low excitation direction). Whether computing the ship responses using frequency models, which inherently concentrate the wave field energy at the propagation direction, over-estimations are expected to be obtained if the ship is approached from high excitation directions, as the total energy will be considered to

be given at that direction, and so on. Nevertheless, similar results are still possible, as obtained in this case. The differences between frequency and directional models depend, therefore, strongly on the relation between the wave energy spectrum and the RAO, where θ_H plays quite an important role.

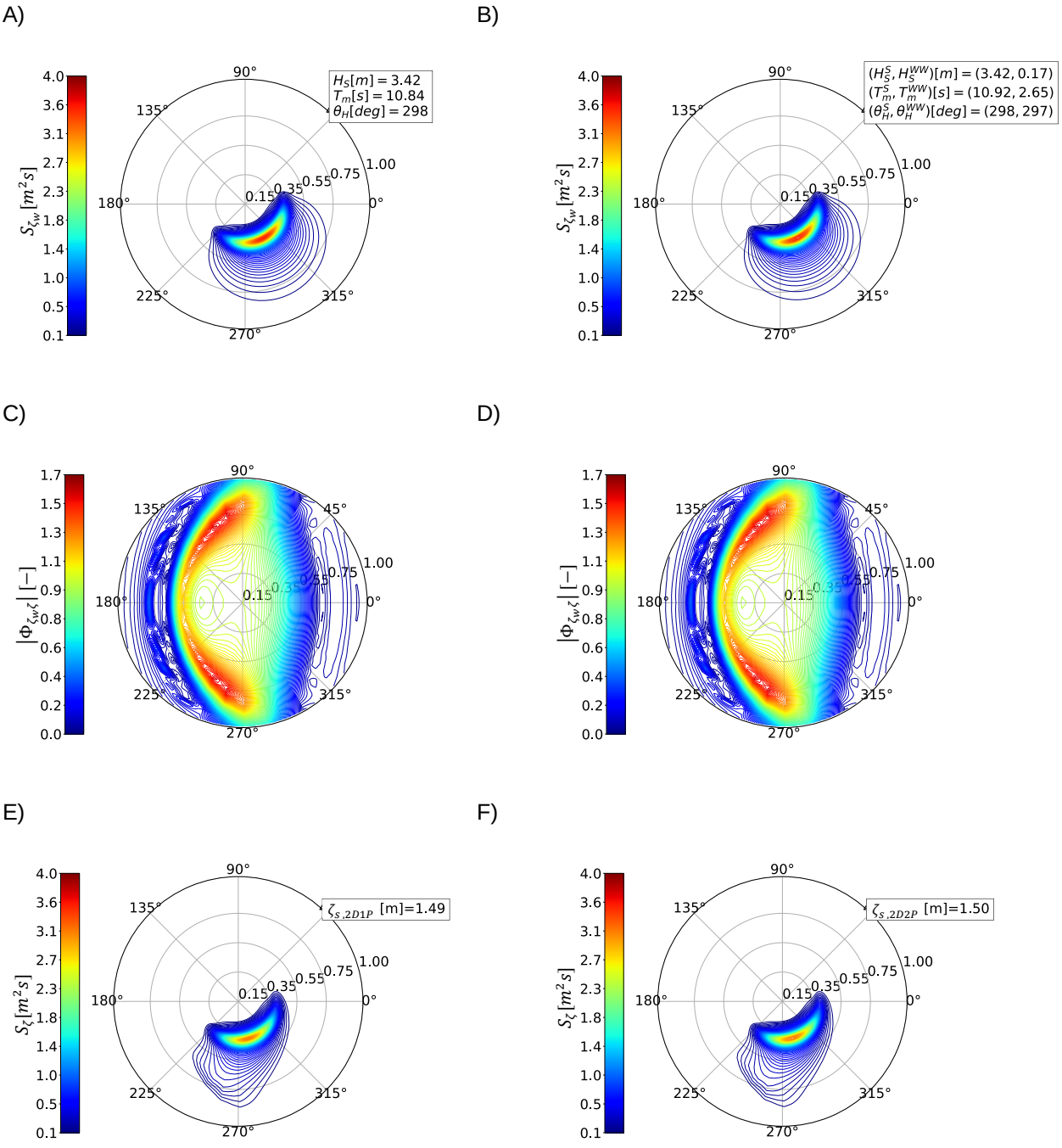

Figure 8. Directional spectra models (2D1P and 2D2P) for date (1) on the heave response. A) and B) are the wave spectrum about the 2D1P and 2D2P models, respectively. C) and D) are the heave RAO and E) and F) are the heave response spectra about 2D1P and 2D2P models, respectively.

The differences between single and double-peaked models, regarding the same energy distribution, mostly depend on the significance of the wave components over the total energy, on the other hand, as it has been shown that if one component is negligible, both models are expected to provide similar results. Not only depending on the stochastic nature of the wave climate but also on the relation between the energy spectrum and the RAO, the difference between frequency and directional models comes, therefore, to be hardly predicted.

4.1.2 Date (2) – Responses to swell waves: Case 2

Table 5. Main wave data about Date (2) for heave response

Date	H_s [m]			$T_{\frac{m_0}{m_1}}$ [s]			θ_w [deg]		
	Combined Wave System (H_S)	Swell Waves (H_S^S)	Wind Sea Waves (H_S^{WW})	Combined Wave System (T_m)	Swell Waves (T_m^S)	Wind Sea Waves (T_m^{WW})	Combined Wave System (θ_W)	Swell Waves (θ_W^S)	Wind Sea Waves (θ_W^{WW})
10/1/2017 06:00 (2)	2.40	2.39	0.22	9.60	9.89	2.17	320	320	70

In this case such as in the previous one, wind-sea waves can be considered to be negligible, as $\left(\frac{H_S^{WW}}{H_S}\right)^2 = 0.007$.

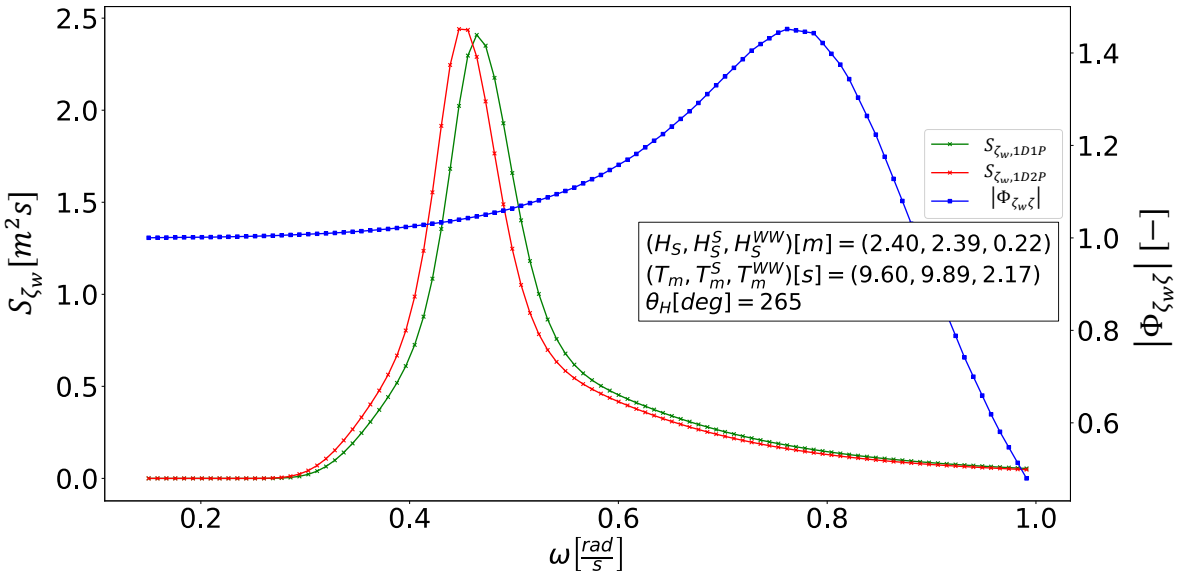

Figure 9. Date (2) – Wave spectra and Heave RAO, 1D models comparison

As the contribution of wind-sea waves over the total sea energy is of low importance, the frequency single and double-peaked models showed to have similar spectrum and agreeing responses are obtained, as shown in Figure 9 and Figure 10, respectively. Similar agreement can be found between the directional

spectral models as seen in Figure 11.A and Figure 11.B. This happens, as before, because the resultant wave field is substantially composed by one wave component, the swell one.

The responses are $\zeta_{s,1D1P} = 1.30$ [m] and $\zeta_{s,1D2P} = 1.28$ [m], which difference is negligible, in practical applications. Even comparing the results of the directional models (Figure 11.E and Figure 11.F), the differences in the amplitude ($\zeta_{s,2D1P} \cong \zeta_{s,2D2P} = 1.16$ [m]) are irrelevant.

The differences between the results obtained with the 1D and 2D models (greater than 10%) deserve attention, in this case. The reason has to be searched in the relation between the heave RAOs and relative wave direction. Differently from Date (1), the θ_H of the combined wave field in Date (2) is close to beam sea (see textbox in Figure 9). Analyzing the RAO displayed in Figure 9, yields that ship excitations about heave motion for the given forward speed are likely to be higher than those derived when the ship is approached about 60 degrees, as the case verified in Date (1). Clearly, heave motion is more magnified when the ship faces beam seas, which can be considered as a high excitation direction. As the frequency models entirely concentrate the wave field energy at this high excitation direction, they are expected to produce higher responses, whereas in the directional models, the energy is spread into the direction domain, as shown in Figure 11.A and Figure 11.B, in such way that energy is not concentrated uniquely at the high excitation direction.

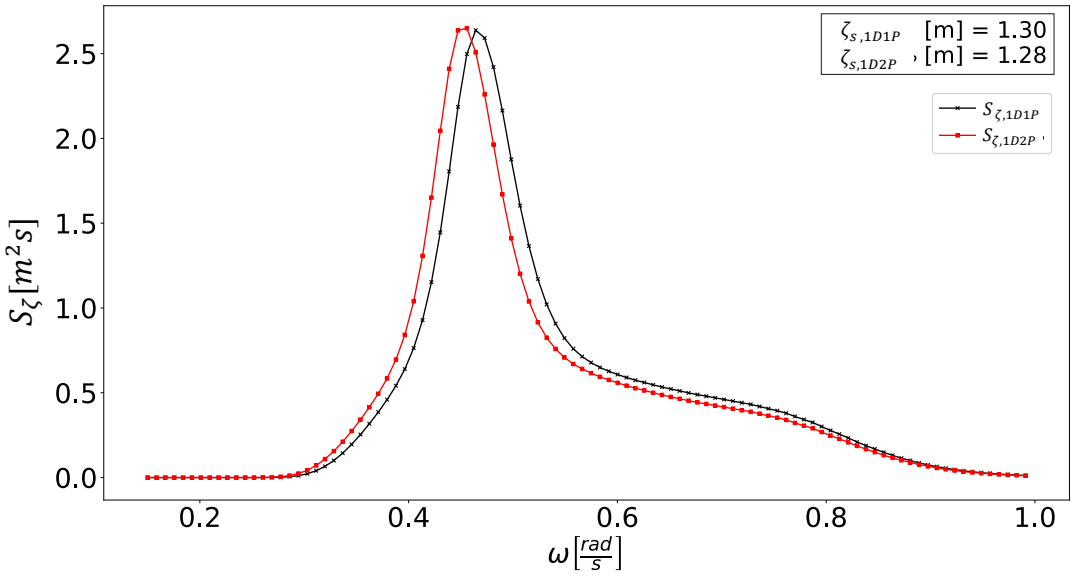

Figure 10. Date (2) – Heave response spectra, 1D models comparison

The energy concentration at a high excitation direction can explain, therefore, why frequency models provided, in this case, higher responses compared to the directional ones. On the other hand, it is further expected that when θ_H configures as a low excitation direction, directional models would tend to produce higher responses, which will be verified in the following example.

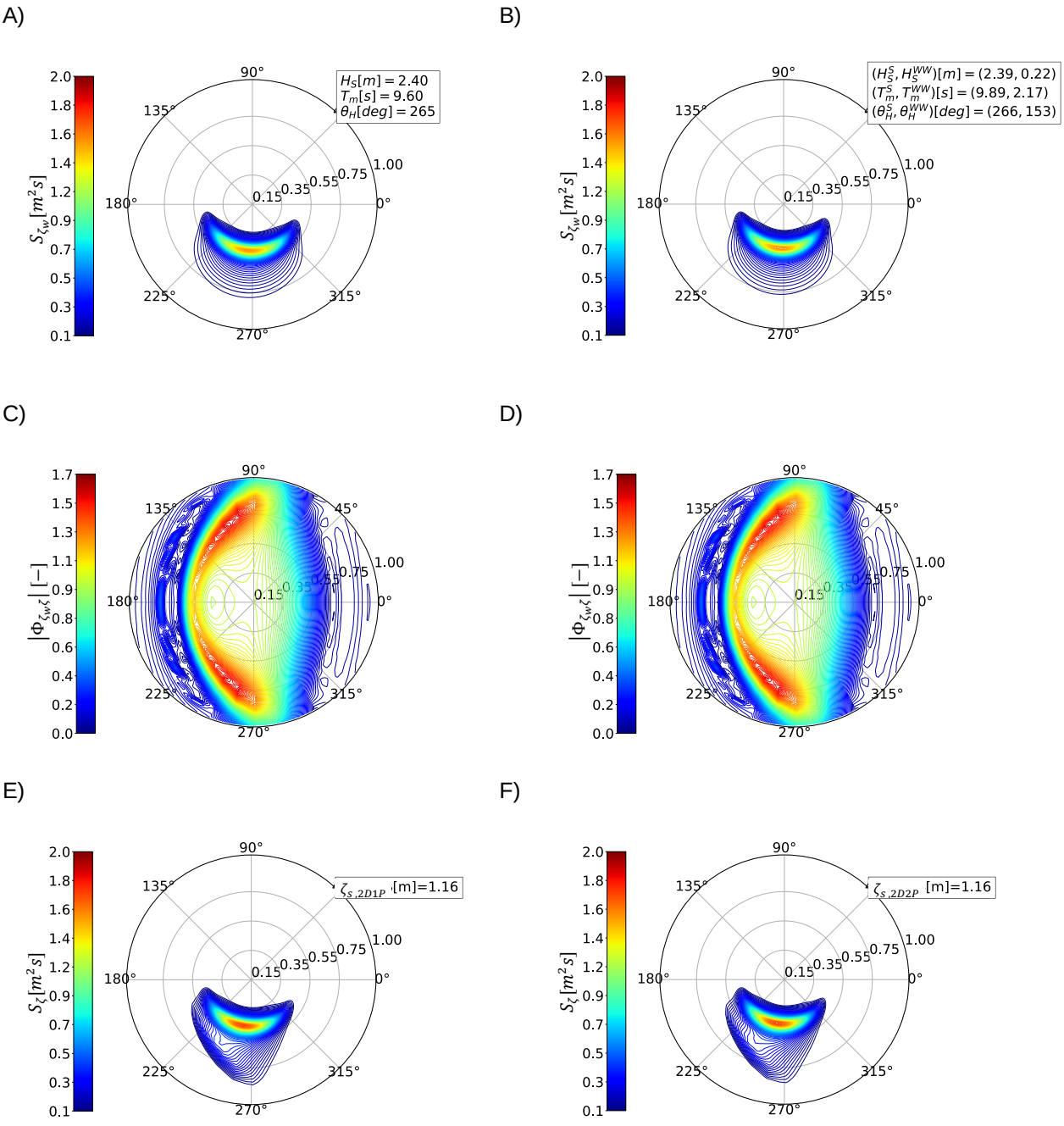

Figure 11. Same as Figure 8, but for Date (2).

4.1.3 Date (3) – Responses to combined wave system: Case 1

Table 6. Main wave data about Date (3) for heave response

Date	H_s [m]			$T_{\frac{m_0}{m_1}}$ [s]			θ_w [deg]		
	Combined Wave System (H_S)	Swell Waves (H_S^S)	Wind Sea Waves (H_S^{WW})	Combined Wave System (T_m)	Swell Waves (T_m^S)	Wind Sea Waves (T_m^{WW})	Combined Wave System (θ_W)	Swell Waves (θ_W^S)	Wind Sea Waves (θ_W^{WW})
16/1/2017 12:00 (3)	3.77	1.72	3.35	7.28	9.80	6.82	161	234	158

Differently from the previous cases, wind-sea waves are now relevant, as $\left(\frac{H_S^{WW}}{H_S}\right)^2 = 0.8$.

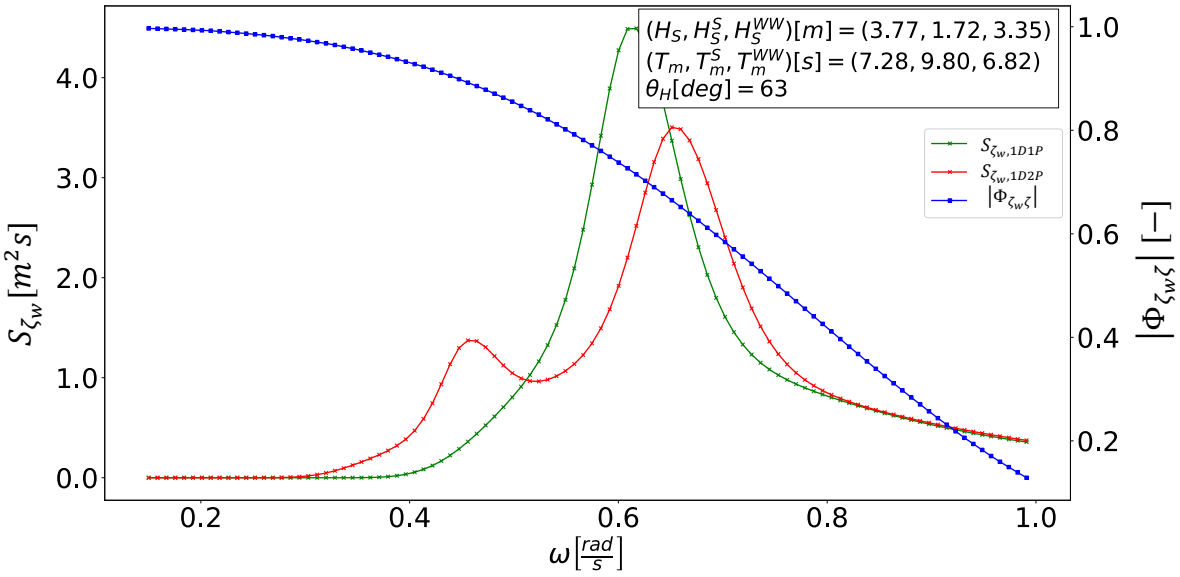

Figure 12. Date (3) – Wave spectra and Heave RAO, 1D models comparison

In this example, strong wind-sea component causes a significant decreasing of the T_m. As reported in Table 6, $T_m = 7.28$ [s], while the periods of swell and wind-sea waves are $T_m^S = 9.80$ [s] and $T_m^{WW} = 6.82$ [s], respectively. Such effect is visually displayed in Figure 12, where is shown that the peak of the combined wave field (1D1P) is located in between the peaks associated to the two wave components (1D2P).

Even though the results on the frequency models are similar, as $\zeta_{s,1D1P} = 1.18$ [m] and $\zeta_{s,1D2P} = 1.19$ [m], see Figure 13, this not necessarily is expected. In fact, as seen previously, both the single and double-peaked models only certainly tend to provide similar results when wave field domination is verified. For instance, whether the heave RAO would be the same as in Date (2), see Figure 9, certainly the heave responses, in this case now presented, due to wind-sea excitation would be substantially amplified, probably yielding higher response for the 1D2P model. The agreement between single and double-

peaked models when wave domination is not recorded is hard to be predicted, as it depends on the relation between the energy spectrum and the RAO, regarding the relevance of θ_H on it. The differences between the directional models are also limited, as the responses obtained are equal to $\zeta_{s,2D1P} = 1.42$ [m] and $\zeta_{s,2D2P} = 1.38$ [m]. A central peak is found in the first model while two peaks at significantly different θ_H and T_m are verified in the latter one, as shown in Figure 14.A and Figure 14.B, which characterizes a crossing-seas condition. The wave energy distributions of these models relate differently with the heave RAO, producing different response spectra, as displayed in Figure 14.E and Figure 14.F. These similarities in the results, however, seem to be specific of the specific case rather than to reflect what can be expected when a relevant wind-sea component is present.

The differences between frequency and directional models, which are quite pronounced in this case ($\zeta_{s,2D1P} \cong 1.20 \times \zeta_{s,2D2P}$) can be assessed in terms of θ_H, but with opposite effects. The combined wave system θ_H is $\theta_H = 63$ [deg], low excitation direction (Figure 14.C), yielding lower responses. As seen in Figure 14.A, the directional energy spreading towards the second quadrant makes the spectrum to sense the peak of the RAO there located, which results in a response energy peak, as seen in Figure 14.E and Figure 14.F, and not interested by the 1D models.

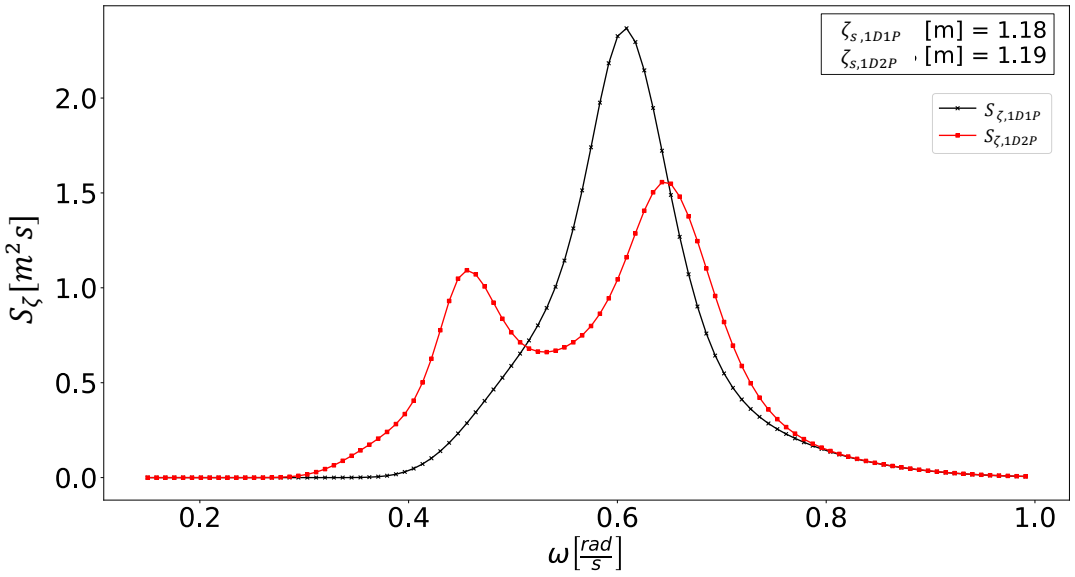

Figure 13. Date (3) – Heave response spectra, 1D models comparison

In this particular case, for instance, the response given by the 1D1P model is almost 20% lower than the 2D1P one, which in fact shows that the simpler models can also under-estimated the environmental forcing.

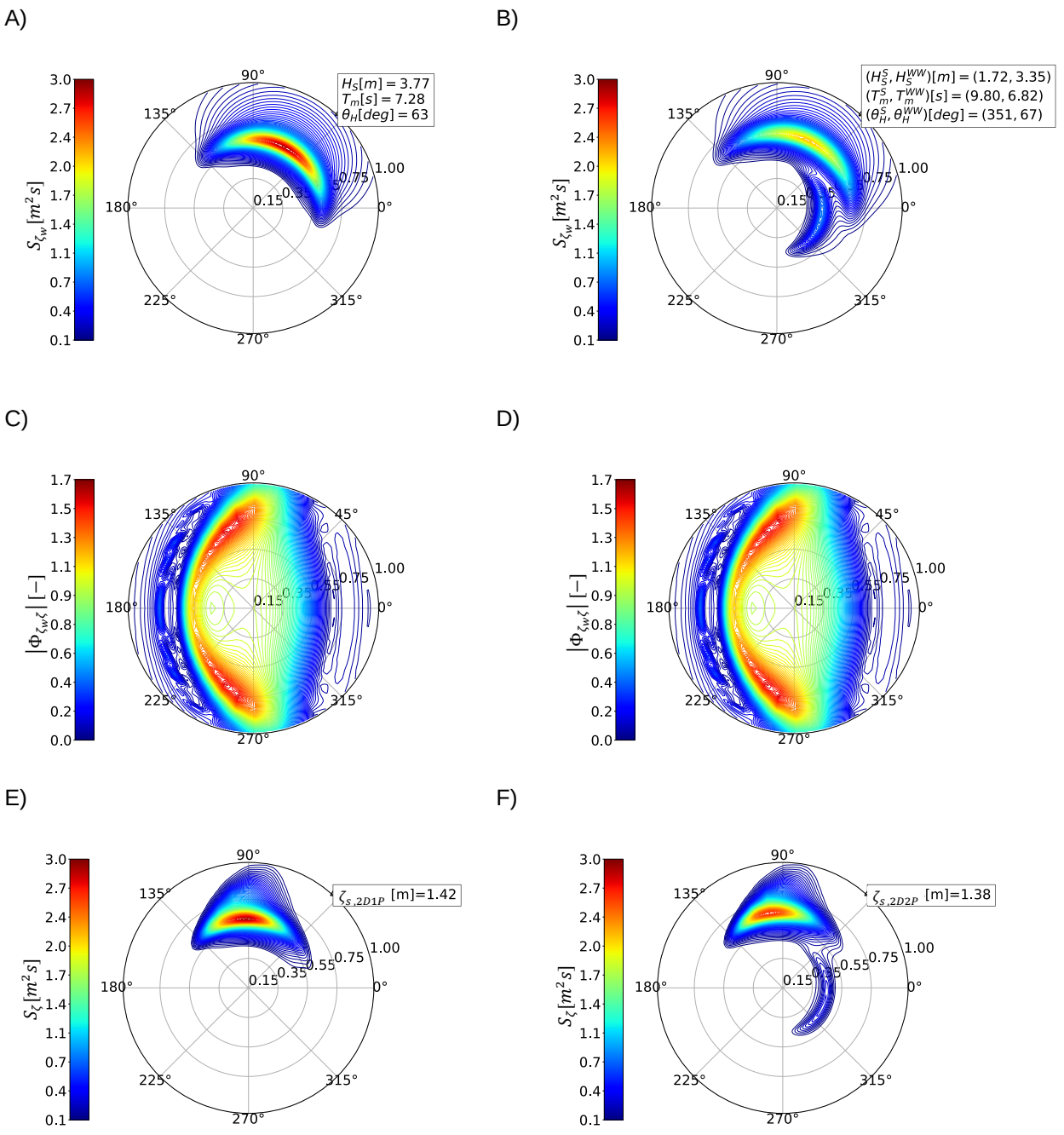

Figure 14. Same as Figure 8, but for Date (3)

4.1.4 Date (4) – Responses to combined wave system: Case 2

Table 7. Main wave data about Date (4) for heave response

	H_s [m]			$T_{\frac{m_0}{m_1}}$ [s]			θ_w [deg]		
Date	Combined Wave System (H_S)	Swell Waves (H_S^S)	Wind Sea Waves (H_S^{WW})	Combined Wave System (T_m)	Swell Waves (T_m^S)	Wind Sea Waves (T_m^{WW})	Combined Wave System (θ_W)	Swell Waves (θ_W^S)	Wind Sea Waves (θ_W^{WW})
7/1/2017 18:00 (4)	2.68	2.47	1.04	7.46	8.76	4.06	123	142	100

Wind-sea waves are considered to be relevant, as $\left(\frac{H_S^{WW}}{H_S}\right)^2 = 0.15$.

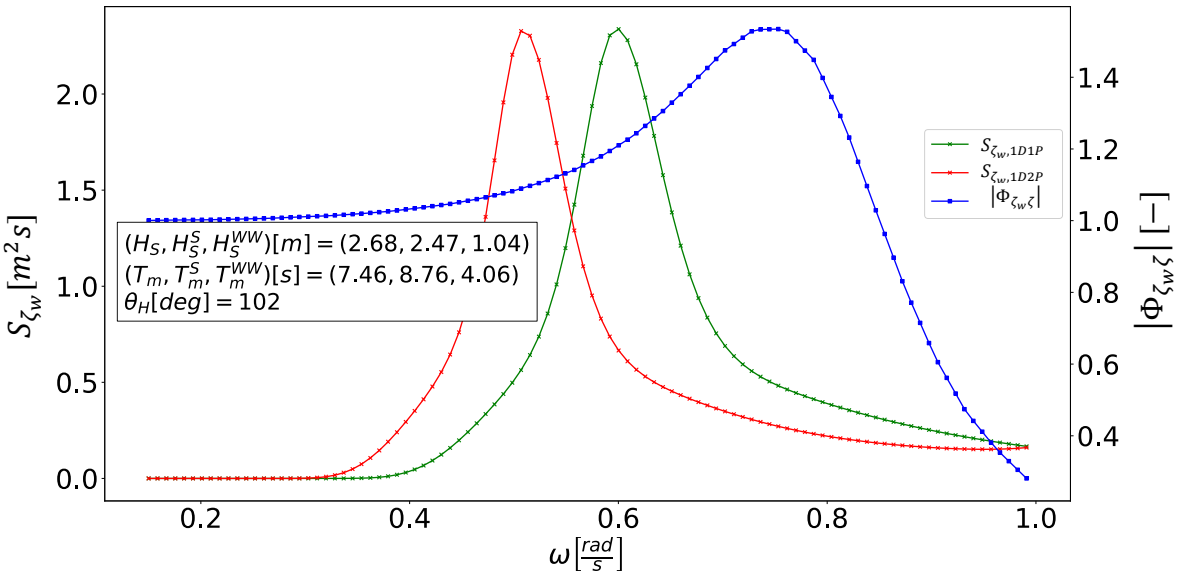

Figure 15. Date (4) – Wave spectra and Heave RAO, 1D models comparison

From Table 7, the T_m of wind-sea is less than half of the swell period, as $T_m^{WW} = 4.06$ [s] and $T_m^S = 8.76$ [s]. As shown either in Figure 15 or Figure 17.B, the energy peak associated to the wind-sea is not represented, as the peak frequency of that component overcomes the frequency threshold until which waves can excite the ship on heave motion. The wind-sea recorded has, in other words, relatively short wave length compared with the ship size, meaning that the heave excitations produced are irrelevant. Nevertheless, the combined wave field is still affected by the contributions of both the swell and wind-sea components, meaning that the resulting energy peak locates in between the peaks of the components. This influence can be seen in Figure 15, as the combined wave field peak (1D1P) is slightly shifted to higher frequencies. The heave RAO shows to amplify the excitations, as the relative wave direction ($\theta_H = 102$ [deg]) is a high excitation direction, in this case. The magnification performed over the 1D1P model ends up to be higher, since the resulting energy peak is shifted towards the increasing RAO

amplification. A more energetic response is obtained compared to the correspondent frequency double-peaked model ($\zeta_{s,1D1P} = 1.56$ [m] and $\zeta_{s,1D2P} = 1.39$ [m]), as seen in Figure 16, in which this latter response is approximately 11% lower than the first one. It shows, therefore, that waves which eventually do not even excite ship motions, but are energetically relevant for the wave field, are inherently sensed on the general measurement of the combined wave field and that can also have an impact on the responses. Such disagreement can eventually be relevant on the design or for operational purposes.

The energy concentration at θ_H, which can be considered as a high excitation direction, makes the frequency model to produce higher responses compared to the directional ones. The significant amplitudes of the single-peaked directional model is $\zeta_{s,2D1P} = 1.30$ [m], which is 17% lower than the correspondent frequency one. The same explains the difference between the double-peaked frequency and directional models ($\zeta_{s,2D2P} = 1.14$ [m], which is 18% less than the 1D2P model and 27% less than the 1D1P one).

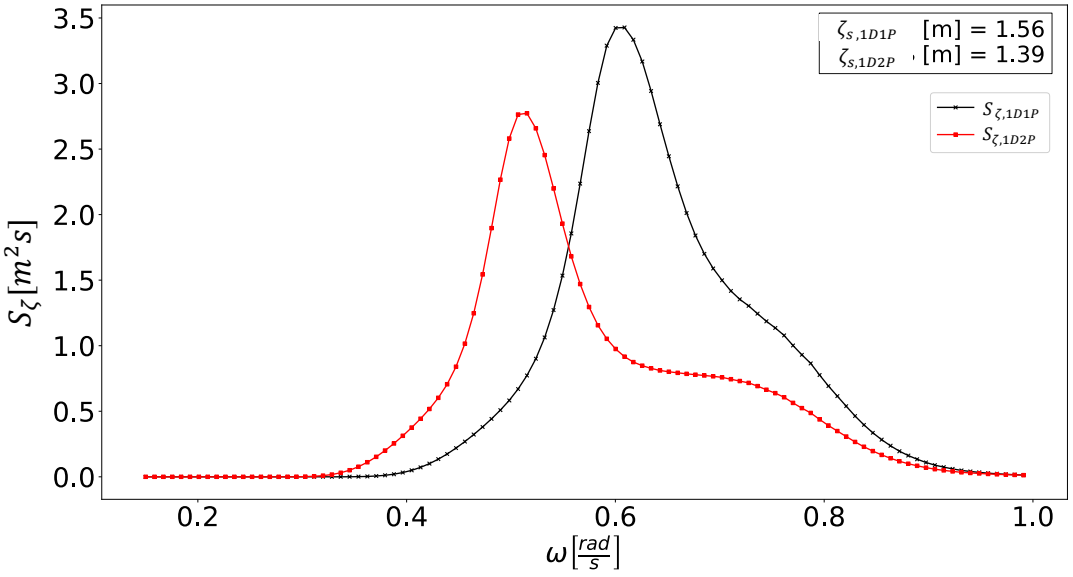

Figure 16. Date (4) - Heave response spectra, 1D models comparison

It is clear that the parametric models can eventually result in disagreeing responses. Such differences are remarkable whether the wave field is energetically influenced by more than one wave system. On the other hand, if one system is negligible, both single and double-peaked models can provide similar responses although the disagreement between the frequency and directional models is still not to be predicted, as the dependency of the responses on the relation between the energy spectrum and the RAO is strong.

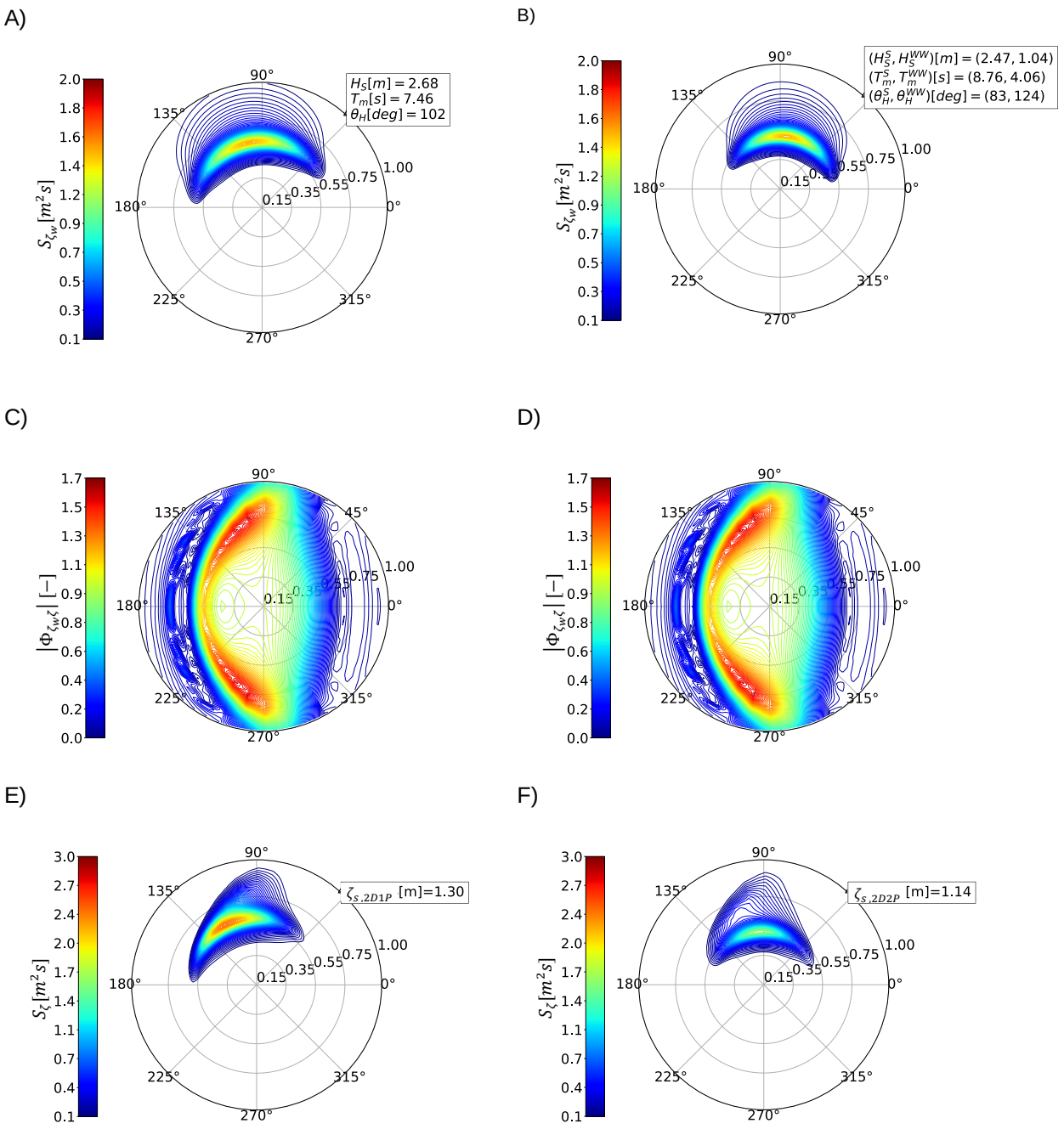

Figure 17. Same as Figure 8, but for Date (4)

4.2 Roll response

Roll is in most of the cases a critical motion for ships, due to, for instance, the difficulties in accurately estimating the damping factor, the possible non-linearities, etc. It will be shown that, even in terms of choice in the wave spectral model, roll responses may be significantly affected, mostly due to the fact that the amplification near to the natural frequency is much more pronounced than for other vertical motions. Some particular events effects have been detected in order to understand the mechanisms that lead to such differences, as performed previously. In Figure 18 are displayed the significant roll amplitudes, $\varphi = 2 \times \sqrt{m_0}$, in degrees, for each parametric model, during the month of January of 2017. Three specific dates are highlighted in the same chart and the wave data respectively to these dates are shown in Table 8.

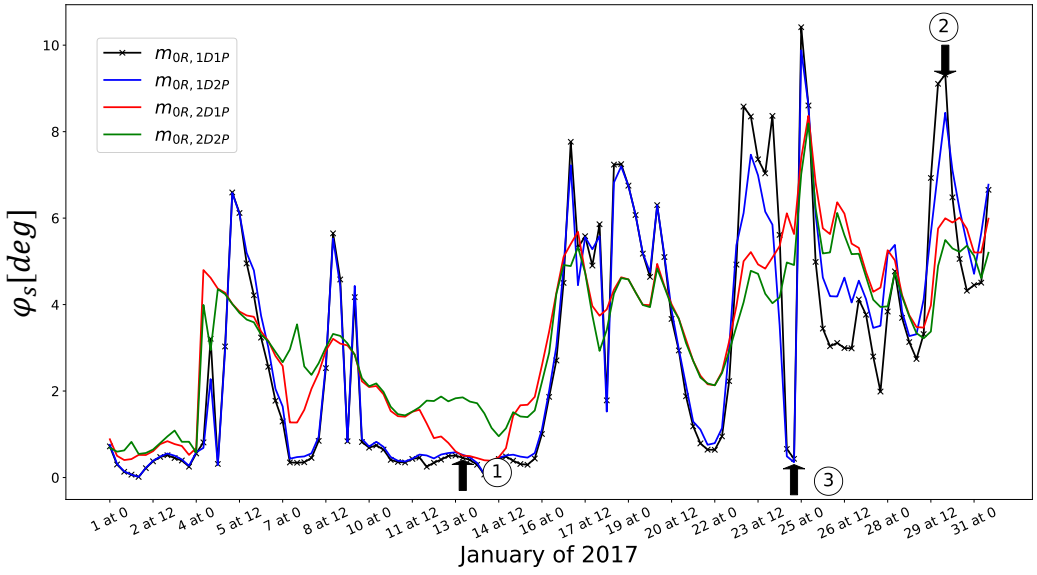

Figure 18. Cases highlighted for roll response

Table 8. Main wave data for the dates highlighted about roll response

Date	H_s [m]			$T_{\frac{m_0}{m_1}}$ [s]			θ_w [deg]		
	Combined Wave System (H_S)	Swell Waves ($H_{S,S}$)	Wind Sea Waves ($H_{S,WW}$)	Combined Wave System (T_m)	Swell Waves ($T_{m,S}$)	Wind Sea Waves ($T_{m,WW}$)	Combined Wave System (θ_W)	Swell Waves ($\theta_{W,S}$)	Wind Sea Waves ($\theta_{W,WW}$)
13/1/2017 06:00 (1)	3.34	2.74	1.91	7.96	10.78	5.17	9.0	337	94
30/1/2017 00:00 (2)	4.06	2.59	3.12	7.96	10.0	6.96	262	266	260
24/1/2017 18:00 (3)	3.71	2.09	3.05	7.27	9.43	6.55	223	263	207

4.2.1 Date (1) – Responses to combined wave system: Case 1

Table 9. Main wave data about Date (1) for roll response

Date	H_s [m]			$T_{\frac{m_0}{m_1}}$ [s]			θ_w [deg]		
	Combined Wave System (H_S)	Swell Waves (H_S^S)	Wind Sea Waves (H_S^{WW})	Combined Wave System (T_m)	Swell Waves (T_m^S)	Wind Sea Waves (T_m^{WW})	Combined Wave System (θ_W)	Swell Waves (θ_W^S)	Wind Sea Waves (θ_W^{WW})
13/1/2017 06:00 (1)	3.35	2.75	1.91	7.96	10.79	5.17	9.0	337	94

All models but the double-peaked directional one provided agreeing responses. That model resulted in significantly higher response when compared to the remaining ones, as seen in Figure 18. Wind-sea waves are considered to be relevant, as $\left(\frac{H_S^{WW}}{H_S}\right)^2 = 0.33$.

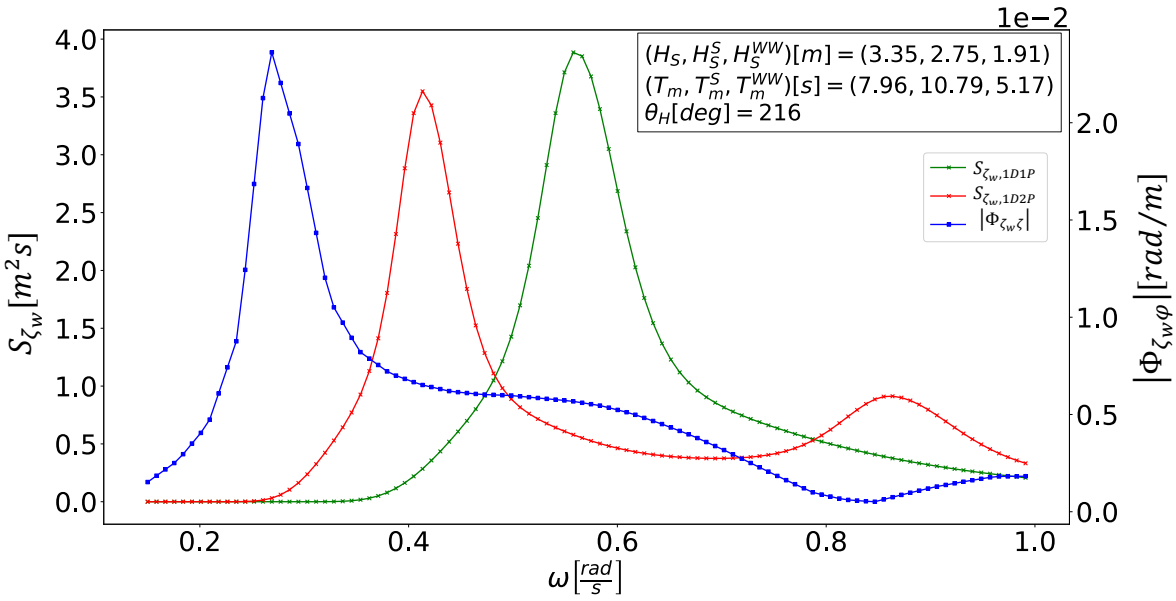

Figure 19. Date (1) – Wave spectra and Roll RAO, 1D models comparison

The combined wave field average wave period, $T_m = 7.96$ [s], is naturally in between those of swell and wind-sea, as $T_m^S = 10.79$ [s] and $T_m^{WW} = 5.17$ [s], according to the data provided in Table 9 and displayed in Figure 19.

The amplification peak represented by the RAO in Figure 19 occurs at small frequencies compared to the energy peaks of the wave energy spectrum, for the given relative wave direction, $\theta_H = 216$ [deg]. As the swell components have higher T_m and, consequently, peak at lower frequency, the first wave energy peak of the 1D2P model ends up to be close to the one of the RAO, yielding a more energetic response, compared to the combined wave field model (1D1P), as seen in Figure 20, as $\varphi_{1D1P} = 0.46$ [deg] and

$\varphi_{1D2P} = 0.53$ [deg] so that this latter is 15% higher than the first one. However, being these values relatively low, the difference is less critical.

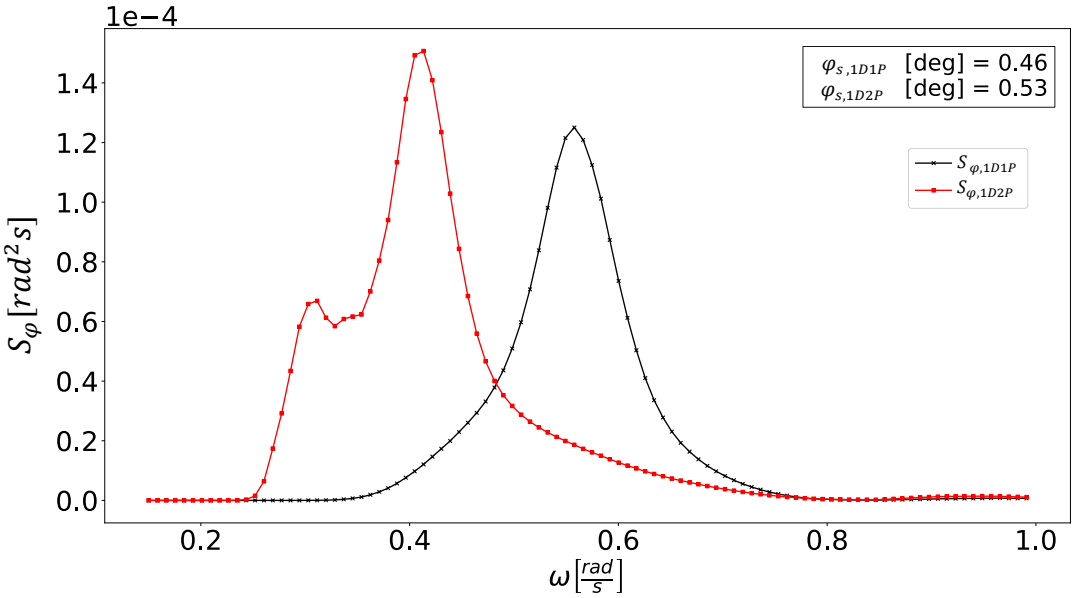

Figure 20. Date (1) - Roll response spectra, 1D models comparison

Even though the 2D1P model yielded a response which order of magnitude resembles to those derived from the frequency ones, such similarity is not expectable for the same reasons before discussed. The combined wave field relative wave direction, $\theta_H = 216$ [deg], is such that the multi-directional spectrum, as presented in Figure 21.A, does not interact with pronounced variations of the roll RAO, which is shown in Figure 21.C, yielding a small response amplitude, $\varphi_{2D1P} = 0.51$ [deg], which is in between the responses derived from the frequency models.

Analyzing the multi-directional spectrum shown in Figure 21.B, both the swell and wind-sea components are clearly identified. It is valuable noticing that the contribution of the wind-sea on the response is of low relevance (in fact the energy spectrum about the relative wave direction, $\theta_H^{WW} = 131$ [deg], is weakly amplified by the roll RAO, yielding low energy contribution about the response spectrum, as seen in Figure 21.F). The swell component, on the other hand, strongly contributes for the energy content of the response spectrum, as the energy spread towards the forth quadrant senses the pronounced variation on the RAO, producing an energetic peak and substantially higher significant amplitude, $\varphi_{2D2P} = 1.85$ [deg], which is, in fact, 300% higher than the one derived from the single-peaked frequency model.

This case clearly shows that whether both the swell and wind-sea components are relevant on the wave field energy and the MWDs and T_m differ significantly, the most appropriate model to be used is the directional double-peaked one. This is due to the fact that it provides a more complete representation of the environmental forcing upon the hull, since the wave energy is better described in terms of direction

and frequency distributions and wave components separate contributions. Nevertheless, it is also evident that the results can be very sensitive to the directional spreading function adopted.

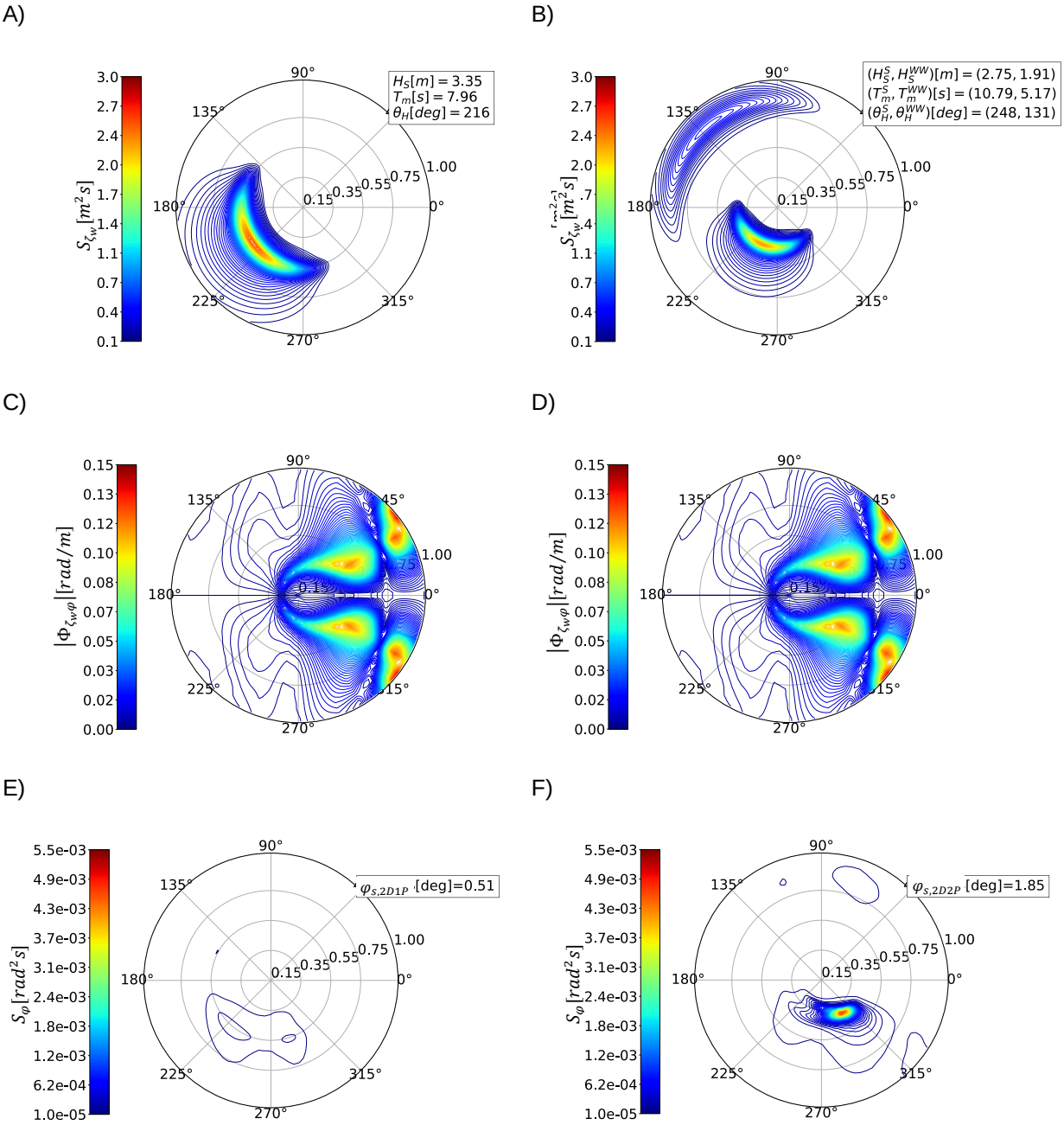

Figure 21. Same as Figure 8, but for roll responses and Date (1)

4.2.2 Date (2) – Responses to combined wave system: Case 2

Table 10. Main wave data about Date (2) for roll response

Date	H_s [m]			$T_{\frac{m_0}{m_1}}$ [s]			θ_w [deg]		
	Combined Wave System (H_S)	Swell Waves (H_S^S)	Wind Sea Waves (H_S^{WW})	Combined Wave System (T_m)	Swell Waves (T_m^S)	Wind Sea Waves (T_m^{WW})	Combined Wave System (θ_W)	Swell Waves (θ_W^S)	Wind Sea Waves (θ_W^{WW})
30/1/2017 00:00 (2)	4.06	2.59	3.12	7.96	10.0	6.96	262	266	260

No agreement is verified, as seen Figure 18. Wind-sea waves are relevant, as $\left(\frac{H_S^{WW}}{H_S}\right)^2 = 0.6$.

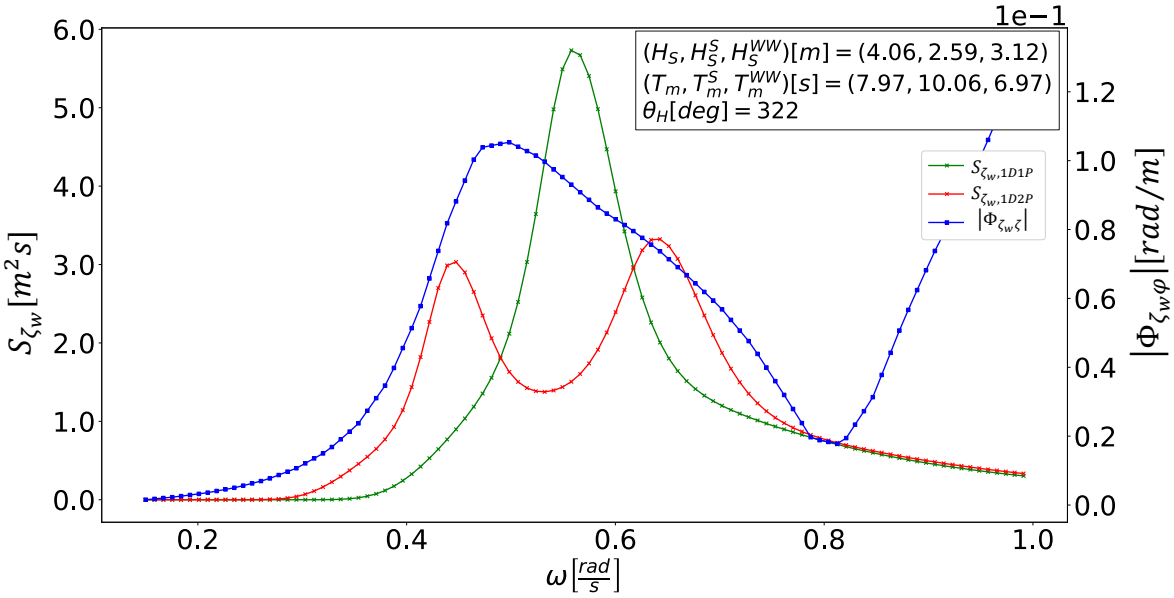

Figure 22. Date (2) – Wave spectra and Roll RAO, 1D models comparison

Both the swell and wind-sea components, and consequently the combined wave field, approach the ship from a similar direction (about 320 degrees), corresponding to high roll excitations, as shown by the roll RAO in Figure 22. As the frequency models concentrate the energy at the mean direction, which is a high excitation direction, therefore, they tend to produce higher responses compared to the directional ones. The responses derived from the frequency models, which are $\varphi_{1D1P} = 9.32$ [deg] and $\varphi_{1D2P} = 8.44$ [deg] (Figure 24), are considerably higher than those derived from the 2D ones, since $\varphi_{2D1P} = 6.00$ [deg] and $\varphi_{2D2P} = 5.49$ [deg] (Figure 23.E and Figure 23.F). Therefore, the single-peaked frequency model provides approximately 70% higher amplitude than the double-peaked directional one, which disagreement is relevant.

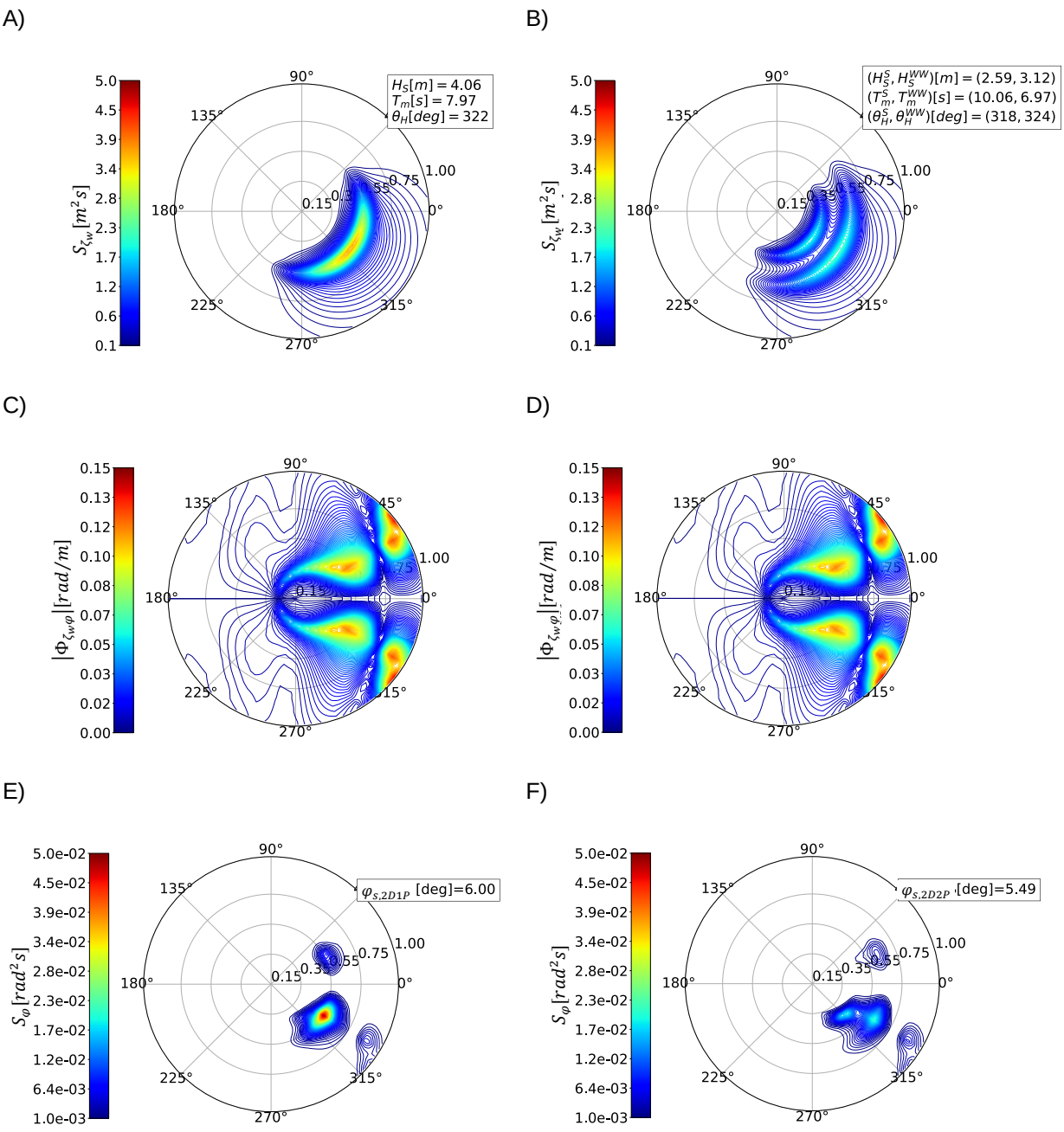

Figure 23. Same as Figure 21, both for Date (2)

Frequency single and double-peaked models showed to be in disagreement, as $SRA_{1D1P} = 1.10 * SRA_{1D2P}$, which difference should not be overlooked either for design or operational purposes.

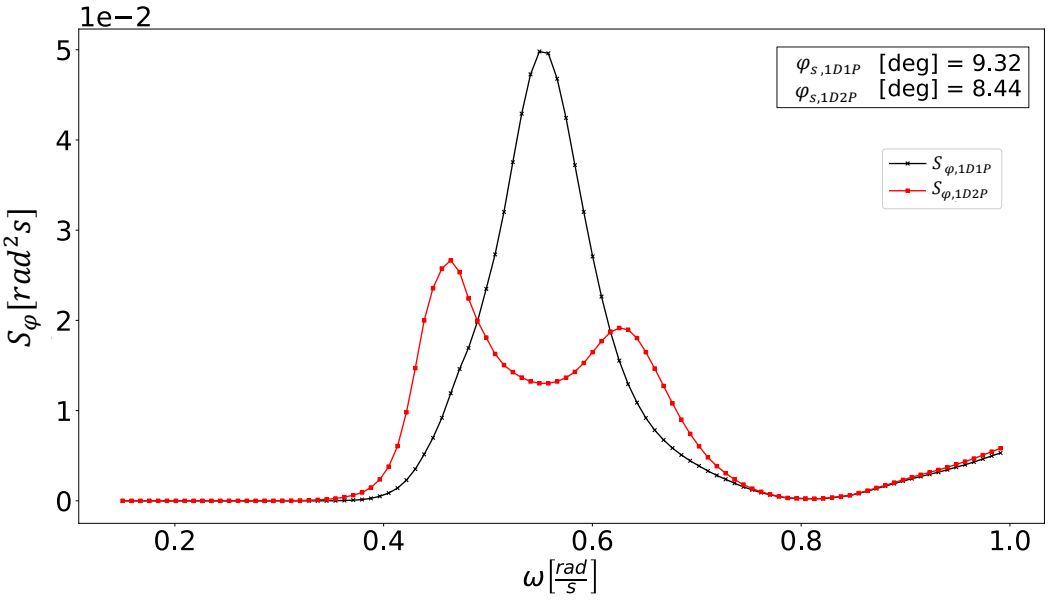

Figure 24. Date (2) - Roll response spectra, 1D models comparison

4.2.3 Date (3) – Responses to combined wave system: Case 3

Table 11. Main wave data about Date (3) for roll response

Date	H_s [m]			$T_{\frac{m_0}{m_1}}$ [s]			θ_w [deg]		
	Combined Wave System (H_S)	Swell Waves (H_S^S)	Wind Sea Waves (H_S^{WW})	Combined Wave System (T_m)	Swell Waves (T_m^S)	Wind Sea Waves (T_m^{WW})	Combined Wave System (θ_W)	Swell Waves (θ_W^S)	Wind Sea Waves (θ_W^{WW})
24/1/2017 18:00 (3)	3.71	2.09	3.05	7.27	9.43	6.55	223	263	207

In this case, as seen in Figure 18, frequency models resulted in significantly lower responses compared to the directional ones. Wind-sea waves are considered to be relevant, as $\left(\frac{H_S^{WW}}{H_S}\right)^2 = 0.67$.

The combined wave field relative wave direction is $\theta_H = 2$ [deg], as shown in Figure 25, which is not considered as a high excitation direction, being roll absent for following waves (within the linear theory). High amplifications are expected for quartering seas, however, as indicated in Figure 27.C. Due to the energy being concentrated at θ_H when frequency models are considered, the roll responses produced ($\varphi_{1D1P} = 0.43$ [deg] and $\varphi_{1D2P} = 0.35$ [deg], see Figure 26), are much lower compared to those derived from the directional models ($\varphi_{2D1P} = 5.63$ [deg] and $\varphi_{2D2P} = 4.91$ [deg], see Figure 27.E and Figure 27.F)

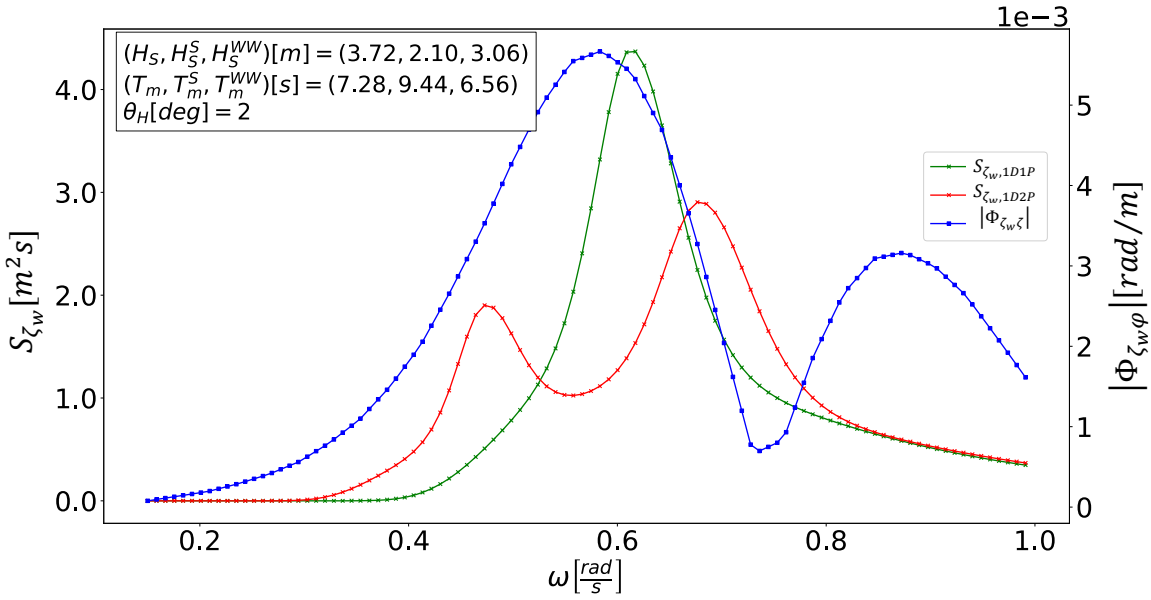

Figure 25. Date (3) – Wave spectra and Roll RAO, 1D models comparison

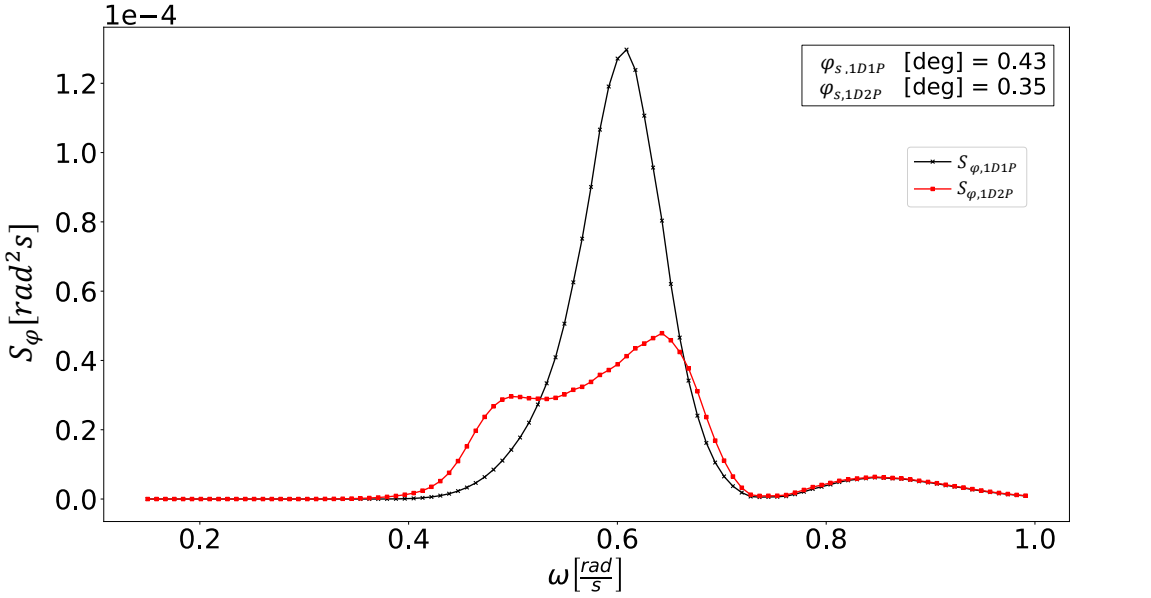

Figure 26. Date (3) - Roll response spectra, 1D models comparison

Even though θ_H is the same about the 2D1P model, meaning following waves, it is clear that the directional spreading of the energy spectrum plays in important role about the final response, as the spread spectrum towards the first and the fourth quadrants senses the roll RAO peaks at, approximately, +30 and -30 degrees. Hence, the response derived from the directional model is considerably higher compared to those from the frequency ones, and response peaks can be found at the mentioned quadrants, as shown in Figure 27.E. The same can be concluded about the 2D2P and 1D2P models. Wind-sea waves at $\theta_H^{WW} = 18$ [deg] and swell at $\theta_H^S = 322$ [deg], as seen in Figure 27.E, makes the

directional double-peaked spectrum to sense the RAO peaks at those high excitation directions, resulting in roll response peaks, as seen in Figure 27.F. The double-peaked directional spectrum model (2D2P) provided 10 times higher response than the single-peaked frequency spectra one (1D1P).

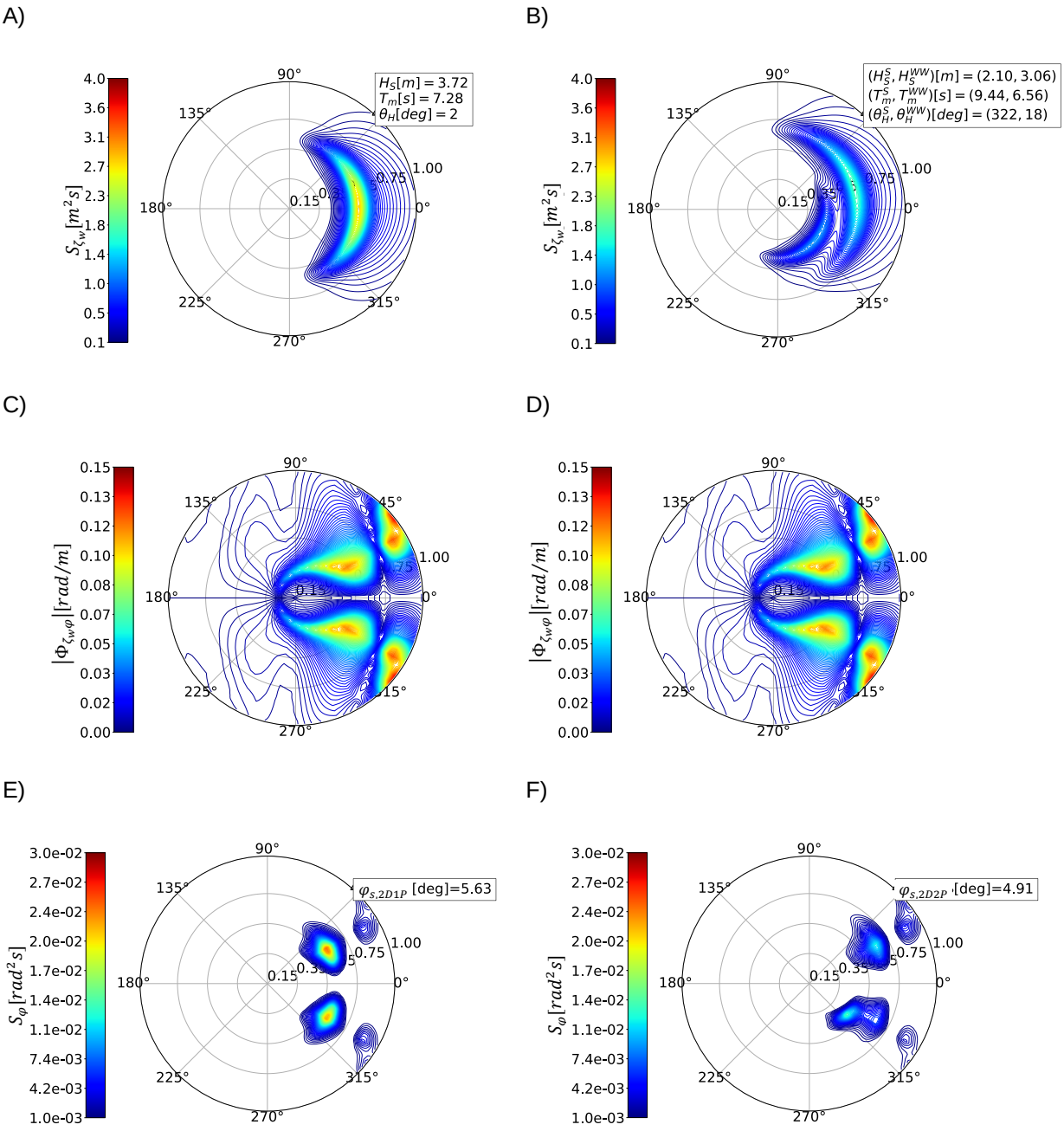

Figure 27. Same as Figure 21, but for Date (3)

Chapter 5

Ship responses on the North Atlantic

In this chapter, heave and roll responses computed over a grid about the North Atlantic are shown. Visual evidences of the differences between the models over the grid are shown and assessed in sight of the general wave climate expectable on the North Atlantic.

In order to take into account all possible courses that the ships can assume in each location, a discrete probability distribution function has been calculated for each considered grid point by analyzing the reports provided within the Voluntary Observing Ships (VOS) scheme [33] by vessels navigating in these areas. These ships are recruited by National Meteorological Services to sense and transmit these meteorological data, including visually observed wave heights, periods and directions of swell and wind-sea waves. That data are associated to the coordinates where the voluntary ships sail through. Furthermore, the measurements of the average H_S are in general over-estimated in comparison to those generated by remote sensing and numerical methods, in areas with small amplitudes, as shown in [34]. The dependency of ship responses on the course is then eliminated by weighting the responses at each direction by the correspondent course probability of occurrence, providing a map of the generic expectable behavior of the ship about the desired responses.

In Figure 28, are presented the weighted averages of each model on the significant heave amplitudes. Different ship courses are considered, from $0°$ to $315°$ with step of $45°$, and for each, the models are applied in order to compute the ship responses at every single point of the grid, in which the North Atlantic is represented. A trade-off between mapping resolution and computational time was carried out, so that the $3° \times 3°$ grid was found to provide fairly good resolution such that the computations could also be performed within the available time. The responses are calculated for the 6-hourly, 1-yr data. The time average of the significant amplitudes is computed for each point after all points get suitably weighted with the ship course probabilities, as shown in Equation 19.

$$\overline{\zeta_s}_{m,p} = \frac{\sum_{h=1}^{N} \sum_a P_{a,p} \times \zeta_{s_{m,a,p,h}}}{N} \tag{19}$$

Where:

- $\overline{\zeta_s}$ is the significant heave amplitude time average respectively to a given model, at a given point.
- *m* is the parametric model, belonging to [1D1P, 1D2P, 2D1P, 2D2P].

- *p* is an arbitrary point of the grid.
- *h* is a specific event within the 6-hourly, 1-yr data.
- *N* is the amount of events of the 6-hourly, 1-yr data.
- *a* is the ship course, belonging to $[0°, 45°, 90°, .., 315°]$.
- *P* is the probability at point *p* of the ship to sail towards *a.*
- ζ_s is the significant heave amplitudes respectively to a given model for a certain course, at given point and event.

Furthermore, the following is verified:

$$\sum_{a} P_{p,a} = 1 \tag{20}$$

5.1 Mapping heave responses

In Figure 29.A and Figure 29.B are displayed the relative differences between the single and double-peaked models for the 1D and 2D cases, respectively. These plots allow verifying that the differences, in these cases, tend to decrease towards the extratropical area. It is interesting to relate these results with the analysis outlined in the previous chapter. By assessing the sources that lead to the differences between the models, it was found that when the wave system is dominated by one wave component, swell or wind-sea, both the single and double-peaked models tend to produce agreeing responses. The oceans, in general, tend to be dominated by swell, as the local probabilities of swell to carry less than 50% of the wave field energy are very low, as shown in [35]. Future findings also provided that the probability of dominated wave fields is high on the North Atlantic in the area within 20ºN and 40ºN, 10ºW and 60ºW (this will be better discussed in Chapter 6). These considerations can be related with the fat that single and double-peaked models visually presented a better general agreement (Figure 29.A and Figure 29.B) compared to the differences between frequency and directional ones (Figure 29.C and Figure 29.D) and with the similarities verified at the locations mentioned about single and double-peaked models. In areas where wave system domination is verified, single-peaked models could preferably be used over double-peaked ones, which decision can be time saving from the computational point of view, such that, nevertheless, fairly good results are provided compared to the more complete and detailed models.

In Figure 29.C and Figure 29.D are shown the differences between the single-peaked frequency model and the 2D1P and 2D2P ones, respectively. It is shown that, in general, the directional models tend to produce higher responses for heave. It is difficult, though, to compare such differences in sight of the local wave climate as did previously, as predicting how differently both the frequency and directional spectra will relate to the RAOs is very complex.

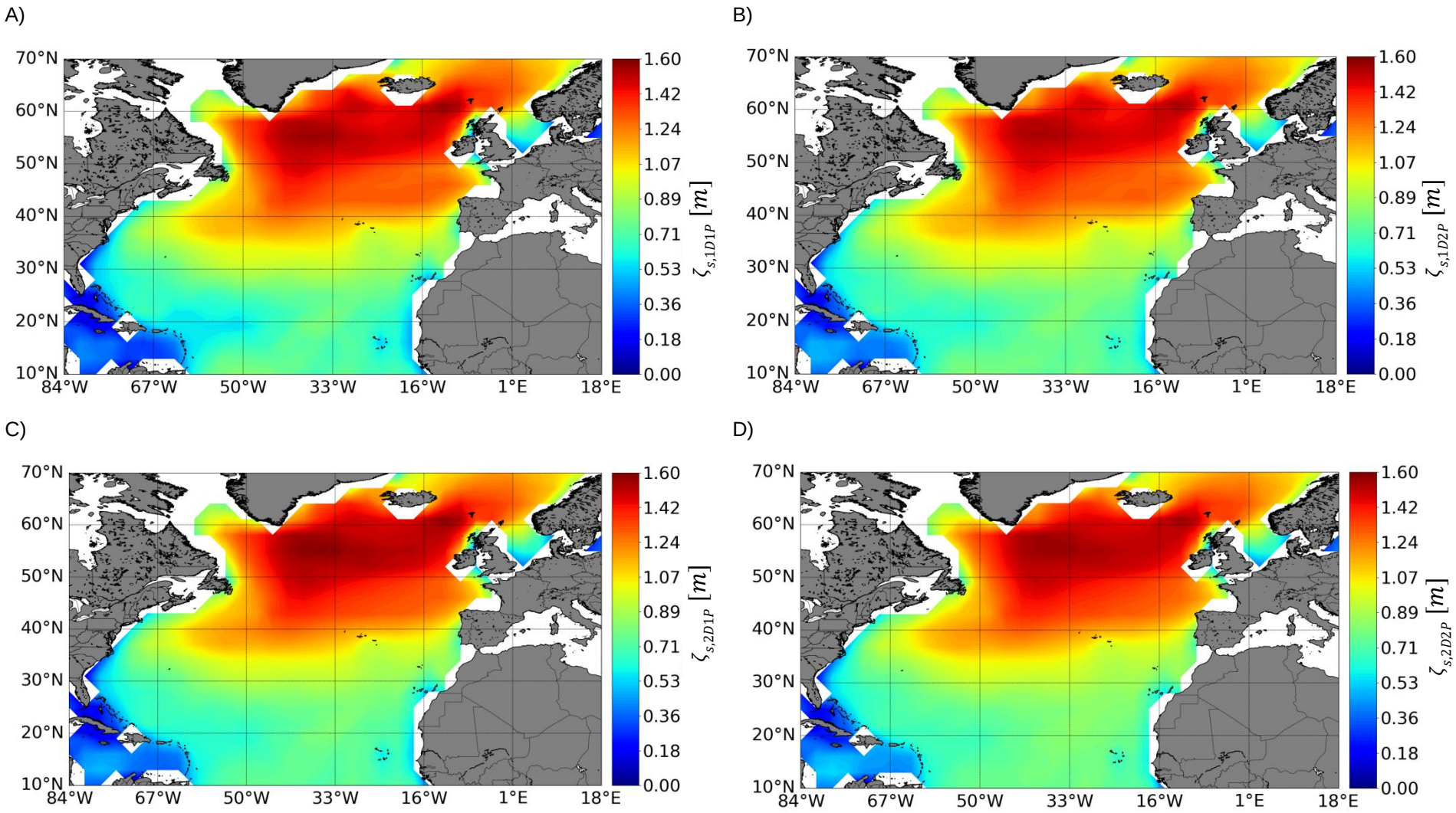

Figure 28. Weighted average mappings for the North Atlantic on the Heave Response. A) 1D1P, B) 1D2P, C) 2D1P and D) 2D2D

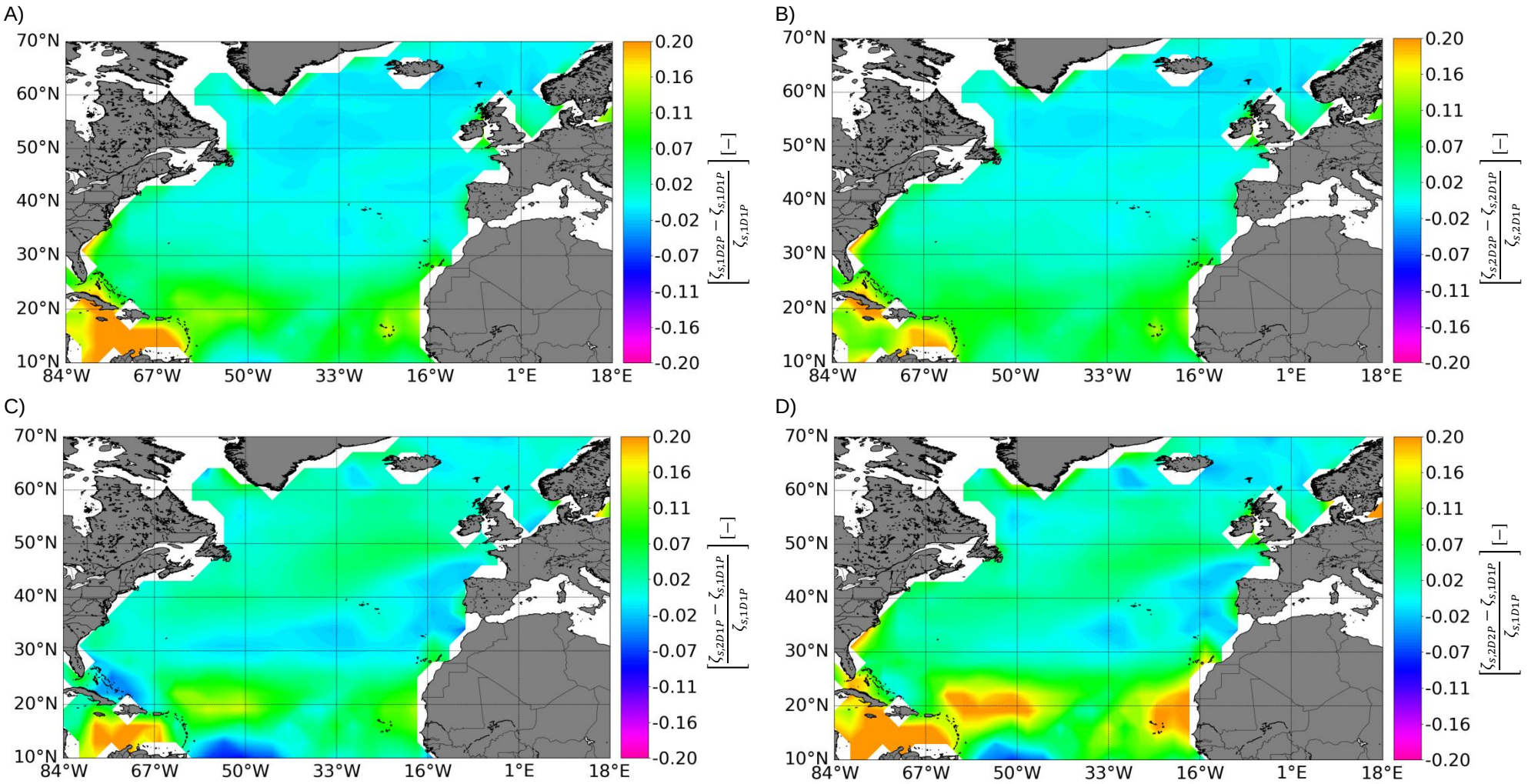

Figure 29. Relative difference mappings for the North Atlantic on the Heave Response. A) 1D2PX1D1P, B) 2D2PX2D1P, C) 2D1PX1D1P and D) 2D2PX1D1P

The responses can be directly compared without considering the time averaging, as shown in Figure 30. The weighted significant heave amplitude average in terms of the ship course probability is performed, however. The Pierson Correlation Coefficient is used to provide a quantitative measurement of how strongly are the models related to each other. All locations of the North Atlantic at each event of the 1-yr 6-hourly data are presented.

As shown in Figure 30.A and Figure 30.F, the single and double-peaked models tend to be strongly correlated, as $CORR = 0.994$, from the comparison between the 1D1P and 1D2P models and $CORR = 0.996$, from the comparison between the 2D1P and 2D2P ones. These models tend to produce agreeing responses under the occurrence of dominated wave fields, which is not necessarily true when comparing frequency and directional models. For that reason, more often than not, single and double-peaked models yielded similar results, resulting in stronger correlations.

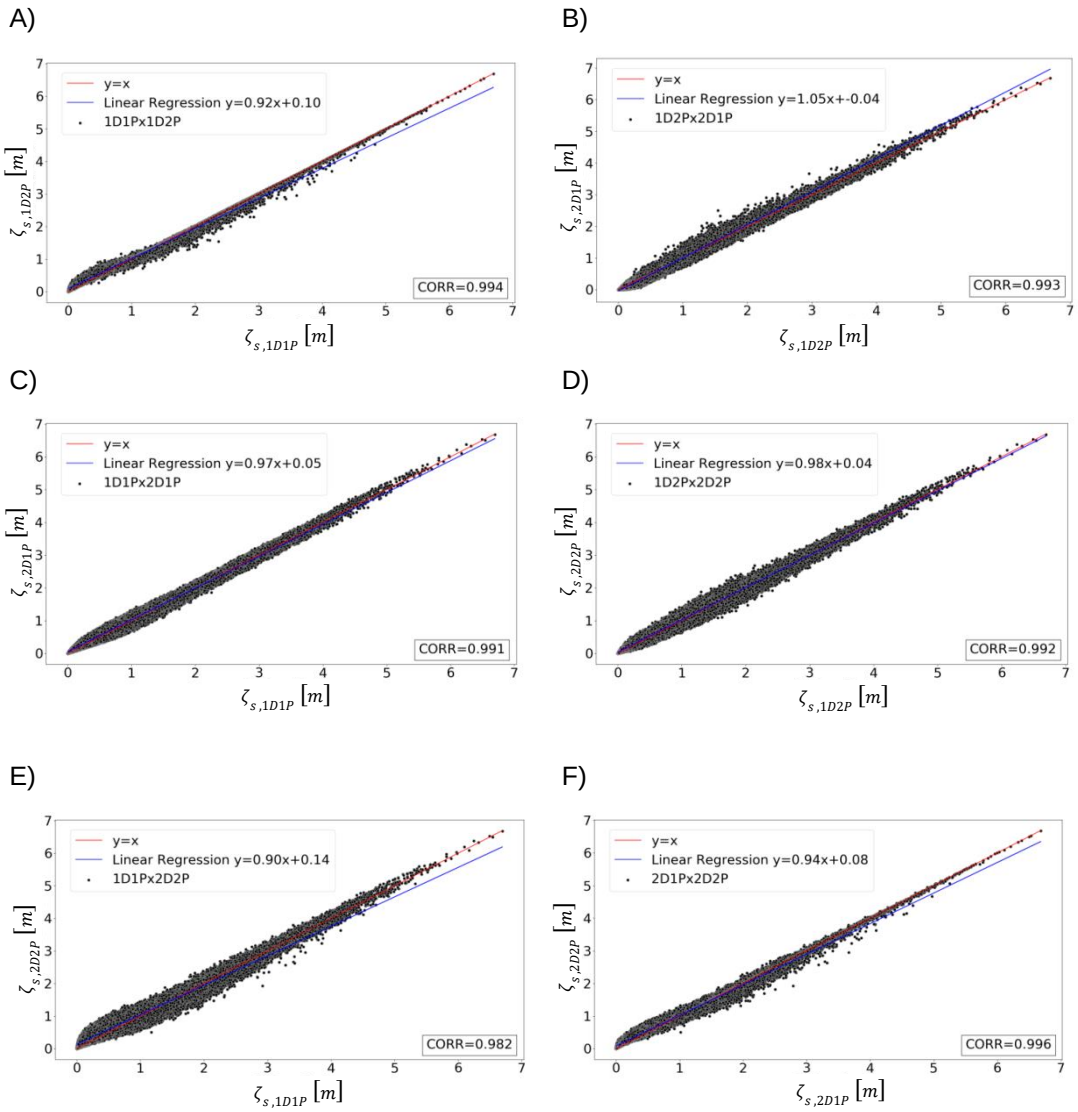

Figure 30. Correlation between the models. A)1D1PX1D2P, B)1D2PX2D1P, C)1D1PX2D1P, D)1D2PX2D2P, E)1D1PX2D2P and F)2D1PX2D2P

Such discussion can be assisted by the results shown in Figure 31, where are displayed the algebraic difference between the models and its relation with the part from the total wave field energy carried by the wind-sea component. As shown in Figure 31.A and Figure 31.F, the algebraic difference between both the single and double-peaked models tend to increase as wind-sea becomes relevant, $\left(\frac{H_S^{WW}}{H_S}\right)^2 > 0.1$, and tend to decrease as swell becomes negligible, $\left(\frac{H_S^{WW}}{H_S}\right)^2 > 0.9$.

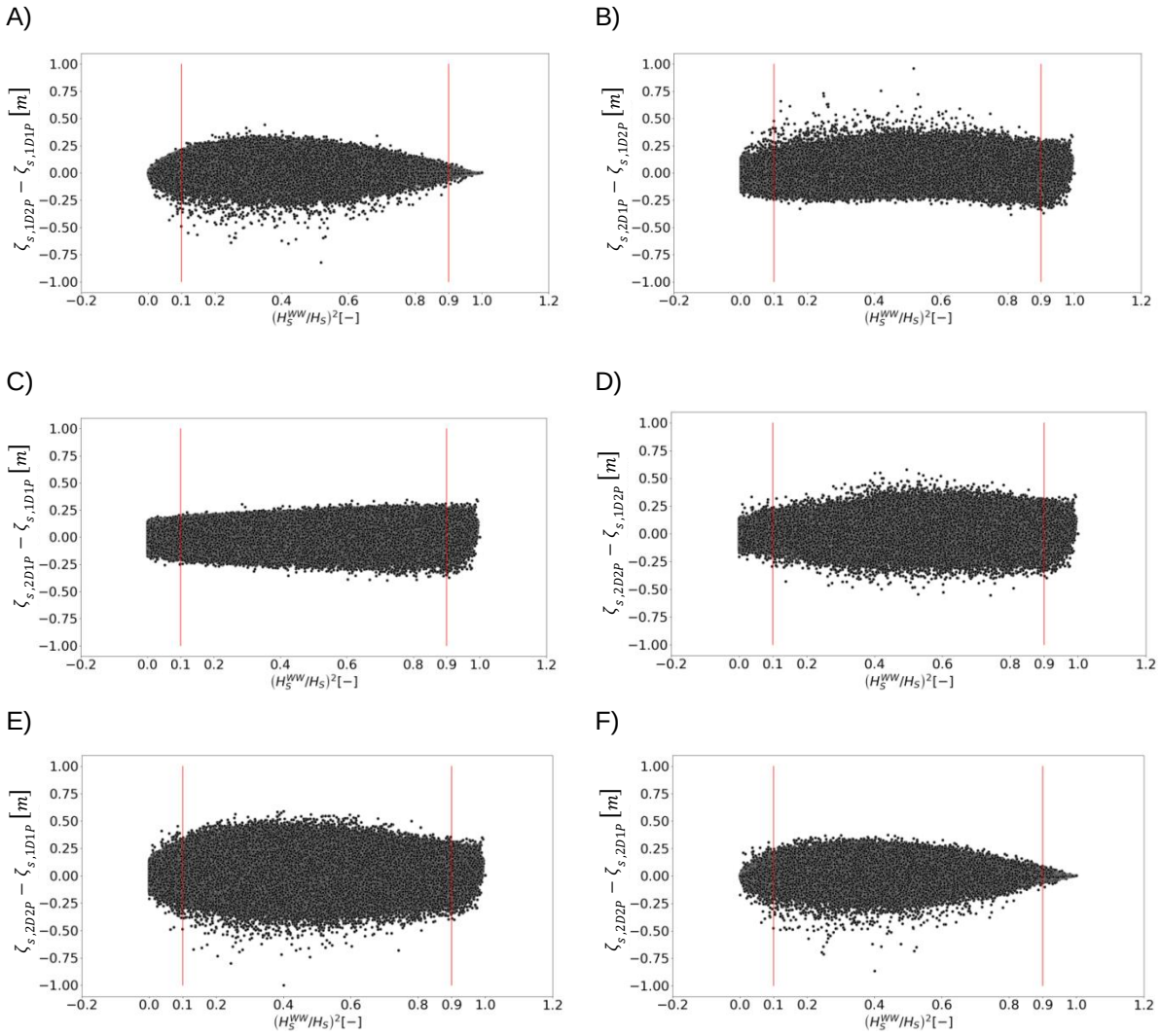

Figure 31. Relation between the significant heave amplitude absolute difference and the part of wind-sea energy from the total one, same disposition as in Figure 30

Such pattern is not recognized about the differences between the 1D and 2D models, as shown from Figure 31.B to Figure 31.E. Since the difference decreases as long as one wave component becomes negligible, inherently the 1P and 2P models will present stronger global correlation, as increased is the number of events when they provide agreeing responses.

Further discussions can be outlined regarding the scatter plots shown. All models are strongly correlated, according to the Pierson coefficient shown in Figure 30. The models source of variability uniquely derives from the different ocean-wave energy spreading methods and from the representation of the wave-field energy spectrum either by a resultant system or by accounting for individual contributions of swell and wind-sea. Further analysis in such aspect would be the study of the variability on the correlations when wave data are derived from different databases.

From Figure 30, one notices that, in general, for heave responses higher than 5 meters, the model comparison method adheres the $y = x$ line quite strongly. The number of points regarding such extreme response is decreased compared to the total amount of events, though. Stormy weather is, in general, scenario in which these responses are more likely to occur. The low differences in these events, mostly those verified in Figure 30.A and Figure 30.F, suggests that the wave-field was dominated by one wave component, as the agreement between the single and double-peaked models is significant. According to studies on sea-state classification shown in Table 1 from [36], the wave-field in Azores can be considered to be wind-sea dominated when stormy events are verified, where the H_S usually exceeds 8 [m]. In sight of that, wind-waves generated by the local wind in extreme wave climate dominate the wave field in such way that ocean-going waves as swell tend to play a smaller role. Therefore, one can attribute the strong correlation between single and double-peaked models when extreme heave responses are verified due to wind-sea dominated wave fields in stormy conditions.

As general rule, the higher the responses, the stronger the correlation between the models. The general aspect of the correlations in all combined cases is the pronounced spreading around the $y = x$ line about lower responses and the clear sharpening as long as higher amplitudes are verified. A quasi-perfect adherence in high responses is obtained from the single and double-peaked models comparison, Figure 30. A and Figure 30.F, and one verifies the same behavior, less marked though, about the correlations between frequency and directional models, as seen in the remaining figures.

These findings allows to draw some important conclusions about the usage of different models for design or operational purposes. At the design stage regarding seakeeping under extreme weather conditions, the selection of simpler models is not expected to lead to substantial disagreements compared to results from more complete ones. Thus the traditional and simpler 1D1P model can be recommended. The general agreement in less severe sea-states, $SHA \leq 5.0$ [m], is not conclusive, though, as the pattern shows an increased disagreement about the ideal line. In sight of that, when considering the optimization of the operability in average climate, the parametric model to be used should be accurately selected. In this case, it is suggested to gather more information about the sea-ways the ship is supposed to sail through, as to determine if they are likely to be dominated by one wave component, or rather composed by more wave systems, possibly from different directions. This allows, eventually, the selection of the most suited model.

The results shown in Figure 29 and Figure 30 about the agreement in high responses complete each other. The general tendency of the models on providing disagreeing results at locations where responses are expected to be less severe is verified in Figure 29, as at the intertropical zone, the amplitudes are significant lower compared to those verified at the extratropical one, as seen in Figure 28. Here, intertropical zone here means up to 30°N while extratropical means starting from 50°N. Cleary the relative differences show to be higher where lower responses are verified, overcoming in some cases, 20% of the amplitude as seen in Figure 29.D. However, at locations within 30°N and 50°N, single and double-peaked models, as shown in Figure 29.A and Figure 29.B, seemed to provide similar results, as the differences are negligible. This pattern is different from the one observed at the extratropical zone, where the single-peaked model seemed to over-estimate the responses compared to the double-peaked one, even though the differences there are much lower compared to those verified at the intertropical zone. The same pattern is not observed about the comparison between 1D and 2D models, Figure 29.C and Figure 29.D, as within 30°N and 50°N, the 1D1P model clearly over-estimates the responses compared to the 2D1P and 2D2P, respectively. Differences around -5% are observed although from the intertropical towards the extratropical one, the differences visually tend to decrease, in absolute value. The similarities observed in Figure 29.A and Figure 29.B within 30°N and 50°N have to be better analyzed as it suggests that the wave field in that location is likely to be dominated by one wave component, since the single and double-peaked models provided such agreeing results.

5.2 Mapping roll responses

In Figure 32 are shown the roll responses computed in the same way as discussed in the beginning of this chapter. Higher responses are obtained at the extratropical area such as in heave, as seen in Figure 28. The relative differences between the models are shown in Figure 33.

Single-peaked models showed to under-estimate the responses compared to the double-peaked ones about the intertropical zone, as seen in Figure 33.A and Figure 33.B, which pattern is the same from the one observed on heave responses shown in Figure 29.A and Figure 29.B. Such differences in this former case, however, showed to decrease towards the extratropical zone where higher responses are expected. Single peaked models slightly over-estimated the responses within 50°N and 60°N while similar results appeared within 30°N and 50°N. On roll response, though, such a pattern is not found and single peaked models significantly over-estimated the responses from 40°N towards North. A significant variability on the differences about frequency and directional models is furthermore observed in Figure 33.C and Figure 33.D.

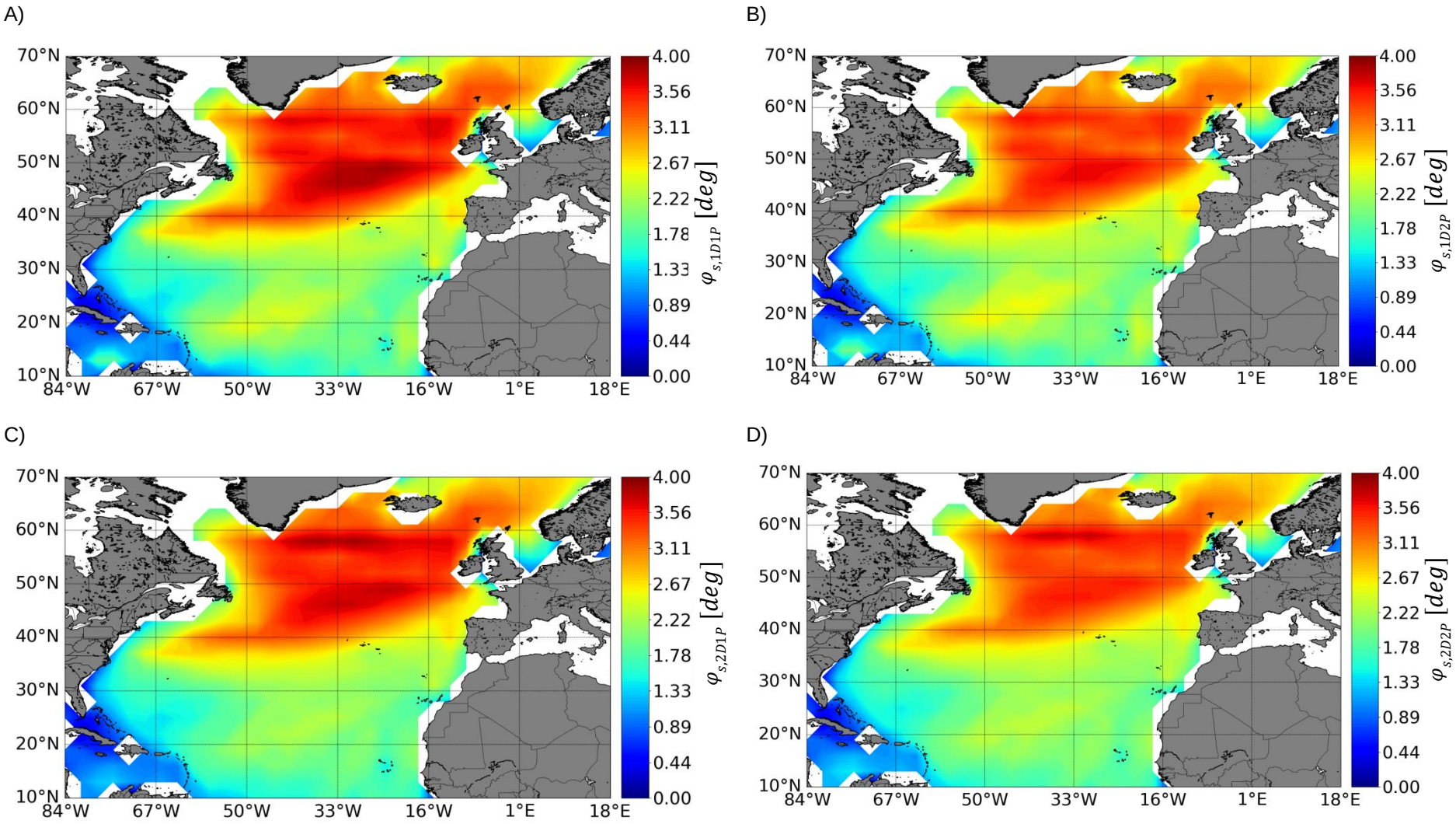

Figure 32. Weighted average mappings for the North Atlantic on the Roll Response. A) 1D1P, B) 1D2P, C) 2D1P and D) 2D2D

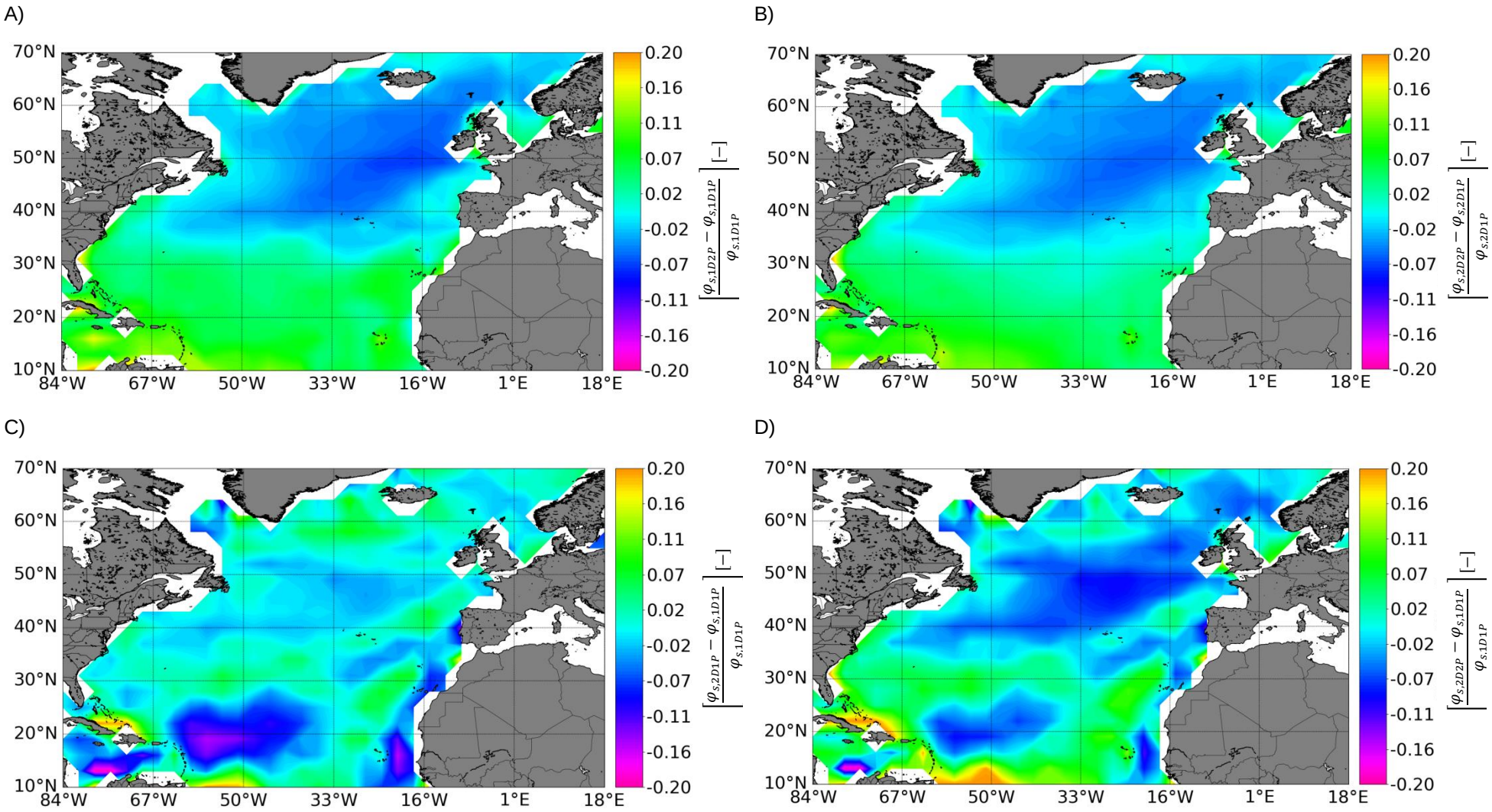

Figure 33. Relative difference mappings for the North Atlantic on the Roll Response. A) 1D2PX1D1P, B) 2D2PX2D1P, C) 2D1PX1D1P and D) 2D2PX1D1P

When studying the mechanisms that lead to the differences between the models in Chapter 4, the agreements in roll responses (Figure 18) showed to be more uncommon compared to those from heave motion, as seen in Figure 5. Single and double-peaked models on roll response will provide similar results in quite specific events, majorly when the wave field is dominated either by swell or wind-sea.

The next chapter presents the methodology used in this work to know whether the wave-field is expected or not to be dominated by a single component. Such tool will be used to show how the models differ under the consideration of single-peaked dominated wave-fields and how it differs from the results shown in Figure 29, which are also to be analyzed in sight of a probabilistic mapping showing the likely occurrence of single-peaked dominated wave-fields.

Chapter 6

Sea-state classifications

Up to this stage, this work presented the spectral parametric models which the ship responses are obtained from and the differences on the results were investigated. Cases in which the models produced either similar or disagreeing responses were presented and discussions were outlined in order to identify where such differences could come from. Maps about the heave responses on the North Atlantic were displayed, in which the disagreement between the models was visually evidenced. It was found that when the wave field is dominated by one wave component, either swell or wind-sea, both the 1P and 2P models tend to provide similar responses. Less definitive conclusions can be derived on the agreement between the frequency and directional models, though, as the first concentrates the wave field energy at the mean direction, providing either considerably higher, lower, or even similar responses compared to the directional models.

It becomes vital to foreknow if the wave field is expected to be dominated, as in this case single-peaked models are sufficiently accurate to compute the desired responses. The knowledge of the relevance of the wave components on the wave climate can be achieved if the wave field is classified according to pre-defined parameters and if statistical analysis are performed over a certain time record in order to determine the probability of occurrence of each class. Wave fields can be classified as swell or wind-sea dominated (single-peaked wave field), for instance, once verified if the corresponding wave component is likely to be irrelevant over the period recorded. Once known the statistical significance of single-peaked events over a grid of points, the locations where high probability of occurrence is verified are those where 1P models are expected to produce agreeing responses compared to the correspondent 2P ones.

If the full directional wave energy spectrum is known, one can set it to be the target spectrum of an optimization procedure that attempts to approximate it by a spectral function, which variables are the number of wave components and the main wave data, as shown in [36]. These variables are the output of the optimization process, resulting that the full spectrum ends up to be accurately described by a spectrum with known integral parameters (H_S, T_m and MWD) and number of wave system components. The wave field which the full spectrum was derived from can then be classified accordingly. The optimization process itself first assumes the approximation function to be composed uniquely by one wave system with given initial characteristics. The target function is the total square difference over both the frequency and directional domains, which when computed under the mentioned conditions, yields $J^{(0)}$.

That first attempt is compared with the derived one, assuming now two wave components, $J^{(1)}$, and so on. In summary, if the ratio between the measurement $J^{(N)}$ and the $J^{(N+1)}$ one, meaning $\frac{J^{(N)}}{J^{(N+1)}}$, does not exceed a certain threshold, so N terms are enough for the description of the wave field.

The classification methodology used in this work differs from the above briefly described. It was indeed preferred to propose a more straightforward parametric classification methodology. This is due to the fact that the application of the previously method is quite time demanding and, especially, because complete information about wave spectra are not available in practical applications.

The classification is based on the wave field main characteristics. Three parameters are used to distinguish the further presented classes. They are:

$$\tilde{H} = \left(\frac{H_S^{WW}}{H_S}\right)^2 \tag{21}$$

$$\tilde{T} = abs(T_m^S - T_m^{WW}) \tag{22}$$

$$\tilde{\theta} = abs(\theta_W^S - \theta_W^{WW}) \tag{23}$$

The Equation 21 compares both wind-sea waves and total wave system energies. Equation 22 and Equation 23 measure the absolute difference between the mean periods of swell and wind-sea waves and mean directions, respectively. The classes whose nomenclature is displayed below are:

- One-peaked swell dominated – OPS;
- One-peaked wind sea dominated – OPWS;
- Two-peaked, no crossing-seas occurrence – TPNCS;
- Two-peaked, with crossing-seas occurrence – TPCS;
- Undefined Mixed Condition – UMC.

The separation is made according to the methodology presented in Table 12.

The following comments can be outlined:

- Class OPS: as swell wave components are substantially more significant than wind-sea ones, so the part of the energy content of the spectrum relatively to the contribution of wind-sea can be neglected, thus the resulting spectrum is considered to be single-peaked, swell waves dominated.
- Class OPWS: as wind wave components are substantially more significant than swell ones, so the part of the energy content of the spectrum relatively to the contribution of swell can be neglected, thus the resulting spectrum is considered to be single-peaked, wind-sea waves dominated.

- Class TPNCS: the contributions of both wave components are relevant and whether the mean directions are similar but not the average periods, the spectra is considered to be double-peaked but crossing-seas are not verified;
- Class TPCS: the contributions from both wave components are relevant and whether the mean directions are significantly different, the spectra is directly considered to be double-peaked, crossing-seas;
- Class UMC: the contributions from both wave components are relevant and whether the average periods and mean directions are similar, the resulting wave spectrum is neither single nor double-peaked. As for the classification method this is an uncertain case about the real contribution of the components on the resulting spectrum shape, responses under sea-states as such classified will not be assessed. Only in restricted seas such as in the Caribbean one, the UMC class showed to be relevant as found and shown in Figure 35.B. As this work mainly concerns about the responses on the open North Atlantic, whether not taking this case into consideration will not compromise the statistical relevance of the remaining classes on the open sea.

Table 12. Mathematical description of the classes

Class	Description
OPS	$\widetilde{H} \leq 0.1$
OPWS	$\widetilde{H} \geq 0.9$
TPNCS	$0.1 < \widetilde{H} < 0.9$ $\tilde{T} > 4.0\ s$ $\tilde{\theta} \leq 30°$
TPCS	$0.1 < \widetilde{H} < 0.9$ $\tilde{\theta} > 30°$
UMC	$0.1 < \widetilde{H} < 0.9$ $\tilde{T} \leq 4.0\ s$ $\tilde{\theta} \leq 30°$

As an example, the results of the classification method applied to a location near the Azores Archipelago (GPS coordinates: 40º N, 26º W) are shown in Figure 34, where are displayed the probability of occurrences of each class about the 6-hourly, 1-yr wave field data. One concludes that during this period, the wave field in that particular location was majorly dominated by swell. Besides, wind-sea dominated events showed to be irrelevant.

Single-peaked events probability of occurrence can be computed over the North Atlantic grid, as shown in Figure 35.A. It represents the sum of both the swell (OPS) and wind-sea (OPWS) probability of occurrences, meaning when the wave field is likely to be dominated by a single component. A better

conclusion about the differences shown in Figure 29.A and Figure 29.B within 30°N and 50°N can now be outlined. It was verified that single and double-peaked models provided similar results in that location as the relative differences are negligible. Furthermore, such similarity, according to the findings so far obtained, suggests that wave field domination by a single component is likely to occur, which is in fact true, as seen in Figure 35.A. High probability of single-peaked spectra is verified within 20°N and 50°N. The decreased differences observed in Figure 29.A Figure 29.B in that area can, therefore, be in part attributed to the higher occurrence of single-peaked energy spectrum events as well as to the fact that the amplitudes tend to increase from the intertropical towards the extratropical zone, as models tend to provide similar results as higher the amplitudes.

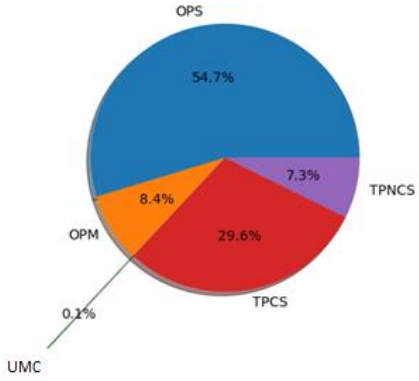

Figure 34. Class percentages in Azores (GPS coordinates: 40º N, 26º W)

In Figure 35.B is shown the probability of occurrence of the UMC events. The relevance of sea-states within this class is higher on the Caribbean Sea, being of low importance on the rest of the North Atlantic. This suggests that further analysis are required for characterizing the wave spectral conditions in closed seas. As the work presented concerns more about the study of the effect of the wave climate on the differences between the models in open seas, detailed analysis regarding weather that characterizes accordingly to such classification will not be outlined. In Figure 35.C is shown the probability of occurrence of double-peaked, not crossing seas events, where it is clear that sea-states as such classified are less likely to occur, while the occurrence of crossing seas are relevant, especially at extratropical area, as seen in Figure 35.D.

The direct influence of the classified sea-states upon the differences between the models can be verified conditioning the statistical analysis of the wave field to the classifications proposed. It is expectable, indeed, that OPS and OPWS classes will be fairly represented by 1D1P or 2D1P models, TPNCS class will require at least 1D2P model, whereas TPCS must include both double peak and directionality in the spectral model as to catch the real physics of the wave field.

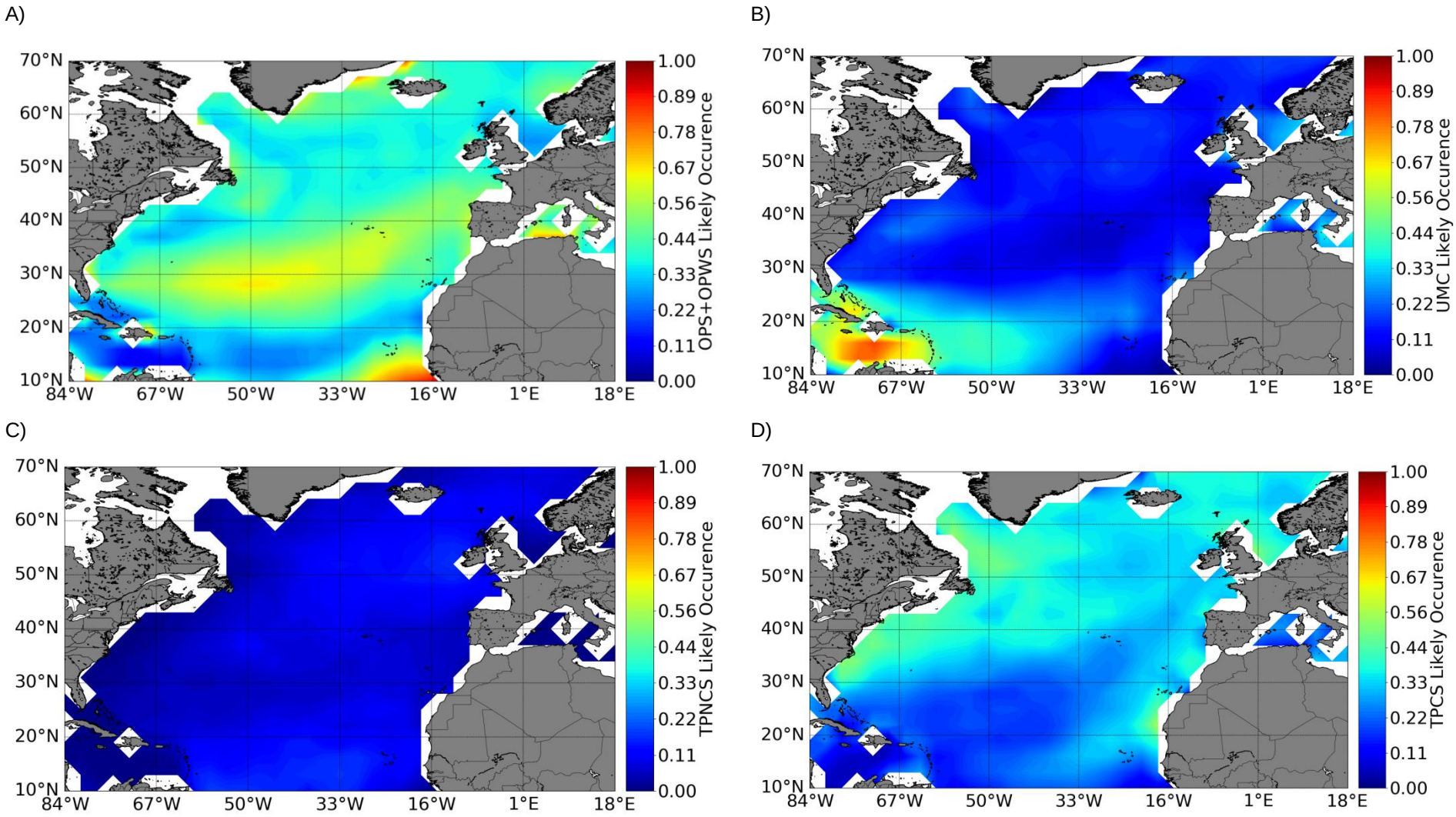

Figure 35. Probability of occurrence of each sea-state classification. A) OPS+OPWS, B) UMC, C) TPNCS and D) TPCS

6.1 Mapping heave responses in conditioned seas

6.1.1 Single-peaked dominated wave fields

In Figure 36 are shown the relative differences conditioned to single-peaked wave field. The differences between single and double-peaked models are negligible over the whole area, excepting in marginal seas such as the Caribbean one, as seen in Figure 36.A and Figure 36.B. The differences on the extratropical area, around the parallel $50°$N, are even closer 0%, as these are the locations where high responses are verified. These figures provide visual evidence that in fact single and double-peaked models output agreeing responses as long as the wave field is dominated by a specific component as well as show the particular tendency of the differences to be lower in higher responses. Figure 36.C and Figure 36.D show the differences between the single-peaked frequency spectrum and the directional models, 1P and 2P, respectively. No general rule about the agreement between frequency and directional models can be derived, even considering the wave field dominated by one wave component. As energy directionality is not considered in frequency models, both the sea spectrum and RAOs relate differently in such way that expectations about the agreement between 1D and 2D models are not necessarily assertive. Frequency models can yield much higher or lower responses compared to those from the directional ones, as shown in Chapter 4, even at single-peaked events. The same is seen in the mentioned figures, where in some locations the 1D1P model over-estimates the responses and vice-versa. However, the differences showed to slightly decrease towards more severe response locations.

It is concluded that in dominated wave fields, single and double peaked models tend to provide similar responses in open seas, as expected. Differences between frequency and directional models showed to not present a general patter to be outlined, although the differences slightly decrease towards the extratropical zone. The frequency model can be suggested to be used over the double-peaked directional one in more severe locations, where the differences showed to not be significant. The more complete model is, on the other hand, suggested whether optimal seakeeping in average wave climate is desired. In this case, nevertheless, the single-peaked directional model can be used, as it showed to be in agreement with the directional double-peaked one in the whole open North Atlantic.

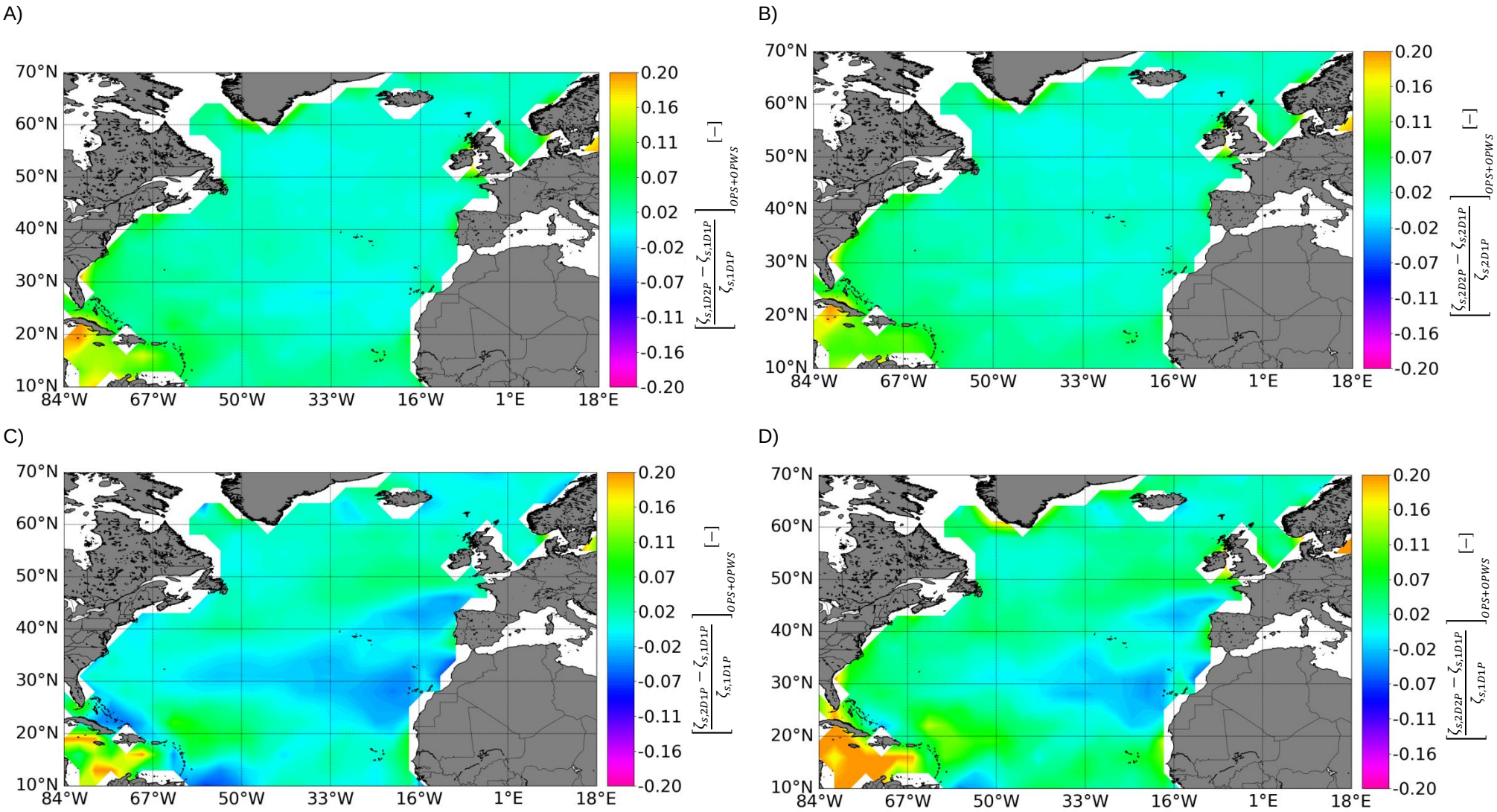

Figure 36. Same as Figure 29 but conditioned to single-peaked wave field. A) 1D2PX1D1P, B) 2D2PX2D1P, C) 2D1PX1D1P and D) 2D2PX1D1P

6.1.2 Double-peaked not crossing seas

In Figure 37 are shown the differences conditioned to double-peaked not crossing seas events. The general agreement between single and double-peaked models is not precisely predictable as a considerable variability is verified, as seen in Figure 37.A and Figure 37.B. The effect of the motion amplitude over the differences is quite clear, as towards the extratropical zone they showed to decrease. Locations where lower responses are observed, up to 30°N, presented several cases where the relative differences overcame 20%, as seen in all combinations. Single-peaked models showed to under-estimate the responses in that zone, compared to the double-peaked ones (Figure 37.A and Figure 37.B). The energy directionality showed to play important role in double-peaked sea-states as from the comparison in Figure 37.C and Figure 37.D, a significant variability is observed. Figure 37.D shows that the differences between the simplest and the most complete models are significant, especially in less severe climate locations. The 1D1P model substantially under-estimated the significant heave amplitudes at that same location compared to the 2D1P one (Figure 37.C), and the same pattern repeats at the extratropical zone, although less marked.

In case the sea-ways the ship is designed to sail through are characterized according to the TPNCS class characteristics, if the optimal operability in average wave climate (about the intertropical zone) is the design objective, the more complete models should be taken into consideration. The frequency single-peaked one, in this case, showed to in general under-estimate the responses compared to the directional models, highlighting the relevance of a more complete wave energy representation through the directionality. Comparing with the cases when dominated wave field was verified (Figure 36.C and Figure 36.D), especially about the intertropical zone, more accentuated under-estimations derived from double-peaked wave fields, suggesting that in dominated ones, the energy directionality does not play such an important role as it does when both swell and wind-sea contributions are relevant.

It is concluded that the energy directionality should be taken into consideration as frequency models tend to generally under-estimate the responses compared to directional ones. To decide whether to use single or double-peaked directional models, the ship operability location should be taken into consideration, as the 2D1P model showed to slightly under-estimate the responses about the intertropical zone (Figure 37.B), although towards higher response areas the differences generally became negligible.

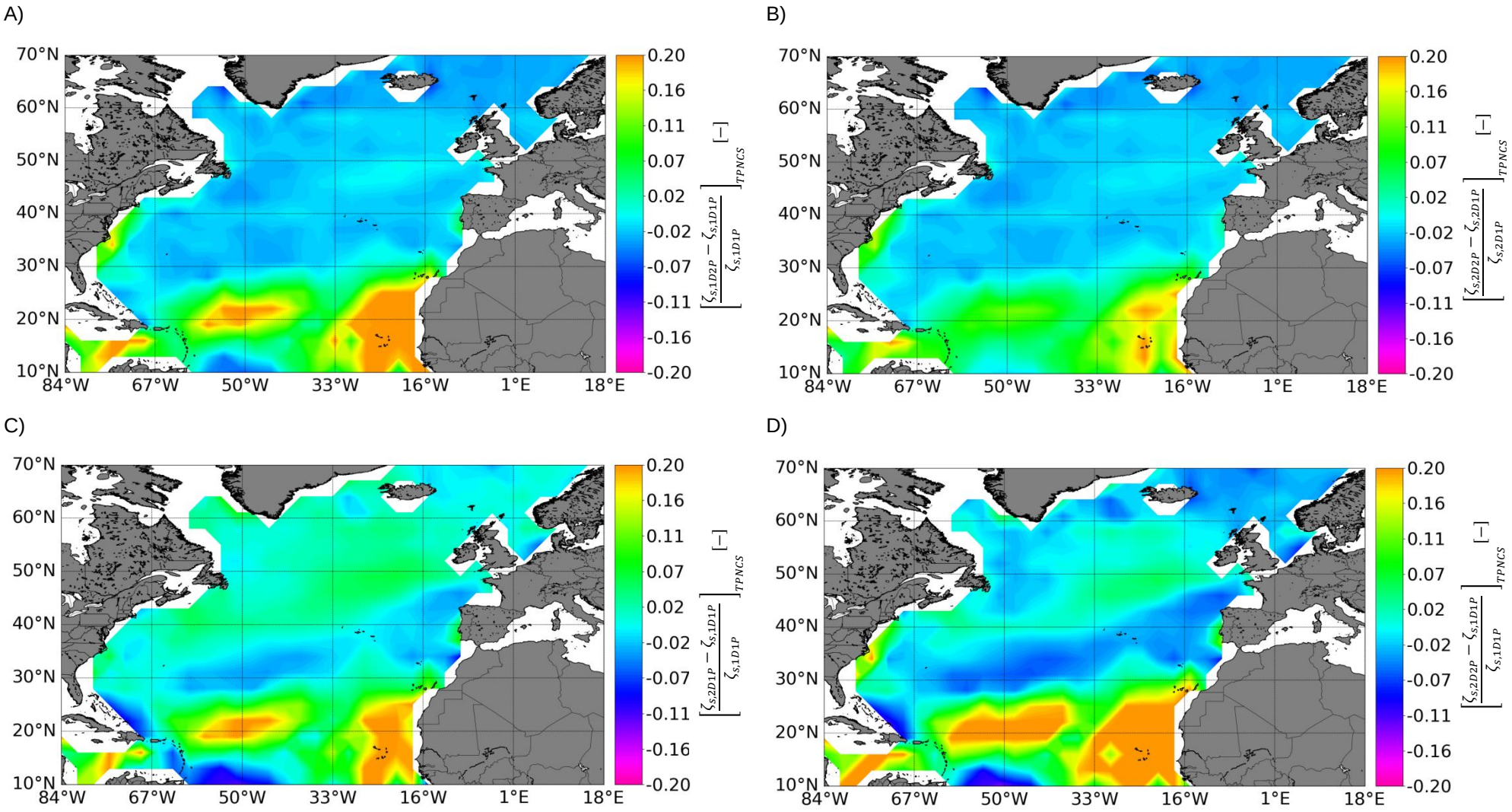

Figure 37. Same as Figure 29 but conditioned to not crossing seas, double-peaked wave field. A) 1D2PX1D1P, B) 2D2PX2D1P, C) 2D1PX1D1P and D) 2D2PX1D1P

6.1.3 Double-peaked crossing sea wave fields

Differences between the models regarding the wave field conditioned to crossing seas, double-peaked events are shown in Figure 38. The single-peaked frequency model showed to under-estimate the responses around the parallel 20°N compared to the 1D2P one, as seen in Figure 38.A. The differences showed to decrease towards the extratropical zone, though. Compared to the case presented in Figure 37.A, visually lower disagreements are verified as few are the cases where the relative differences overcome 20%, although it is believed that the lower statistical significant of the previous case could have led to such results, as wave fields with two aligned wave systems are less likely to occur compared to the crossing events. Nevertheless, the pattern showed to be the same, which was expected, as the separate wave components directionality is not taken into consideration in both models (1D1P and 1D2P), meaning that the general aspect of the differences between these models in both crossing and not crossing wave fields are expected to be the same. The 1D1P model showed to generally under-estimate the responses compared to the directional models, as exposed in Figure 38.C and Figure 38.D. The disagreements in that case are stronger about the intertropical zone and are more significant when comparing with the 2D2P model, as shown in this latter figure. As seen in Figure 38.B, the differences between both the single and double-peaked directional models are more pronounced at less severe wave climate zones, while towards the extratropical area, where higher responses are verified, the results showed again to converge.

The same outlined on the previous case is now found, in such way that frequency models should be avoided as they generally tend to under-estimate the responses compared to those from the directional ones. Furthermore, the single-peaked directional model seemed to provide fairly good results compared to the more complete one in locations where higher responses are expected, although about the intertropical zone the usage of the double-peaked one is suggested.

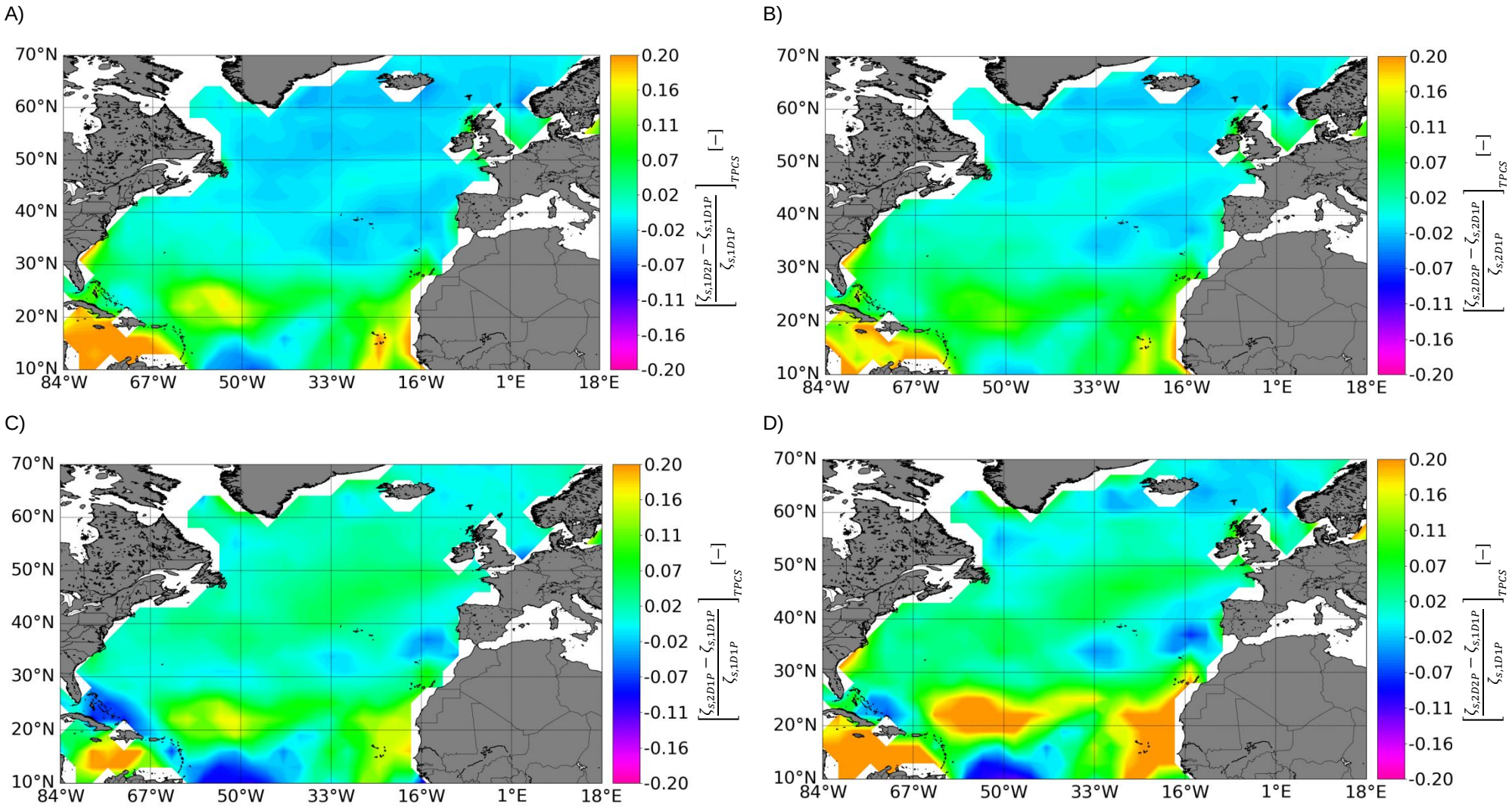

Figure 38. Same as Figure 34 but conditioned to crossing seas, double-peaked wave field. . A) 1D2PX1D1P, B) 2D2PX2D1P, C) 2D1PX1D1P and D) 2D2PX1D1P

6.2 Mapping roll responses in conditioned seas (general overview)

Differences regarding conditioned single-peaked sea-states are shown in Figure 39. The agreement between single and double-peaked models at panels A and B showed to be significant. Single-peaked models slightly over-estimated the responses about the parallel 50°N, though. Nevertheless, one can observed that both models kept the same pattern on providing similar responses in dominated wave field, which conclusion was also outlined for heave response. On the other hand, the differences between frequency and directional models showed strong variability, as seen in Figure 39.C and Figure 39.D. One notices that the frequency model either under or over-estimate the responses, in such way that similar results are quite uncommon to be found. Differently from the heave motion where the differences tended to decrease towards the extratropical area, regions where agreeing responses are expected cannot be observed since in roll motion the differences between frequency and directional models seem to have a random nature.

On the regards of the conditioned double-peaked, not crossing seas wave field, single-peaked models under-estimate the responses about the intertropical zone while it over-estimates them about the extratropical one, compared to the double-peaked models, as shown in Figure 40.A and Figure 40.B. Locations where frequency and directional models provided similar results cannot be highlighted, as well as on the previous case, as seen in Figure 40.C and Figure 40.D.

Both the double-peaked not crossing and crossing seas have the same pattern regarding the differences between single and double-peaked models, Figure 41.A and Figure 41.B, and frequency and directional models, Figure 41.C and Figure 41.D.

On the roll response it is outlined, therefore, that the selection of a more complete model such as the double-peaked directional one is suggested. The agreement between this latter and frequency models is quite uncommon. This is mainly due to the urgency of correctly represent the wave energy content in a relatively narrow range of frequencies and directions next to the natural frequency of roll, where responses can be largely amplified. Moreover, the single-peaked directional model only provide similar results when dominated wave field is expected. Even in locations where dominated seas are more likely to occur, the differences between single and double-peaked directional models showed to be considerable in such way that describing the wave field energy by taking into account the separate contributions of each component plays an important role such as the energy directionality does.

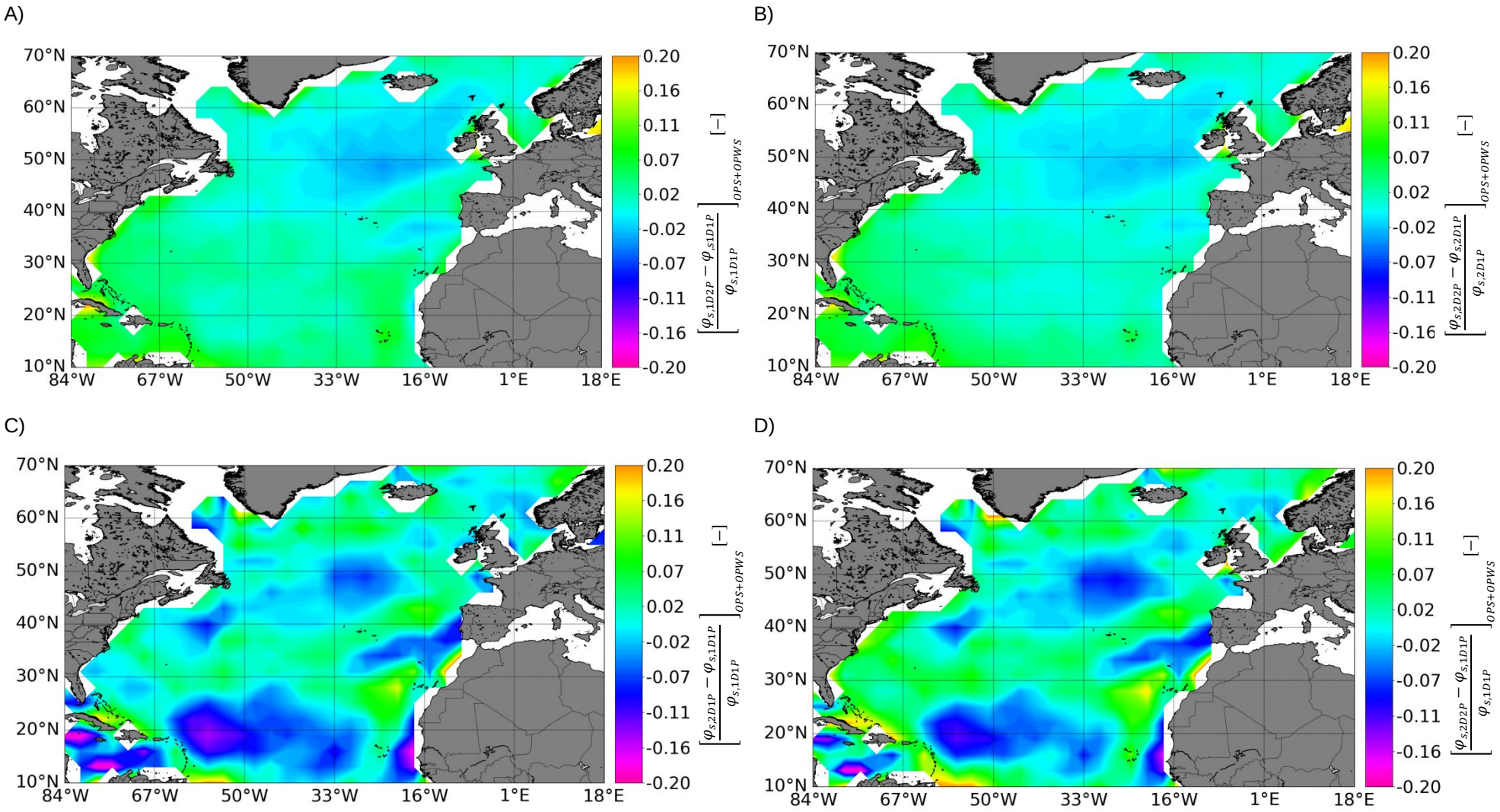

Figure 39. Same as Figure 33 but conditioned to single-peaked wave field. A) 1D2PX1D1P, B) 2D2PX2D1P, C) 2D1PX1D1P and D) 2D2PX1D1P

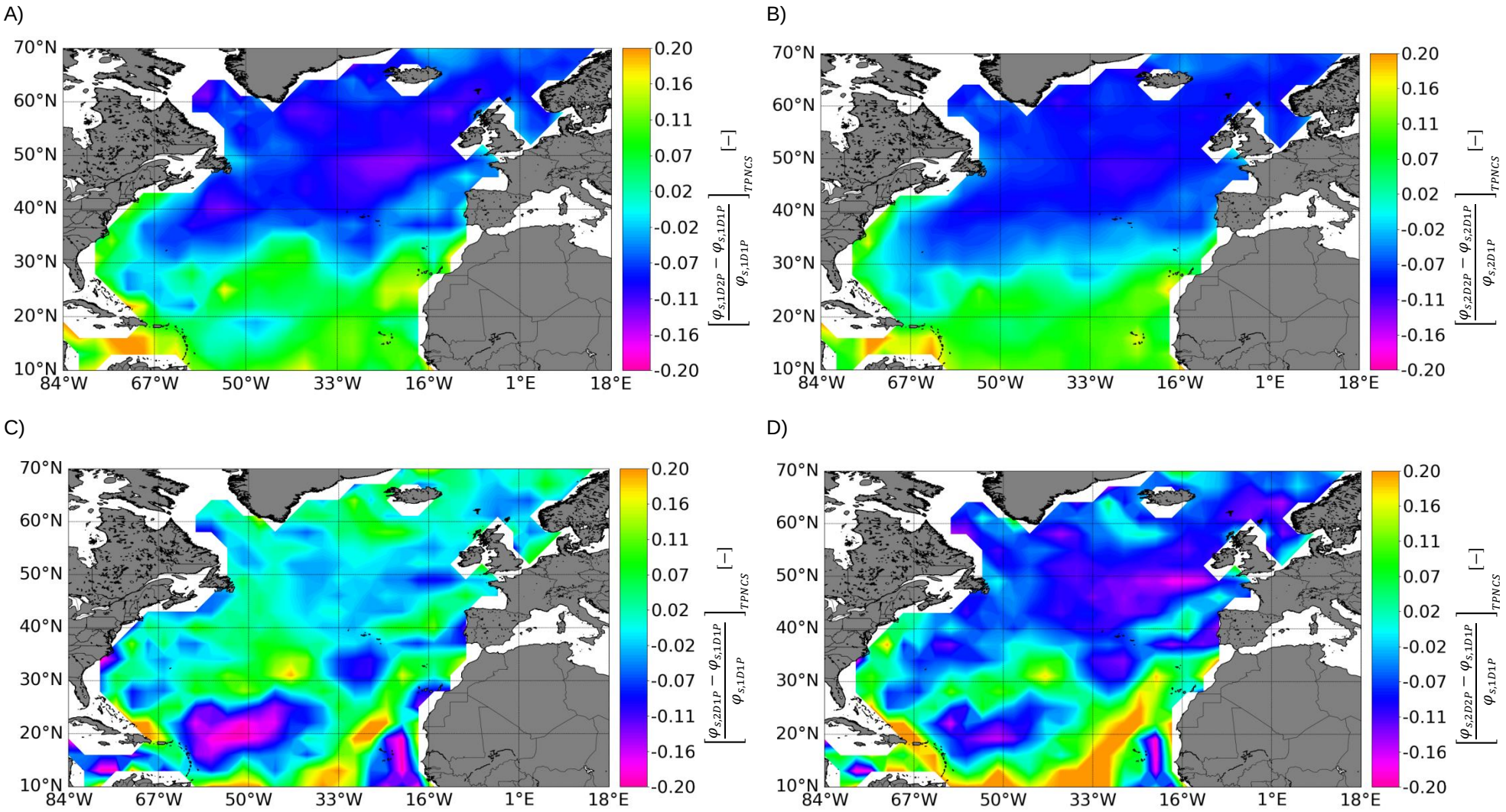

Figure 40. Same as Figure 33 but conditioned to not crossing seas, double-peaked wave field. A) 1D2PX1D1P, B) 2D2PX2D1P, C) 2D1PX1D1P and D) 2D2PX1D1P

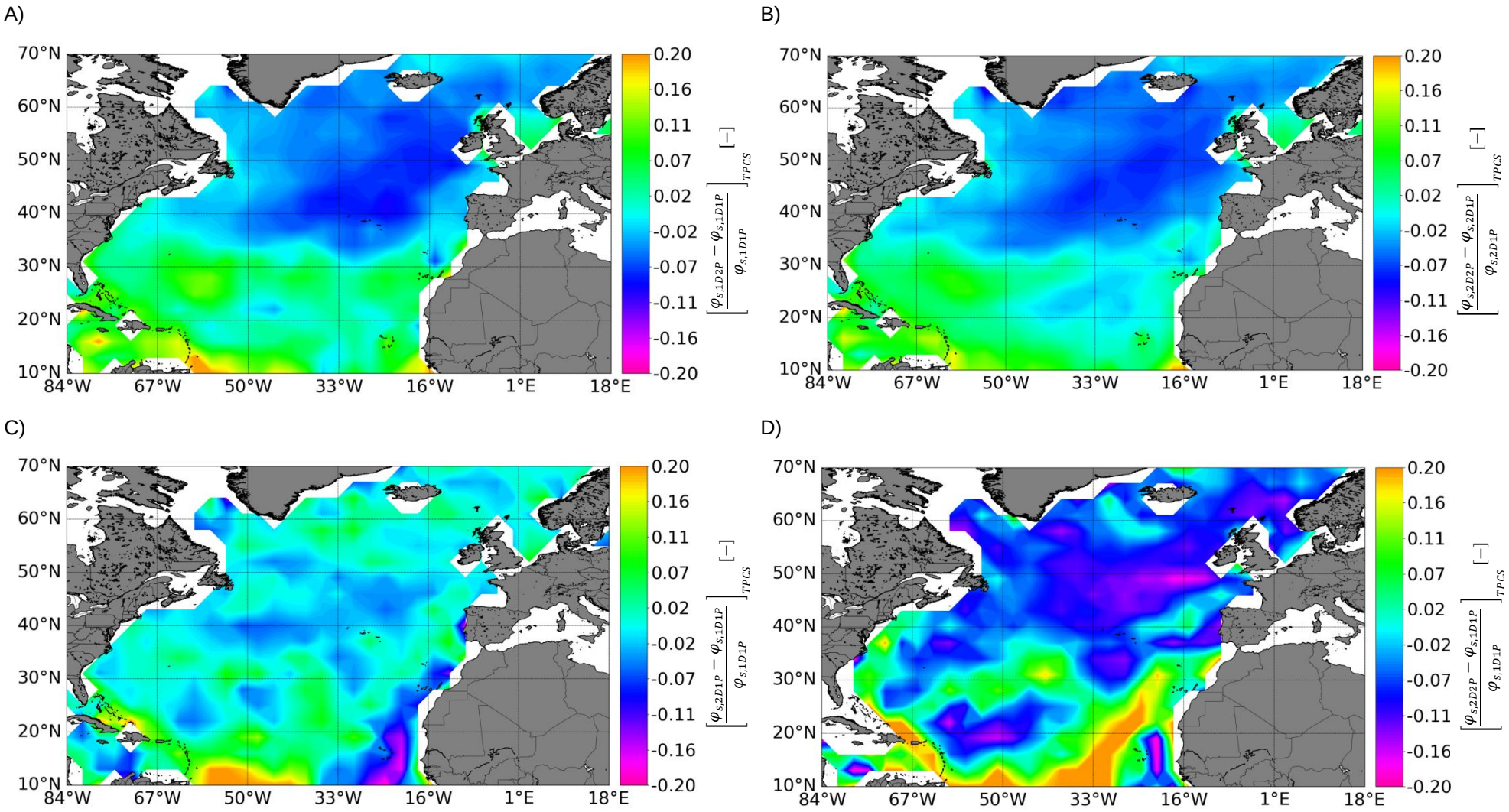

Figure 41. Same as Figure 33 but conditioned to crossing seas, double-peaked wave field. A) 1D2PX1D1P, B) 2D2PX2D1P, C) 2D1PX1D1P and D) 2D2PX1D1P

Conclusions

In this work, the influence of the spectra model on the ship response is analyzed. The responses are computed from the product between the RAO and the wave energy spectrum. The first is obtained computationally, where numerical methods such as strip theory are applied to solve the potential problem. Heave and roll TFs are then obtained from the seakeeping code, regarding the hull of a container ship, the S175 one. Pitch motion has been also analyzed, though the results are not presented in this thesis due to the general similarity with the results of heave.

The wave spectrum, which shape is evaluated according to well-established parametric models, requires as prior information the wave field main characteristics such as the H_S, MWD and T_m to be built. Such environmental information is obtained from ERA-Interim, which agglutinates numerical models and data assimilated via satellite and radar altimeter observations in order to provide an historical database of the wave climate particulars. The parametric models vary in number of peaks and energy distribution. Single-peaked models describe the energy distribution of the combined wave field, as a single wave system, possibly resulting from the interaction between wave components, wind-sea due to local wind and one (or more) swells. Double-peaked models, on the other hand, describe the energy distribution taking into account the contribution of swell and wind-sea, separately. In this latter case, one spectra for each component is generated and the total energy of the wave field is represented by the sum of the two. The distribution of wave energy can be limited to the frequency domain, or consider directional domain as well. Four different parametric models are then implemented, varying from the single-peaked frequency to the double-peaked directional one.

The differences on the ship responses regarding the application of each parametric model and how they can be related to the wave climate in general is the main focus of this work. First, an understanding on the mechanisms that lead to the differences between the models is outlined and finally a relation between them and the wave climate is studied, as the agreement between the models vary according to the environmental characteristics recorded at each event. In sight of the sea-ways climate that the vessels are designed to work at, simpler parametric models such as the single-peaked one can be eventually suggested as long as they provide similar results compared to the more complete one. Avoiding the usage of more complete model in fact can be preferable for computational time saving and modeling simplicity.

Regarding relation between different models for the same sea-state condition, as outlined in Chapter 4, it was found that, in general, when both swell and wind-sea are energetically relevant about the wave field energy, the models tend to provide different results. The differences between single and double-peaked

models regarding the same energy distribution tend to decrease as long as the relevance of one of the components shows to be lower compared to the total energy. In these cases, the resultant spectrum of the double-peaked model mostly represents the energy distribution of the most energetic component, often being swell. Both the single and double-peaked models yield then to similar energy distributions, as shown, for instance, in Figure 6, Figure 8.A and Figure 8.B. Since the RAO is the same, the models provided similar response spectra, as shown in Figure 7, Figure 8.E and Figure 8.F. The differences between frequency and directional models, even considering dominated wave field, vary according to the θ_H. Frequency models can provide similar, and either significantly higher or lower results compared to the directions ones, depending if θ_H is a high excitation direction or not. Such differences became clear when analyzing the case proposed in 4.2.3, when whether considering the frequency model, a low excitation direction was recorded by the relative wave direction, while it was the opposite for the directional model, as at such direction, the wave spectrum sensed the energy peaks of the roll RAO. In that case, therefore, single peaked models clearly under-estimate the responses compared to those from the directional ones. On the other hand, frequency models provided higher responses in both cases, such as those shown in 4.1.2 and 4.2.2. In these examples, the wave field energy was completely concentrated at a excitation direction. The energy directionality clearly spread the wave energy towards lower excitation directions, resulting in lower responses about the directional models. The energy concentration at the MHD as inherent aspect of both the 1D1P and 1D2P models is, hence, a mechanism that can eventually lead to disagreements between them and the directional models. This variability is even more evident for roll motion than for heave. During the analysis outlined in Chapter 4, the differences between the models clearly showed to vary according to the sea-state characteristics. It appeared then to be interesting to study the differences over a grid of points on the North Atlantic, so that the relation between them and the wave climate could be studied in detail.

The differences between the models over the grid on the North Atlantic, as shown in Figure 29 on Chapter 5 provided a visual evidence of their variability according to the locally dependent wave climate. As to take into account the variability of ship courses in navigation at each different location, the analyzed results derive, in this case, from a weighted average over the ship courses, for which a realistic probability distribution is computed from VOS database. Furthermore, to draw general conclusions with respect to the wave climate, the temporal 1-yr average is computed. Thanks to the scatter plots shown in Figure 30, one can verify that the differences on the heave responses tend to decrease as the responses themselves become higher. High response locations about the extratropical zone, as seen in Figure 28 are those where the models showed to be in higher agreement. Low response locations, those about the intertropical zone, presented higher disagreement between the models and the same is verified on the scatter plots, as in lower responses the correlations show to be more spread around the $y = x$ line. Single and double-peaked models regarding the same energy distribution showed to present higher agreement, according to the Pierson correlation coefficients shown on the scatter plots. Part of such higher agreement can be attributed to the similar responses that they provide when dominated wave field

occurs, that is, one of the wave components carries more than 90% of the total energy. An example can be seen in Figure 31.A and Figure 31.F, where the relative differences showed to be negligible. The same behavior is not verified regarding the differences between frequency and directional models, as the absolute minimum of the relative differences between the models compared from Figure 31.B to Figure 31.E showed to not be directly related to the wave field domination. Besides, the substantial agreement in more severe conditions ($SHA \geq 5.0$ [m]) seen in Figure 30.A and Figure 30.F can be attributed to the the fact that the wave field is dominated by local wind excitation at extreme weather conditions. It can be outlined, therefore, that whether considering seakeeping under extreme responses as design parameter, the usage of simpler models does not lead to significant differences compared to the more complete one, although whether the design focus on the seakeeping in average climate where the responses are not expected to be violent, the selection of a suitable parametric model is suggested to be taken into account, as in this case simpler and more complete models not necessarily provide similar results.

The analysis performed in Chapter 5 showed that in between 30°N and 50°N, single and double-peaked models tended to provide similar results, as the relative differences are generally negligible. As such behavior does not verify regarding the difference between frequency and directional models, it suggests that dominated wave fields are likely to occur in that location. In fact, according to the classification proposed, single-peaked dominated wave fields have higher probabilities in this region (approximately 65%), as seen in Figure 35.A. This justifies the tendency on single and double-peaked models on providing similar responses in between 30°N and 50°N.

The sea state classification discussed in Chapter 6 showed its importance, as the differences between the models could be analyzed regarding similar wave fields recorded in each classification. For instance, OPS is the class which holds only events when swell dominated wave fields were recorded. Conditioning the study to the classified wave fields permits to visualize how the differences vary spatially within each classification and, eventually, to recommend different models depending on the sea-state class to be expected. Regarding the heave conditioned to single-peaked events, both the single and double-peaked models showed to provide similar results all around the open North Atlantic, as seen in Figure 36.A and Figure 36.B. A higher variability is presented when comparing frequency and directional models, as expected, since the agreement between them strongly depends on θ_H and how the energy spectrum relates with the heave RAO, see Figure 36.C and Figure 36.D. The differences in this latter case tended to decrease towards the extratropical zone, where higher responses are expected. About both the TPNCS and TPCS classifications, it was found that single-peaked models tend to under-estimate the responses compared to those from the double-peaked ones, although towards the extratropical zone, higher agreement is observed, as seen in Figure 37 and Figure 38, panels A and B. The same pattern is seen on the comparison between frequency and directional models, Figure 37 and Figure 38, panels C and D. In sight of that it, depending on the sea-ways the marine structure is designed to operate at, more

complete models are suggested to be used, as the responses showed to be under-estimated by the frequency single-peaked model at no violent locations.

On regards of roll responses, on the other hand, aside the agreement verified between single and double-peaked models in dominated wave field (Figure 39.A and Figure 39.B), a general higher variability on the differences between the models was observed. When one component is not dominant, more often than not frequency models misestimated the responses compared to those from the double-peaked ones. The differences between frequency and directional models showed quite high variability in all conditioned seas. More complete and detailed models such as the directional double-peaked one showed to be more appropriate than the simpler ones, as the contribution of both the swell and wind-sea are separately taken into consideration. Besides, the energy directionality showed to be perform quite important role on roll responses, as frequency and directional models showed to not agree all around the open North Atlantic, regardless of the wave climate.

It is clear that different parametric models can provide different responses depending on the wave climate and on the location. The prior knowledge of the climate of the sea-ways the structures are designed to operate at can be fundamental for the selection of a suitable model, as in some cases, simpler models can present fairly reliable results compared to those from more complete ones. In general, in dominated sea-states, the single-peaked directional model can be used rather than the double-peaked one. Besides, for the usage of frequency models in dominated seas, one should take into consideration whether extreme responses are expected, as the differences between them and the directional models tend to decrease under severe weather conditions. In locations where both the swell and wind-sea components are relevant, more complete models should be taken into consideration.

The findings of the present work allow to provide some important recommendation for the selection of the most appropriate spectral model:

- for design purposes, when limit state values are to be evaluated, the traditional approach to single-peak model can be accepted, however taking into account directional spreading is recommendable, especially when roll motion is considered.
- in case of design parameter influenced by frequent events of lower intensity, such as fatigue, more complex models may be needed, however further research on structural loads should be carried out to better investigate these aspects;
- for operational purposes, the expected sea-state should be carefully categorized and guided towards the model that better reflects the physics of such a wave field.

Finally, the performed analysis opens the path to further investigations in this directions. First of all, since the responses have been shown to be sensitive to the directional distribution of the wave energy, more effort should be put on the identification of the most appropriate parameters for the directional spreading function, depending on the wave component and, possibly, on the location. The complexity of the wave

climate on closed seas and coastal areas suggests to study in more details the ship responses in these regions, especially considering that these are often the busiest operational areas. Moreover, a similar analysis, but focused on structural stresses can also lead to important conclusions for the design of marine structures.

Bibliography

[1] E. Spentza, G. Besio, A. Mazzino, T. Gaggero, and D. Villa, “A ship weather-routing tool for route evaluation and selection: Influence of the wave spectrum,” in *Maritime Transportation and Harvesting of Sea Resources.*, no. 1, 2017, pp. 453–462.

[2] R. Lawford, J. Bradon, T. Barberon, C. Camps, and R. Jameson, “Directional Wave Partitioning and Its Applications to the Structural Analysis of an FPSO,” in *OMAE*, 2008, pp. 333–341.

[3] J. Jiao, C. Chen, and H. Ren, “A comprehensive study on ship motion and load responses in short-crested irregular waves,” in *International Journal of Naval Architecture and Ocean Engineering*, vol. 11, no. 1, Elsevier Ltd, 2019, pp. 364–379.

[4] C. Guedes Soares, “Effect of spectral shape uncertainty in the short-term wave induced ship resposnes,” in *Applied Ocean Research*, vol. 12, no. 2, 1990, pp. 54–69.

[5] C. Guedes Soares, “Effect of transfer function uncertainty on short-term ship responses,” in *Ocean Engineering*, vol. 18, no. 4, 1991, pp. 329–362.

[6] F. Belga, S. Sutulo, and C. Guedes Soares, “Comparative study of various strip-theory seakeeping codes in predicting heave and pitch motions of fast displacement ships in head seas,” in *Progress in Maritime Technology and Engineering*, 2018, pp. 599–610.

[7] D. Hoffman, “The Impact of Seakeeping on Ship Operations,” in *Marine Technology*, vol. 13, no. 2, 1976, pp. 241–262.

[8] J. Prpić-Oršić, R. Vettor, O. M. Faltinsen, and C. Guedes Soares, “The influence of route choice and operating conditions on fuel consumption and CO2 emission of ships,” in *Journal of Marine Science and Technology (Japan)*, vol. 21, no. 3, Springer Japan, 2016, pp. 434–457.

[9] E. M. Bitner-Gregerse, C. G. Soares, and M. Vantorre, “Adverse Weather Conditions for Ship Manoeuvrability,” *Transp. Res. Procedia*, vol. 14, pp. 1631–1640, 2016.

[10] B. Guo, E. M. Bitner-gregersen, H. Sun, and J. B. Helmers, “Statistics analysis of ship response in extreme seas,” in *Ocean Engineering*, vol. 119, Elsevier, 2016, pp. 154–164.

[11] J. M. . Journée and W. W. Massie, *Offshore hydromechanics*, 1st ed., no. January. Delft Univeristy of Technology, 2001.

[12] J. N. Newman, *Marine Hydrodynamics*. Cambridge, MA: The MIT Press, 2017.

[13] N. Fonseca and C. Guedes Soares, “Comparison of numerical and experimental results of nonlinear wave-induced vertical ship motions and loads,” in *Journal of Marine Science and Technology*, vol. 6, no. 4, 2002, pp. 193–204.

[14] N. Salvesen, E. O. Tuck, and O. M. Faltinsen, “Ship motions and sea loads,” in *The society of naval architects and marine engineers*, vol. 6, 1970, pp. 1–30.

[15] E. R. Miller, “Roll Damping, Technical Report 6136-74-280, NAVSPEC,” 1974.

[16] ITTC Seakeeping Committee, “Comparison of results obtained with compute programs to predict ship motions in six-degrees-of-freedom and associated responses,” *Proceedings of the 15th ITTC*. pp. 79–92, 1978.

[17] J. Miles, “On the generation of surface waves by shear flows,” in *Journal of Fluid Mechanics*, vol. 3, no. 2, 1957, pp. 185–204.

[18] O. Phillips, “On the generation of waves by turbulent wind,” *J. Fluid Mech.*, vol. 2, no. 5, pp. 417–445, 1957.

[19] W. H. Munk, “Origin and Generation of Waves,” in *Coastal Engineering*, 1950.

[20] W. H. Munk, G. R. Miller, F. E. Snodgrass, and N. F. Barber, “Directional recording of swell from distant storms,” in *Philosophical Transactions of the Royal Society A: Mathematical, Physical and Engineering Sciences*, vol. 255, no. 1062, 1963, pp. 505–584.

[21] C. Lucas and C. Guedes Soares, “On the modelling of swell spectra,” in *Ocean Engineering*, vol. 108, no. November, 2015, pp. 749–759.

[22] I. R. Young, “Seasonal variability of the global ocean wind and wave climate,” in *International Journal of Climatology*, vol. 19, 1999, pp. 931–950.

[23] A. Semedo, K. Sušelj, A. Rutgersson, and A. Sterl, “A global view on the wind sea and swell climate and variability from ERA-40,” in *Journal of Climate*, vol. 24, no. 5, 2011, pp. 1461–1479.

[24] W. J. Pierson and L. Moskowitz, “A proposed spectral form for fully developed wind seas based on the similarity theory of S. A. Kitaigorodskii,” in *Journal of Geophysical Research*, vol. 69, no. 24, 1964, pp. 5181–5190.

[25] R. Vettor and C. Guedes Soares, “Rough weather avoidance effect on the wave climate experienced by oceangoing vessels,” in *Applied Ocean Research*, vol. 59, Elsevier B.V., 2016, pp. 606–615.

[26] K. Hasselmann, T. P. Barnett, E. Bouws, H. Carlson, D. E. Cartwright, and K. Enke,

"Measurements of wind-wave growth and swell deacy during the Joint North Sea Wave Project (JONSWAP)," *Dtsch. Hydrogr.*, vol. 8, no. 12, pp. 1–95, 1973.

[27] N. Hogben *et al.*, "Environmental conditions.pdf," *Report of Committee I.1 - 6th International Ship Structures Congress*. Boston, 1976.

[28] C. Guedes Soares, "Representation of double-peaked sea wave spectra," in *Ocean Engineering*, vol. 11, no. 2, 1984, pp. 185–207.

[29] M. A. Hinostroza and C. Guedes Soares, "Parametric estimation of the directional wave spectrum from ship motions," in *Transactions of the Royal Institution of Naval Architects Part A: International Journal of Maritime Engineering*, vol. 158, no. A2, 2016, pp. A121–A130.

[30] D. P. Dee *et al.*, "The ERA-Interim reanalysis: Configuration and performance of the data assimilation system," in *Quarterly Journal of the Royal Meteorological Society*, vol. 137, 2011, pp. 553–597.

[31] R. M. Campos and C. Guedes Soares, "Comparison and assessment of three wave hindcasts in the North Atlantic Ocean Comparison and assessment of three wave hindcasts in the North Atlantic Ocean," in *Journal of Operational Oceanography*, vol. 9, no. 1, Taylor & Francis, 2016, pp. 26–44.

[32] "ERA Interim: What is the direction convention for wave fields?" [Online]. Available: https://confluence.ecmwf.int/pages/viewpage.action?pageId=111155338.

[33] J. Fletcher, "Meteorological observations from ships," *Seaways - The Nautical Institute*, pp. 7–10, 2008.

[34] R. Vettor and C. Guedes Soares, "Assessment of the Storm Avoidance Effect on the Wave Climate along the Main North Atlantic Routes," in *Journal of Navigation*, vol. 69, no. 1, 2016, pp. 127–144.

[35] R. Vettor and C. Guedes Soares, "A Global View on Bimodal Wave Spectra and Crossing Seas from ERA-interim [Not Published]."

[36] C. Lucas, A. Boukhanovsky, and C. Guedes Soares, "Modeling the climatic variability of directional wave spectra," in *Ocean Engineering*, vol. 38, no. 11–12, 2011, pp. 1283–1290.